Fabrication of composite scaffolds impregnated with an optimized fibrin-alginate hydrogel for cartilage tissue engineering

A Thesis Submitted to the College of
Graduate Studies and Research in
Partial fulfillment of the
Requirements for

the

Degree of Master of Science

in the

Department of Biomedical
Engineering
University of Saskatchewan
Saskatoon

By

Christopher James Little

Permission to Use

In presenting this thesis/dissertation in partial fulfillment of the requirements for a Postgraduate degree from the University of Saskatchewan, I agree that the Libraries of this University may make it freely available for inspection. I further agree that permission for copying of this thesis/dissertation in any manner, in whole or in part, for scholarly purposes may be granted by the professor or professors who supervised my thesis/dissertation work or, in their absence, by the Head of the Department or the Dean of the College in which my thesis work was done. It is understood that any copying or publication or use of this thesis/dissertation or parts thereof for financial gain shall not be allowed without my written permission. It is also understood that due recognition shall be given to me and to the University of Saskatchewan in any scholarly use which may be made of any material in my thesis/dissertation.

Disclaimer

Reference in this thesis/dissertation to any specific commercial products, process, or service by trade name, trademark, manufacturer, or otherwise, does not constitute or imply its endorsement, recommendation, or favoring by the University of Saskatchewan. The views and opinions of the author expressed herein do not state or reflect those of the University of Saskatchewan, and shall not be used for advertising or product endorsement purposes.

Requests for permission to copy or to make other uses of materials in this thesis/dissertation in whole or part should be addressed to:

Head of the Department of Biomedical Engineering
University of Saskatchewan
Saskatoon, Saskatchewan, S7N 5A9
Canada

OR

Dean
College of Graduate Studies and Research

University of Saskatchewan
107 Administration Place
Saskatoon, Saskatchewan S7N 5A2
Canada

Abstract

Osteoarthritis (OA) is a painful degenerative joint disease that affects millions of North Americans. OA could be better managed if tissue engineers can develop methods to create long-term mechanically stable engineered articular cartilage tissue substitutes. Many of the tissue engineered cartilage constructs currently available lack the chemical stimuli, cell-friendly environment, and/or mechanical strength needed for use in joint cartilage repair. The goal of my research was to test the efficacy of composite scaffolds comprised of a solid synthetic polymer framework impregnated with a fibrin/alginate hydrogel containing hyaluronic acid (HA) and/or chondroitin sulphate supplements (CS).

The suitability of a polylactic-co-glycolic acid (PLGA) and iron(III) oxide material slurry as the synthetic polymer framework was determined. It was found that a solid three-dimensional scaffold with an interconnected porous structure could be fabricated from this material using dispensing-based rapid prototyping. Moreover, films of the PLGA-iron oxide material supported higher cell populations of porcine chondrocytes compared to a previously reported PLGA-hydroxyapatite material film. In addition, an experiment examining the effects of HA and/or CS macromolecule supplementation on chondrocytes cultured in a fibrin-alginate hydrogel was performed. Chondrocytes cultured in fibrin-alginate hydrogels retained their phenotype better than chondrocytes cultured in monolayer as analysis of expression of type I collagen and type II collagen mRNA transcripts. HA or CS supplementation of the hydrogels increased matrix production during the first week of culture. However, the effects of these supplements on matrix accumulation were not additive and were no longer observed after 2 weeks of culture. Supplementation of the hydrogels with HA and/or CS increased the chondrocyte cell population after two weeks of culture, and the effects of these macromolecule on cell numbers were additive. Finally, composite scaffolds were successfully fabricated by impregnating the solid PLGA-iron oxide scaffold with a CS-supplemented fibrin-alginate hydrogel. However, a large amount of cell death that occurred during the cell seeding prevented quantification of cellular DNA or sulphated GAG accumulation in these composite scaffolds. Nevertheless, my research suggests that, with refinement of the cell seeding process, a CS supplemented fibrin-alginate/PLGA-iron oxide composite may be a superior three-dimensional scaffold system for use in articular cartilage tissue engineering applications.

Acknowledgements

First and foremost, I would like to thank my co-supervisors, Dr. William Kulyk and Dr. Daniel Chen, for their guidance and support throughout my entire M.Sc. degree. Whether it be providing feedback on a problem in the lab, or guiding me through the peer-review process for my first publication, you have both far exceeded my expectations of mentorship. I thank you both and would like you to know that you excelled in your roles as my supervisors.

I would also like to thank the other members of my advisory committee, Dr. David Cooper and Dr. James Johnston. I appreciate your helpful comments throughout my project and eventual thesis submission. In addition, I would like to thank Dr. Cooper for his help with the microtomography portion of my scaffold characterization and Dr. Johnson for his help with my questions on the mechanical testing of cartilage.

To my lab-partner Lindsay Jacobi, I would like to thank you for showing me many of the protocols necessary for the sizeable biological portion of my project. You went above and beyond what I would expect from a fellow M.Sc. student and showed me where everything was and who to talk to in the Department of Anatomy and Cell Biology. I'm sure teaching biological procedures to an engineer was not an easy task and I thank you for taking the time.

I would also like to thank Dr. Ovsenek, Dr. Ziola, and their respective graduate students and technicians for their help with the qPCR portion of this project. In addition, Karen Yuen for showing me how to cryogenically section my samples, Tangyne Berry for teaching me cell culture techniques, and Doug Bitner for processing all of my early purchase orders. Finally, I would like to thank my fellow graduate students in Dr. Chen's research group for their help with the scaffold fabrication portion of this project. These include, Ajay Rajaram, Dr. Minggan Li, Nahshon Bawolin, and Dr. Ning Zhu.

Dedication

To my father Dr. David Little, who has had the patience to edit my writing since grade school without complaint, and has set an example for higher education that helped inspire me to pursue this degree.

Table of Contents

List of Figures

List of Tables

List of Abbreviations

3D	Three-Dimensional
ACT	Autologous Chondrocyte Transplant
ANOVA	Analysis of Variance
BMP	Bone Morphogenetic Protein
CC	Confined Compression
CS	Chondroitin Sulphate
DMEM	Dulbecco's Modified Eagle Medium
DMMB	1,9-Dimethylmethylene Blue
DS	Dynamic Shear
ECM	Extra-Cellular Matrix
ES	Equilibrium Shear
FBS	Fetal Bovine Serum
FGF-2	Fibroblast Growth Factor 2
GAG	Glycosaminoglycans
GAK	0.292 mg/ml glutamine; 100 U/ml penicillin; 100 µg/ml streptomycin, 0.25 µg/ml amphotericin B, 100 µg/ml kanamycin
HA	Hyaluronic Acid
HACS	containing both HA and CS
HAP	Hydroxyapatite
I	Indentation

IO	Iron(III) Oxide
mRNA	messenger RNA
MSC	Mesenchymal Stem Cell
NRT	No Reverse Transcriptase Control
NSERC	Natural Sciences and Engineering Research Council of Canada
NTC	No Template Control
NTMT	100 mM Tris HCl, pH 9.5, 50 mM $MgCl_2$, 100 mM NaCl, 1 mg/ml Triton X-100, 0.5 mg/ml levamisole
OA	Osteoarthritis
PBS	Phosphate Buffered Saline
PBST	Phosphate Buffered Saline with 0.01% Tween 20
PCL	Polycaprolactone
PCR	Polymerase Chain Reaction
PEGT/PBT	Poly(ethylene glycol)-terephthalate-poly(butylene terephthalate)
PG	Proteoglycans
PGA	Polyglycolic acid
PLA	Poly(L-lactide)
PLGA	Poly(D,L-lactide-co-glycolide)
qPCR	Real-Time Quantitative Polymerase Chain Reaction
REST	Relative Expression Software Tool
RH	Relative Humidity

RP	Rapid Prototyping
RV	Representative Volume
SFF	Solid Free Form
SHRF	Saskatchewan Health Research Foundation
TCSR	Tensile Constant Strain Rate
TEC	Tissue-Engineered Construct
TGF-β	Transforming Growth Factor Betas
TSR	Tensile Stress Relaxation
UC	Unconfined Compression

Chapter 1: Introduction

1.1 Adult Articular Cartilage and Osteoarthritis

Adult articular cartilage is a complex, organized tissue made up of numerous components such as collagens, proteoglycans, and chondrocytes. These components work together to form a tissue that can withstand the heavy biomechanical loads normally applied to articular cartilage.

The main component of cartilage is water, which constitutes 70-85% of its total weight. The next most prevalent component is collagen, making up between 60 and 70% of the dry weight[1]. Collagen gives structure and tensile/shear strength to cartilage. The collagen matrix is primarily made up of collagen type II fibrils which have small amounts of collagen types IX and XI associated with them. In addition collagen types I, III, V, VI, XII, and XIV are also present to a much lesser degree[2, 3].

Proteoglycans are also heavily concentrated within the cartilage extra-cellular matrix (ECM), making up approximately 30% of the dry weight[1, 2]. Both non-aggregating and aggregating proteoglycans (PG) are present in cartilage. Aggregating PG are made up of a large number of sulfated glycosaminoglycans (GAG) such as keratan sulfate, chondroitin sulfate, and dermatan sulfate attached laterally to the core protein aggrecan. These aggregating PG are bound to a hyaluronic acid (HA) backbone via Link Protein. Non-aggregating PG, such as decorin or biglycan, consist of a core protein (not aggrecan) with a relatively small number of GAG attached laterally. The GAG interact with the water present in cartilage matrix, providing flow resistance, which results in the cartilage becoming extremely stiff when subjected to impact loading[2].

The aforementioned ECM components almost completely account for the composition of adult hyaline cartilage. The chondrocytes responsible for producing these components make up only approximately 2% of the cartilage's total volume[4]. A population of healthy, differentiated chondrocytes would be expected to produce high levels of collagen type II and aggregating PG. On the other hand, expression of collagen type I (rather than collagen type II) is often interpreted as a marker of chondrocyte de-differentiation, which in this context means a change in cell shape and protein expression.

Osteoarthritis (OA) is a debilitating degenerative joint disease involving the degradation of the articular cartilage at the distal ends of bones. There are two types of OA. Primary OA

describes cases with no identifiable cause. Secondary OA cases are usually the result of acute injury to the articular cartilage[5], whereas primary OA could result from a slow age-related erosion of the joint cartilage associated with a decrease in the tissue's proteoglycan content [6]. Eventually this degraded cartilage leads to bone-on-bone contact, making OA a painful and sometimes debilitating disease, and one that affects the day to day lives of millions of North Americans[7]. Over 50% of people over the age of 65 are affected by OA[8], representing an annual $65 billion dollar burden on the US economy alone, both from medical costs and lost wages[9]. In addition to the monetary costs, there are the emotional costs carried by patients and their families. Therefore, there is much incentive to find a method to regenerate articular cartilage to repair the joints of OA patients.

There are a number of established methods that have been used to repair joints of patients suffering from OA. One method drills to the subchondral bone, releasing mesenchymal stem cells (MSCs) from the bone marrow into the cartilage lesion. The MSCs will form a fibrin clot and will start to proliferate and produce their own ECM[10, 11]. Another method is autologous chondrocyte transplantation (ACT), which has been performed on over 12,000 patients worldwide[12]. In this procedure chondrocytes from a non-load bearing portion of the joint are removed from the patient, expanded in monolayer, and placed in a suspension which is subsequently injected into the cartilage lesion. ACT has problems with donor site morbidity[10], and both ACT and subchondral drilling produce cartilage that is mechanically inferior to the surrounding native cartilage[10, 13].

A promising alternative is cartilage tissue engineering, which is aimed at repairing articular cartilage lesions with artificial cartilage constructs that have mechanical properties similar to those of native cartilage tissue. Tissue engineering in general is an interdisciplinary field combining engineering, biology, and materials science, with the goal of replacing damaged or diseased tissue with artificial tissue substitutes grown in a lab. In most cases, tissue engineers seed a biocompatible three-dimensional (3D) construct called a scaffold with a cell suspension. This scaffold provides initial mechanical support for the cells, as well as providing a micro-environment that supports cell proliferation and a differentiated phenotype. Eventually, the cells produce their own ECM capable of withstanding the biomechanical loads the tissue is subjected to *in-vivo* while the scaffolds biodegrade away, leaving only the engineered tissue. If tissue

engineers succeed in producing a cartilage implant with mechanical properties and composition near those of natural hyaline cartilage, these could be used to effectively fill in cartilage lesions. Filling these lesions with engineered cartilage will be a significantly more effective method of treating OA compared to those used today, such as ACI and prosthetics.

1.2 Brief Introduction to Cartilage Tissue Engineering

1.2.1 Stimulation of Chondrocytes with Macromolecules

A variety of molecules have been used to help chondrocytes increase ECM output, proliferate, and/or maintain their phenotype[2]. For example, different types of transforming growth factor betas [14-17] and bone morphogenetic proteins [15, 18, 19] have been widely used in cartilage tissue engineering. In addition, both fibroblast growth factor 2 (FGF-2) and insulin-like growth factor 1 have also been shown to help chondrocytes maintain their phenotype in traditional monolayer culture conditions[15, 17]. These growth factors are small peptides which interact with receptors on the cell surface which directly affect cytoplasmic protein kinase pathways[20].

HA and chondroitin sulphate (CS) are both components found in natural cartilaginous tissue. It has been shown that the addition of HA to cell medium or hydrogel enhances the production of GAG and collagen type II, as well as significantly increasing cell proliferation[21, 22]. In addition, chondroitin sulphate has been shown to increase cell proliferation and PG synthesis[23, 24]. Both HA and CS are much larger than the aforementioned growth factors and are known as macromolecules. These macromolecules also interact with receptors on the surfaces, which are in turn associated with the cells' cytoskeleton. This stimulation of the cytoskeleton will ultimately also lead to downstream effects on cytoplasmic protein pathways[20].

While the effects of HA and CS on chondrocytes have been studied previously, there has been no investigation to determine if the effects of these molecules on chondrocyte proliferation and matrix synthesis is additive or not. If these molecules have additive effects or interact synergistically with one another, it may be worth the extra expense of adding both of them to engineered cartilage cultures before implantation. On the other hand, if they interfere with one

another supplementing the cartilage cultures with both molecules may actually result in less desirable chondrocyte behaviour than if one just supplemented with CS or HA on their own.

1.2.2 Hydrogels

A hydrogel is a water swollen polymer network which can be used for drug delivery or as a 3D matrix to support cellular growth and differentiation. Typically, hydrogels exist as viscous liquids unless the cross-linking process is performed to cause polymerization. Different cross-linking methods include: chemical cross-linking[25], photopolymerization[26], and enzymatic cross-linking[27]. These hydrogels can take the shape of any mould they are polymerized in, making them potential candidates for injectable tissue-engineered constructs (TEC).

A number of materials have been used as hydrogels in cartilage tissue engineering, and Table 1 summarizes the common hydrogels reported in the literature. Both alginate and agarose are polysaccharides that are extracted from brown and red algae, respectively. Chitosan is fabricated by the deacetylation of chitin, which is a naturally derived polysaccharide from arthropod exoskeletons[28]. Finally, fibrinogen, which is found naturally within mammalian blood and cleaved by thrombin into fibrin during blood coagulation can also function as a hydrogel[29].

Table 1. Various biomaterials used in hydrogels for cartilaginous TECs. Almost all hydrogel materials are some form of biologically-derived polymer and have low mechanical properties.

Biomaterial	Natural or Synthetic	References
Hydrogels		
Alginate	Natural	[21, 25, 30-32]
Agarose	Natural	[33-35]
Collagen	Natural	[36-38]
Hyaluronic Acid	Natural	[21, 37, 39]
Fibrin Glue	Natural	[16, 40]
Gelatin	Natural	[39]
Chondroitin Sulfate	Natural	[26, 39]
Poly(vinyl alcohol)	Synthetic	[26]
Chitosan	Natural	[41]

Notably, fibrin has numerous advantages over many of the other hydrogels listed in Table 1. It has been shown that fibrin supports higher cell proliferation than alginate[42]. In addition, as it is naturally found in the body, fibrin can decrease the chance of an immune response[29]. It also has cell adhesion capabilities through its linkage to the integrin receptor[43], and will

biodegrade unlike alginate[42]. The use of fibrin in cell scaffolds has been shown to help retain macromolecules within the hydrogel[43] thus stimulating chondrocyte activity. However, the rapid degradation rate of fibrin can cause chondrocytes to de-differentiate[44]. This rapid degradation can be slowed by the addition of more stable hydrogels such as alginate[42], or the addition of macromolecules like HA[45].

Given the long-term stability and biocompatibility of a fibrin-alginate hydrogel, it is ideal for 3D cell culture and as such could be used to support cells while investigating the effects of macromolecule supplementation (Section 1.2.1).

1.2.3 Scaffolds and their Fabrication

Like hydrogels, there are numerous different types of polymers that have been used to create solid scaffolds, as shown in Table 2. There are a number of different fabrication methods used to form these polymers into scaffolds. Some of these methods include porogen leaching[36], freeze-drying[36, 39], electrospinning[46], and rapid-prototyping (RP) methods[16, 47, 48]. Unlike the other types of scaffold fabrication, RP allows for accurate control over pore-size and orientation, which can be created reproducibly.

Table 2. Various synthetic polymers used to create solid tissue engineering scaffolds.

Biomaterial	Natural or Synthetic	References
Solid Polymers		
Poly(L-lactide) (PLA)	Synthetic	[49]
Poly(ethylene glycol)-terephthalate-poly(butylene terephthalate) (PEGT/PBT)	Synthetic	[50]
Poly(propylene fumarate) (PPF)	Synthetic	[37]
Polyurethane	Synthetic	[40]
Polyethyleneoxide-terephtalate/ polybutylene-terephtelate (PEOT/PBT)	Synthetic	[51]
Poly(D,L-lactide-co-glycolide) (PLGA)	Synthetic	[36, 39, 52]
Polyglycolic acid (PGA)	Synthetic	[52]
Polycaprolactone (PCL)	Synthetic	[16]

The RP technique currently being used at the University of Saskatchewan for tissue engineering is one based on dispensing[53], in which scaffolds are created by extruding a polymer through and then out a needle, as shown in Figure 1. The material extruded is either

molten[47] or in a material slurry[48]. Materials that have been used in this fabrication process include PEGT/PBT[50], PCL[54], PLA[48, 54], and PLGA[54, 55]. Of these materials, PLGA has some distinct advantages over the rest. First, PEGT/PBT requires high temperatures[47] (not currently achievable at the U of S) to extrude it, while PLGA, PCL and PLA are usually mixed with a solvent such as chloroform, and a non-soluble nano-sized particle to create a material slurry[48, 54, 55]. PCL degrades very slowly, taking more than three years as opposed to the months that it takes for PLA and PLGA to degrade[56]. Finally, PLGA and its copolymers PLA and PGA have been widely used in cartilage tissue engineering[52, 55, 57-60] and as dissolvable clinical sutures[61]. By varying the copolymer concentrations in PLGA, the mechanical and degradation properties can be more finely tuned than if one used PLA or PGA alone[56].

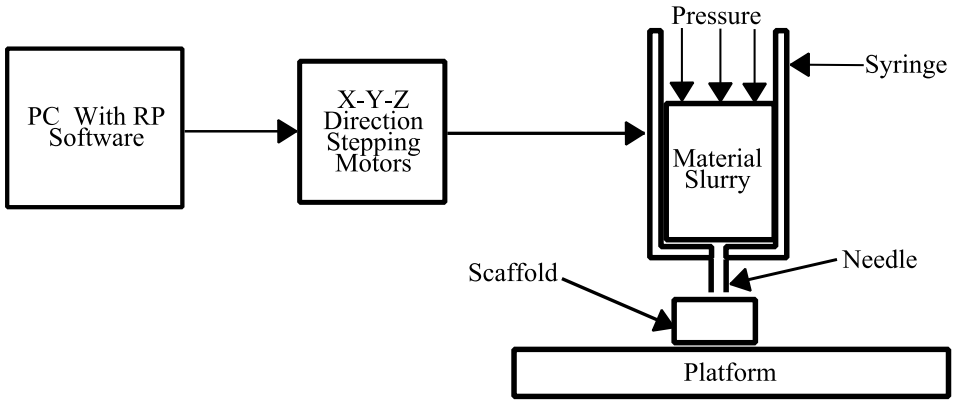

Figure 1. Schematic showing the dispensing-based RP technique. The computer controls the stepping motors to move the syringe in a pre-programmed path as the scaffold material is extruded through the needle. The layers are sequentially deposited on top of one another to create a 3D construct.

The purpose of the aforementioned non-soluble nano-sized particles in the material slurry is to adjust the consistency such that overhanging structures (i.e. interconnected pores) can be created during RP. Hydroxyapatite (HAP) has previously been used as the micro-sized particle in bone tissue engineering applications[48, 55, 62, 63]. However, the fact that HAP is found in bone rather than hyaline cartilage raises the concern that it might cause chondrocytes to de-differentiate. A promising alternative to HAP is the use of iron oxide nanoparticles, which have extremely low solubility at physiological pH[64], no cytotoxic effects[65], no effect on chondrocyte phenotype[66]. As such, they have been approved by the FDA as an MRI contrast agent[67].

The proven suitability of PLGA in cartilage tissue engineering and the biocompatibility of iron oxide particles suggest that a slurry comprised of these two materials could be used to create a solid scaffold capable of providing mechanical support to a 3D chondrocyte culture.

Several strategies for combining the mechanical stability of a solid scaffold with the cell-friendly environment of a hydrogel have been tested during the past ten years. Compared to solid scaffolds alone, it has been shown that these composite scaffolds are more successful at growing cartilaginous tissue. For example, GAG[31, 40, 57, 59] and collagen type II[31, 68] production per cell is higher in composite scaffolds. In addition, cell proliferation in composite scaffolds is significantly higher than in solid scaffold controls, but not significantly different than in hydrogels alone[40].

Commonly, the composite scaffolds found in the literature use a fibrin hydrogel[40, 57, 68, 69]. As mentioned in section 1.2.2, it has been shown that fibrin alone will rapidly degrade leading to chondrocyte de-differentiation. Based on the properties of alginate it would be beneficial to use a fibrin-alginate mixture[42] to improve the composite scaffolds by enhancing the longevity of the hydrogel component. In addition, there exists a void in the literature regarding a solid scaffold material used for cartilaginous composite scaffolds that can be deposited as a material slurry rather than a high temperature melt.

These solid scaffolds should greatly enhance the mechanical properties of the TEC. However, there has been little work done to determine the mechanical properties of these composite scaffolds. In fact, one of the few examples of mechanical testing of these scaffolds fails to examine widely reported cartilage properties such as aggregate modulus and hydraulic permeability[59], which would be of importance to cartilage tissue engineering.

1.3 Research Goal and Objectives

It is hypothesized that for the reasons postulated in Section 1.2.3, chloroform-solubilised PLGA mixed with iron oxide nanoparticles can prove a suitable material for the solid scaffold component of composite scaffolds. The goal of this research is to fabricate composite scaffolds from the above material impregnated with a macromolecule-supplemented fibrin/alginate hydrogel and to characterize them in terms of chondrocyte phenotype retention and proliferation

as compared to PLGA and iron oxide solid scaffold alone. To achieve this goal, the following specific objectives are proposed:

1. Fabricate scaffolds from a material slurry comprised of PLGA and iron oxide and characterize them by
    a. performing a microtomography examination of the solid scaffolds to determine the actual average pore size and ensure the consistency of the internal overhanging structures (i.e. interconnected pores) and,
    b. culturing primary chondrocytes on this material and comparing cell survivability to that of a similar material that uses HAP as the micro-sized particle, and a conventional tissue culture plate.
2. To identify the combination of CS and HA that best stimulates chondrocyte activity, as determined by
    a. the amount of PG, collagen types I and II produced and expressed as mRNA and,
    b. the amount of cell proliferation and PG matrix accumulation.
3. Perform a preliminary experiment showing that chondrocytes can be cultured within the composite scaffolds by
    a. measuring PG production and cell population and,
    b. comparing these measurements to solid scaffold controls

1.4 Organization of this Thesis

This thesis is organized into five separate chapters: Introduction; Mechanical Properties of Natural Cartilage and Tissue-Engineered Constructs; Materials and Methods; Results; and General Discussion. These chapters are followed by a References section which lists all cited sources.

Chapter 2 is a publication which was accepted by *Tissue Engineering Part B: Reviews* in early 2011. A description of the relevance of this manuscript to the project as a whole is briefly

outlined at the beginning of the Chapter. Chapter 3 outlines the methodology used during all experimental work reported in this thesis and Chapter 4 presents the results from said experiments. Finally, the discussion in Chapter 5 examines these results and compares them to previously reported findings. In addition, it draws come conclusions about the import of this work and makes some suggestions for future experiments which could help clarify some of the observed relationships.

Chapter 2: Mechanical Properties of Natural Cartilage and Tissue-Engineered Constructs

2.1 Relevance of this Manuscript within the General Project

As mentioned in Section 1.2.3, one of the primary benefits of using composite scaffolds compared to a hydrogel is the mechanical robustness of the solid scaffold. As such, it will be of great importance to characterize the mechanical properties of these composite scaffolds and compare them to the mechanical properties of natural articular cartilage.

Due to the importance of this mechanical characterization, it was initially included as a part of this Master's project. As such, an extensive literature review was performed on both the mechanical properties of natural cartilage and TECs and the mechanical tests used to ascertain these properties. This literature review has led to a paper[70] published in August of 2011 in *Tissue Engineering Part B: Reviews*, a leading journal in the field with an impact factor of 4.636. It is reprinted as a chapter in this thesis with permission from Mary Anne Liebert, Inc. It is noted that this paper is co-authored and that it is the mutual understanding of all authors that Chris Little, as the first author, made primary contribution to its publication. The contributions of the other authors are acknowledged.

As a further note, due to the fact that the work presented in other chapters in this thesis is sufficient for a Master's project, the mechanical testing potion of the project was not pursued, as approved by the Advisory Committee. Testing the mechanical properties of scaffolds is crucial to the success of cartilage tissue engineering applications and as such the aforementioned review paper is included to aid future researchers or students who will build on the work presented in this thesis.

2.2 Manuscript

2.2.1 Abstract

There has been much research over the past two decades with the aim of engineering cartilage constructs for repairing or restoring damaged cartilage. To engineer healthy neocartilage, the constructs must have mechanical properties matching those of native cartilage as well as appropriate for the loading conditions of the joint. This paper discusses the mechanical behaviour of native cartilage and surveys different types of tensile, compressive, and shear tests with their limitations. It also comprehensively reviews recent work and achievements in developing the mathematical models representing the mechanical properties of both native and engineered cartilage. Different methods for enhancing the mechanical properties of engineered cartilage are also discussed, including scaffold design, mechanical stimulation, and chemical stimulation. This paper concludes with recommendations for future research aimed at achieving engineered cartilage with mechanical properties matching those found in native cartilage.

2.2.2 Introduction

Osteoarthritis (OA) is a degenerative joint disease characterized by progressive erosion of the articular cartilage that covers the distal surfaces of bones. Because articular cartilage is responsible for cushioning compressive forces in the joint, its destruction leads to joint pain, stiffness, and impaired mobility. Currently, OA afflicts the daily life of millions of Americans [7] whose articular cartilage has been damaged either through trauma or the effects of aging [5]. In addition to the emotional costs carried by patients and families dealing with this disability those, who suffer from this disease represent a large burden on both the economy and the health care system, as lost wages and medical costs related to OA are estimated to be as much as $65 billion in the US alone [9]. Therefore, it is desirable to develop technologies that would allow for regeneration of damaged articular cartilage.

Tissue engineering aims to replace damaged tissues with artificial tissues grown in the controlled laboratory environment. For this, three-dimensional (3D) constructs, or scaffolds, are created from biocompatible and biodegradable materials and then seeded with cells such as chondrocytes. The scaffold provides cells with a 3D structure and mechanical support for their attachment and proliferation, ultimately growing into a functional tissue engineering construct (TEC). The TEC is then implanted into a patient and, with time, hopefully integrates itself with the surrounding natural cartilage. Eventually, the cells will secrete their own extra-cellular matrix (ECM) that is able to withstand the mechanical forces seen in the joints, while the scaffold biodegrades. In this healing process, a crucial role is played by the mechanical properties of the TEC, which, ideally, must match those of native cartilage. Considerable progress has been made in the past two decades to fulfill the requirement of mechanical properties imposed on the TEC as applied to the repair of damaged cartilage. This paper aims to review this progress with emphasis on the different mechanical testing procedures, mathematical representations or models of the mechanical properties of cartilage and TECs, and methods to enhance the mechanical properties of TECs. The challenges in these aspects are also discussed, along with the recommendations for future research aimed at achieving the desired mechanical properties of TECs for cartilage tissue engineering applications.

2.2.3 Cartilage Structure and Response to Mechanical Forces

2.2.3.1 Organization and Composition of Adult Articular Cartilage

Articular cartilage is an organized tissue composed mainly of water, collagens, proteoglycans, and chondrocytes. These components interact with one another to give cartilage the strength to withstand the mechanical forces or loads it experiences. Water, the most prevalent component, accounts for 70-85% of the total weight of articular cartilage; next is collagen, which makes up between 60 and 70% of the cartilage's dry weight [1]. Collagen type II makes up most of the collagen matrix, in addition to types I, III, V, VI, IX, XI, XII, and XIV to lesser degrees [3]. The third most prevalent component of articular cartilage, comprising approximately 30% of the dry weight is proteoglycans, which are made up of a number of sulfated glycosaminoglycans (GAGs) on a hyaluronic acid (HA) backbone [2]. The water, collagen, and proteoglycans together are referred to as the ECM of the tissue. Chondrocytes are responsible for producing and assembling the ECM components but only make up 2% of the volume of adult articular cartilage [4].

There is a large amount of zonal variation in the composition and orientation of the ECM components of articular cartilage. Adult articular cartilage can be divided into four separate zones, i.e., the superficial zone, middle zone, deep zone, and calcified cartilage (Figure 2) [71]. The chondrocyte concentration is at its highest within the superficial zone [50], where the collagen fibrils run parallel to one another and the articular surface [71]. This collagen fibril arrangement gives the superficial zone the highest strength among the four zones [72], allowing the cartilage to withstand the mechanical forces (e.g. shear, compressive stress, tensile stress) experienced at the surface. In addition, while the concentration of aggregating proteoglycans is lowest in the superficial zone, smaller non-aggregating proteoglycans such as biglycan and decorin are most concentrated here[2].

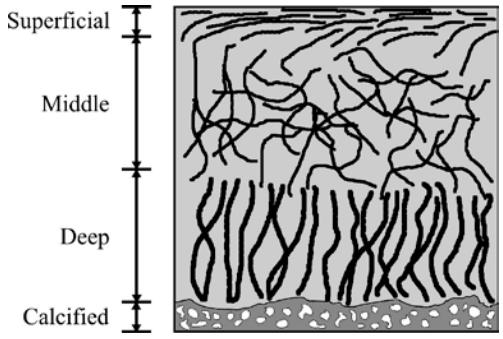

Figure 2. Zonal organization of hyaline cartilage, showing the superficial, middle, deep, and calcified cartilage zones. The dark lines represent the collagen fibrils which are thick and oriented vertically in the deep zone, randomly oriented in the middle zone, and oriented tangent to the surface in the superficial zone.

The middle zone is rich in proteoglycans and contains larger collagen fibrils in a more random arrangement [50]. In the deep zone, the chondrocyte concentration is low and the proteoglycan (PG) concentration and collagen fibril diameter are at a maximum [50, 71]. The high collagen and PG concentration makes the deep zone the most resistant to compressive forces [73]. Next to the subchondral bone, the cartilage becomes mineralized, forming calcified cartilage, that has mechanical properties between the cartilage zones above and the bone below and which provides a good transition between the two [71].

2.2.3.2 Cartilage Responses to Mechanical Forces

Two distinct mechanisms respond to the forces applied to cartilage: the resistance to interstitial fluid (water) flow through the ECM, and deformations of the ECM[74]. As mechanical forces are applied to the cartilage, a pressure gradient is generated in the interstitial fluid, causing fluid flow through the pores within the ECM. Because the pore size is small, fluid flow through them, referred to as the hydraulic permeability, is limited and therefore, causes significant flow resistance [75]. Moreover, the interaction between the negatively charged GAGs and the polar water molecules further limits fluid flow through the ECM pores [2]. This interaction combined with the hydraulic pressure gradient withstands as much as 95% of the mechanical force applied to the cartilage, the remaining 5% is achieved by ECM deformation [74]. This early fluid pressurization reduces the coefficient of friction between the articulating surfaces [76]. In healthy cartilage, the hydraulic permeability of the superficial zone is low and the pressures in the interstitial water in the deep and middle zones are relatively high [77]. These high internal pressures protect the ECM from most of the biomechanical loading. If these forces

are transmitted through the solid ECM, it may lead to cartilage degeneration [78], thus the variability of hydraulic permeability between patients may explain why some are more prone to joint diseases than others [79].

Interstitial water flow through the ECM gives rise to some time-dependent articular cartilage responses [80]. One of these is the displacement response of cartilage to a constant load applied over time, referred to as creep. For example, a creep response following an instantaneous elastic deformation may take approximately 1000 seconds to reach a new equilibrium state [80]. Another response is stress relaxation, which is the force response to a ramped displacement input. The cartilage requires time to react to the applied load or displacement and reach an equilibrium state (Figure 3). Notably, as the ECM deformation increases, the average ECM pore size decreases, which consequently increases the diffusional drag between the interstitial water and the ECM [81]. As a result, the time to reach the equilibrium state varies depending on the load/displacement applied.

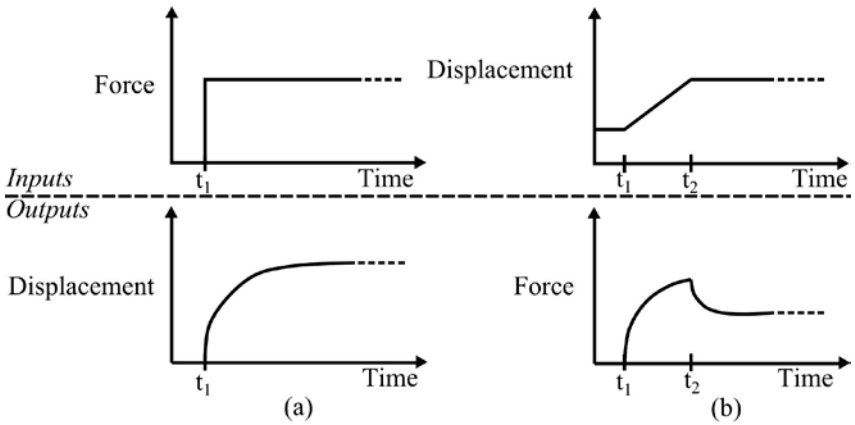

Figure 3. Time-dependent responses of cartilage to (a) a constant load and (b) a ramped displacement. The response in (a) is known as creep, and the response in (b) is stress relaxation.

Measuring and characterizing the aforementioned time-dependent or transient responses of native cartilage or ECM, especially in an *in-vivo* environment, is both complex and difficult and the development of scientific instruments and tools for this purpose faces significant challenges. The mechanical properties of native cartilage or ECM have typically been measured once equilibrium is reached. The equilibrium or time-independent properties of cartilage or ECM include the aggregate modulus, Young's modulus, shear modulus, and Poisson's ratio [82], these are discussed in the following section, along with typical testing methods and procedures. To characterize the time-dependent responses or properties of cartilage or ECM, one promising

alternative to experimental measurements is the use of mathematical models, which are presented below in the mathematical modeling section.

2.2.4 Mechanical Properties of Natural Cartilage and TECs and Testing Methods

Three major methods for determining the mechanical properties of articular cartilage and TECs are tensile, compressive, and shear testing. Tensile testing is typically conducted either at equilibrium after a force is applied or at a constant strain rate. The compressive mechanical properties are often measured in three ways: confined compression, indentation, and unconfined compression, Shear properties are normally measured using either a constant displacement to find the equilibrium properties or a sinusoidal displacement to determine the dynamic properties.

To find the tensile equilibrium modulus, a strip of cartilage is subjected to a stress relaxation test (Figure 4). This procedure subjects the sample to a stepwise series of displacements: at each displacement step, the stress in the cartilage is measured once it reaches its equilibrium value [83, 84]. The equilibrium stress at each step is then plotted as a function of strain, with the slope giving the tensile equilibrium modulus.

In constant strain rate tensile testing, the sample is subjected to a constant strain rate and the tensile stress is measured at a certain sampling rate. The stress-strain plot of this test reveals a non-linear “toe-in” region where the collagen bundles are straightening out. Once the bundles are all straightened, the plot enters a near linear region that represents the stretching of these bundles: the data from this linear region can be used to calculate the tensile Young’s modulus [82, 84, 85]. Samples used in the tensile tests are typically cut in a dumbbell shape with a thickness of 200-300 μm, and strained at a rate of 5mm/min [84-88]. Depending on the specimen, the stress-strain curves obtained either at equilibrium or under a constant rate of strain may not be linear (Figure 5a), suggesting that the modulus is not a constant, but a function of strain or stress (Figure 5b) [88, 89].

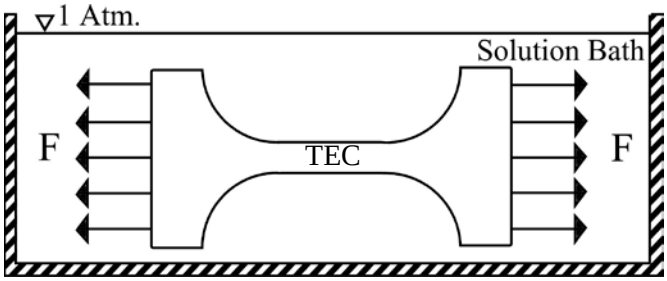

Figure 4. Schematic of the tensile testing apparatus, in which a TEC sample is submerged in a solution (usually phosphate buffered saline (PBS)) and subjected to either a tensile force or a tensile strain rate. Both strain and force (stress) are simultaneously measured and plotted against one another.

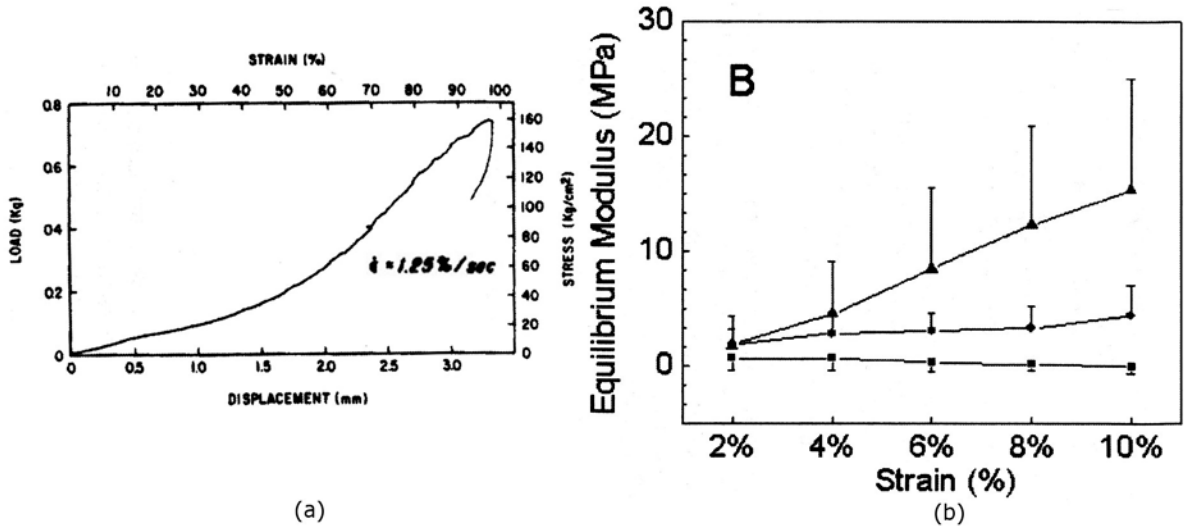

Figure 5. Examples of tensile testing data for (a) a constant strain rate test (reprinted from [88] with permission from ASME) and (b) the relationship between equilibrium modulus and strain (reprinted from [89] with permission from Elsevier). In (b) the top line (triangles) represents adult, middle line (circles) represents adolescent, and bottom line (squares) represents young cartilage.

Confined compression tests are typically pursued to measure properties such as the hydraulic permeability and the aggregate (equilibrium) modulus of cartilage samples outside of the body (*ex vivo* testing) [90-93]. Confined compression places a cylindrical cartilage sample into a tube-shaped container with an inner diameter that is ideally the same as the diameter of the sample, to prevent lateral expansion (Figure 6a) [82]. The test subjects the cartilage to a step load and measures displacement as a function of time (creep) (Figure 2a) or a short ramp displacement with stress measured as a function of time (stress-relaxation) (Figure 2b, Figure 7a). The equilibrium displacement/stress is a function of the cartilage's aggregate modulus[90]. The time it takes for the cartilage to reach the equilibrium displacement/stress is a function of its hydraulic permeability, aggregate modulus, and specimen thickness. A number of factors may

affect the measured mechanical properties in these compression tests. First, the cartilage or TEC samples may not conform exactly to the inner diameter of the confined compression chamber, which results in an initial non-linearity [80, 91]. Next, the use of a porous piston can increase the tissue resistance during compression, which causes the measured material properties to be different from the true ones [80, 91]. The friction between the sample and the chamber has also been shown to affect measurements[94].

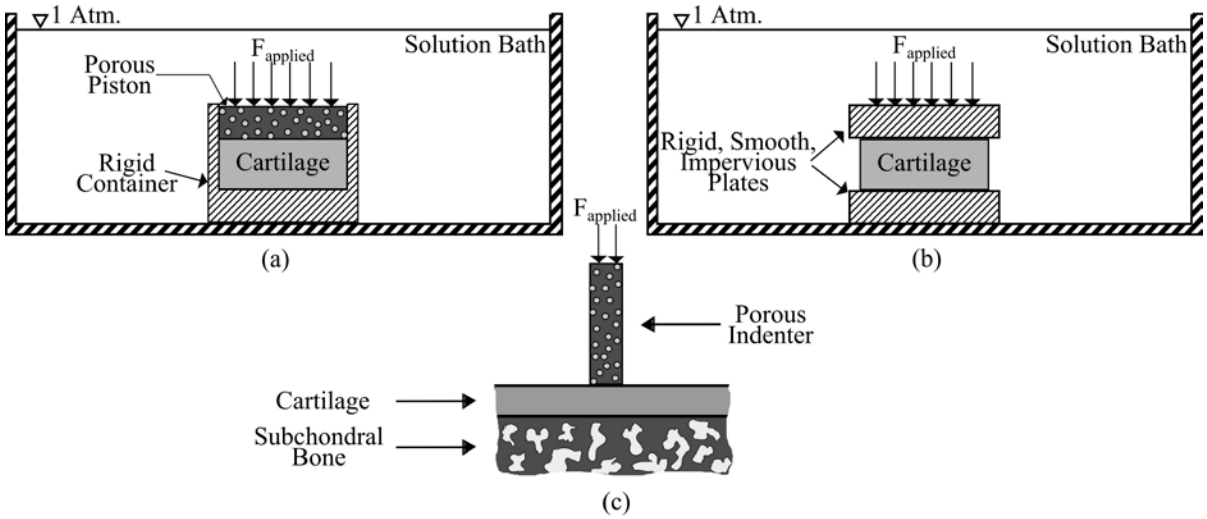

Figure 6. Schematic of types of compressive tests: (a) confined, (b) unconfined, and (c) indentation. Samples in confined compression are constrained on the sides. Unconfined samples are not constrained on the sides. Indentation uses a porous indenter to displace the cartilage, which is measured *in situ*.

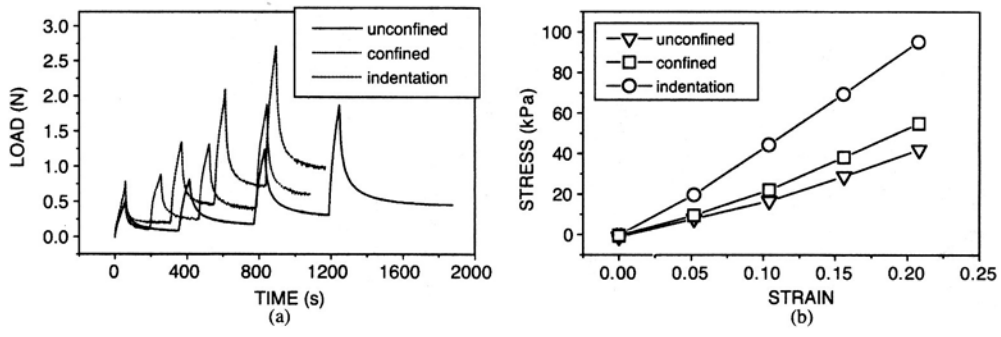

Figure 7. Examples of compression testing data: Data(a) stress-relaxation test of cartilage and (b) stress-strain plot by using the confined, unconfined, and indentation testing methods (reprinted from [95] with permission from Elsevier). In (a) the top line is indentation, the middle line is confined, and the bottom line represents unconfined compression.

Another commonly used compression test is indentation [82, 96, 97]. The indentation test (Figure 6c) is performed with the cartilage still attached to the bone (*in situ*), which suggests that this method has the potential to be used on living models. In this test, a porous indenter is used to

apply a step load to the cartilage and the displacement is measured as a function of time. An *a priori* model [97] is then used to fit the displacement vs. time data by using the non-linear least squares method. By doing so, parameters such as the aggregate modulus, hydraulic permeability, and Poisson's ratio can be identified or estimated [82]. However, a number of assumptions in the indentation test may not reflect reality; the porous indenter may increase tissue resistance, cartilage permeability is not constant, and cartilage is not homogenous or isotropic.

Prior to the biphasic theory developed by Mow *et al.* in 1980 [80], an elastic model was used for fitting the data obtained in the indentation tests [97] in which an approximation of the Poisson's ratio was used to determine the aggregate modulus and hydraulic permeability. Later results from the use of biphasic theory show that the imperfection of Poisson's ratio can result in data off by as much as 200% [97], suggesting that values of the aggregate modulus and hydraulic permeability from these earlier studies should be viewed with caution.

Unconfined compression tests have not been as widely used as the indentation and confined compression tests [82]. In unconfined tests (Figure 6b), the cartilage is ideally compressed between two perfectly smooth, rigid, and impervious plates. However, this condition is nearly impossible, due to suction between the sample and the plates, that causes shear stress [98]. This suction effect can be reduced by applying a lubricant, such as synovial fluid, to the plates [95]. Similar to the other two types of compression tests, the sample is subjected to a step force, while the displacement is measured as a function of time. Hydraulic permeability can be measured and characterized similar to confined compression, with interstitial water flowing along the radial direction [98]. Once the sample reaches equilibrium, the compressive Young's modulus and Poisson's ratio of the ECM can be measured and determined [98].

In shear testing, a cylindrical sample of cartilage is subjected to a torsional displacement. For small torsional displacements, both the change in the sample volume and the pressure-driven fluid flow within the cartilage can be ignored, which allows for measurement of the viscoelastic properties of the ECM [99]. In the equilibrium shear test, the sample is subjected to a sudden constant displacement and the shear stress is allowed to reach an equilibrium value. Again, because of the lack of fluid flow, this equilibrium is reached much more quickly (10 s [82]) than in tensile and compressive tests (1000 s [80]). This test gives the normalized stress relaxation function, which is a ratio of the instantaneous shear stress to the initial shear stress at $t = 0^+$: this

is used in the theory of quasilinear viscoelasticity, as described in the mathematical modeling section below, to determine the stresses present in the cartilage as a function of time for a given strain history [82, 100]. If the sample is subjected to a series of displacements, this test is used to determine the equilibrium shear modulus which is generally determined by calculating the slope of the equilibrium stress/strain plot (Figure 8a). While the stress-strain data are highly linear for shear strains of 0.03 and above, they may be better modelled by a quadratic relationship at lower values [101].

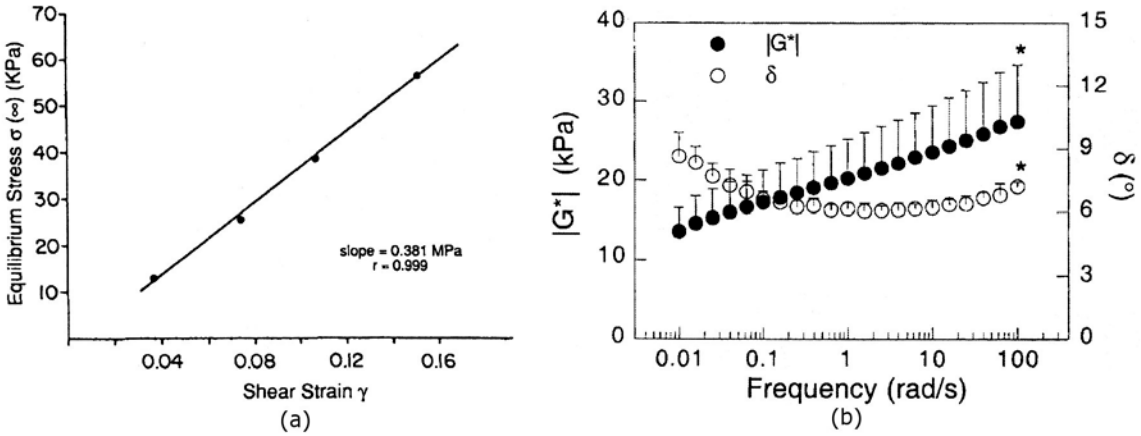

Figure 8. Plots showing (a) the dependence of equilibrium stress on strain in articular cartilage (reprinted from [101] with permission from Wiley) and, (b) the dependence of complex shear modulus and loss angle of alginate on forcing frequency (reprinted from [102] with permission from Wiley).

The complex (dynamic) shear modulus characterizes the overall stiffness of the ECM under shear stress. This parameter can be measured by subjecting the sample to a sinusoidal strain small enough that fluid flow is not generated (0.00003 – 0.005) [99, 103, 104]. The complex shear modulus has a real portion (i.e., the storage modulus) and an imaginary portion (i.e., the loss modulus) (Figure 9) [99]. The storage modulus is in phase with the sinusoidal displacement and proportional to the amount of strain energy stored in the ECM. The loss modulus, on the other hand, is 90° out of phase with the displacement and proportional to the amount of strain energy dissipated in each cycle. The complex shear modulus is a more appropriate representation of the shear properties actually seen during dynamic activities such as running and walking [99]. Importantly, the complex shear modulus is a frequency-dependent measurement (Figure 8b), with values of the shear modulus typically reported for given frequencies in a range of 0.01-100 rad/s [102, 104, 105].

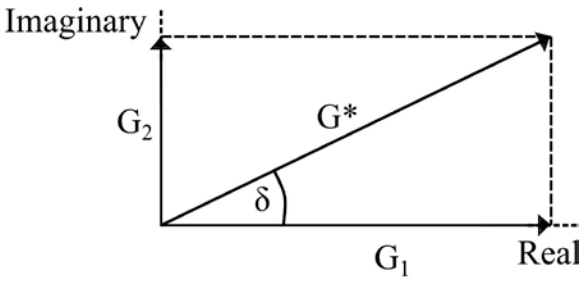

Figure 9. Relationships among the storage modulus (G_1), loss modulus (G_2), complex shear modulus(G*), and loss angle (δ). The storage modulus represents the elastic portion of the modulus, while the loss modulus represents the modulus fraction due to viscous dissipation.

The loss angle (Figure 9) describes how much of the complex modulus is due to the loss modulus and how much is due to the storage modulus. A loss angle of 90° would describe a completely viscous material, whereas a fully elastic material would have a loss angle of 0°. Materials mainly composed of collagen have a loss angle of about 3.6° [82], suggesting that collagen behaves in a very elastic manner. PG-rich materials, on the other hand, have a loss angle of approximately 70° [106], suggesting that the proteoglycans are largely responsible for the viscous portion of the complex shear modulus of cartilage. Articular cartilage has a loss angle of approximately 15°[81], suggesting that the elastic collagen network provides most of the shear stiffness of ECM.

In the tests described above, choosing appropriate testing conditions such as the force and strain-rate applied to the sample, is critical, as is determining when the sample has reached equilibrium. These conditions and the equilibrium time will significantly affect the measured material properties [89]. In the literature, the equilibrium criteria are usually defined at specific times [101, 104] or stress-rates [95, 107], and thus vary from one study to another. It has been argued [89] that in most of the tests reported in the literature, equilibrium has not actually been achieved. Moreover, a higher strain rate can lead to a higher tensile modulus and an excessively large shear strain may drive fluid flow through the ECM, thus increasing the apparent shear modulii. Therefore, experimental designs based on these testing methods should bear the above in mind and involve a rigorous choice of test parameters.

In addition, the type of test chosen may influence the properties measured. The indentation test yields a higher Young's modulus than the confined and unconfined compression tests, possibly be due to the fibrous structure of the tissue being damaged from the sample

extraction process in confined/unconfined compression [95]. On the other hand, some material parameters, such as Poisson's ratio appear to be independent of the test method used [108].

By means of the aforementioned methods, the mechanical properties of articular cartilage and TECs have been extensively investigated. Typical values of the measured mechanical properties are summarized in Table 3. For most entries, values are given within a range; this is due to the variation in the mechanical properties in different joint locations [97], donor species, and donor ages [84].

Table 3. Summary of the mechanical properties of native articular cartilage and TECs as well as the tests used to ascertain each property (CC=Confined Compression, UC = Unconfined Compression, I = Indentation, TSR = Tensile Stress Relaxation, TCSR = Tensile Constant Strain Rate, ES = Equilibrium Shear, DS = Dynamic Shear).

Mechanical Property	Description	Value	Mechanical Test	Native Cartilage	TECs
Aggregate modulus (MPa)	Equilibrium compressive stiffness of cartilage constrained at the sides	0.1-2.0	CC, I	[74, 80, 108, 109]	[51, 110]
Hydraulic permeability (m^4/Ns)	Ease by which interstitial water moves through the solid ECM	10^{-16}-10^{-15}	CC, UC, I	[1, 97]	
Compressive Young's modulus (MPa)	Equilibrium stiffness of cartilage unconstrained at the sides	0.24-0.85	UC	[74, 97, 108]	[26]
Poisson's ratio	Ratio of lateral strain to strain along the stress direction & a measure of the compressibility of pores in the ECM	0.06-0.3	UC, I	[51, 74, 108, 111]	[51, 110]
Tensile Equilibrium Modulus (MPa)	Tensile stiffness of cartilage at equilibrium, usually along the articular surface	5-12	TSR	[83]	
Tensile Young's Modulus (MPa) – constant-strain-rate	Tensile stiffness of cartilage when subjected to a constant-strain-rate, usually along the articular surface	5-25	TCSR	[74, 84, 87]	
Tensile strength (MPa)	Maximum amount of tensile stress endured by cartilage before rupturing, usually along the articular surface	0.8-25	TCSR	[72]	
Equilibrium shear modulus (MPa)	Measure of the shear stiffness of solid ECM after all viscous ECM effects have subsided	0.05-0.4	ES	[101, 104]	
Complex shear modulus (MPa)	Apparent stiffness of ECM which includes both viscous and elastic effects	0.2-2.5	DS	[82, 103, 104, 112]	
Shear loss angle (deg.)	Measurement of how much of the complex shear modulus is due to viscous effects	10-15	DS	[51, 82, 104, 112]	

Mechanical properties, such as the equilibrium shear modulus, Poisson's ratio, and aggregate modulus vary significantly for different joint locations [82, 104, 111, 113]. Some recent research shows that mechanical properties even differ significantly between surfaces that articulate against one another [84]. This mechanical discrepancy between articulating surfaces may contribute to cartilage degradation [113]. Notably, some properties, such as the tensile Young's modulus, are very sensitive to the anisotropies present in the cartilage. In one study [72], the tensile Young's modulus depended not only on the zone from which the sample was taken from but also on the orientation of the sample. For example, a sample taken parallel to the split line[1] leads to a higher Young's modulus than a sample taken perpendicular to the split line. Furthermore, a sample taken from the deep or middle zone has a lower tensile modulus than one from the superficial zone. In addition to joint location, orientation, and depth, donor species also affects the measured mechanical properties. An examination of cartilage samples from human, bovine, canine, monkey, and rabbit donors indicates the hydraulic permeability and Poisson's ratio are significantly different, but the aggregate modulus is quite similar[114]. Finally, donor age will affect the measured properties, which tend to increase into adulthood, and then decrease with old age [72, 84, 85, 89, 90].

2.2.5 Modeling of the Mechanical Properties of Cartilage and TECs

An emerging method that may provide an alternative to mechanical testing of cartilage tissue and TECs is mathematical modelling. The primary advantage of mathematical modelling over experimental methods in TEC design is their ability, once validated by experiments, to predict the behaviour of candidate TEC designs. This allows the optimum design to be identified without the need for extensive experimental investigations. Another unique advantage of mathematical models is that they can be developed and used to derive or estimate the mechanical properties of individual material phases within the cartilage based on the measured bulk behaviour. The progression of many diseases of cartilage results in the changes in mechanical properties [115]. As such, a sequential examination of this change can provide information on the progression of the disease and may lead to the identification of the primary mechanisms of

[1] The split lines mentioned above are presumed to be indicators of the direction of the collagen fibres in the superficial layer[74] and can be determined by puncturing the cartilage with a circular awl. The resulting holes are "stretched out," or elliptical, and the major axis of the ellipse is known as the split line direction[99].

age-related cartilage degeneration. Experimental methods, however, only give the bulk or average properties of the cartilage, rather than the specific mechanical properties of local tissues. One possible experimental approach to this problem is the use of histology combined with micro- and even nano-indentation to measure the 3D distribution of mechanical properties in the tissue. However, in addition the problems of cutting-induced deformation from this approach, even nano-indentation may be unable to directly measure the properties of the individual phases within the cartilage tissue. Another way to estimate the properties of the individual phases within tissue would be to measure of the bulk properties of the tissue at specific locations, and then from these measurements derive the mechanical properties of each individual material phase within the tissue from a mathematical model.

A TEC for cartilage repair is generally composed of three primary material phases: 1) a biodegradable framework or scaffold designed to persist briefly in the body before biological degradation; 2) cartilage tissue that has taken up residence inside the porous scaffold framework; and 3) fluid filled space. The mechanical properties of each of these individual phases and their volume fraction of within the TEC contribute to the effective mechanical behaviour of the three-phase mixture. As an added complexity, the cartilage tissue component of this mixture is itself a complex composite material. A full theoretical treatment of the effective mechanical properties of TECs should first include the development of mechanical models for each of the constituent phases in the system. The resultant models should ideally represent the strain rate-dependent deformation of the phases in tension and compression for small and large deformations, and also include the time-dependent creep behaviour of the material phases of the TEC in tension and compression. These models are then applied in a homogenization scheme to give the effective properties of the mixture.

The tissue scaffold component of the TEC is typically composed of synthetic biodegradable polymers that are either amorphous or semi-crystalline. The stress-strain behaviour of this kind of material under varying strain rates can be represented using models based on the networks of spring and damper elements (Figure 10) [116]. Based on such a model, the strain-rate-dependent behaviour of the polymeric scaffold material can be determined (Figure 11).

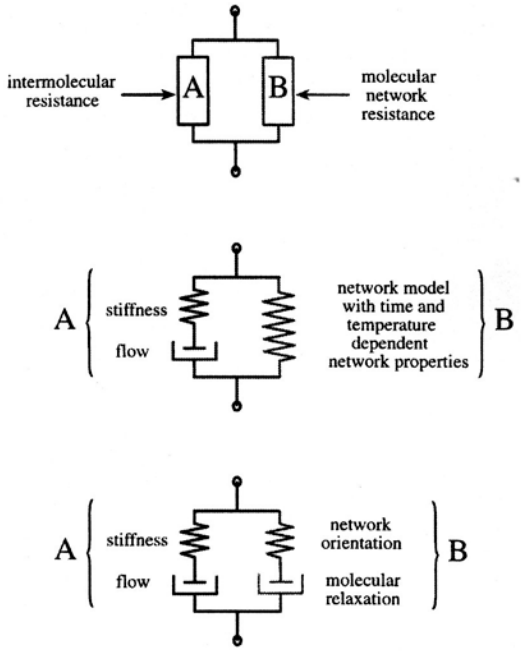

Figure 10. Spring-dashpot networks representing resistance of the polymer to strain as an intermolecular resistance to deformation as well as resistance from molecular network reorientation (reprinted from [116] with permission from Elsevier).

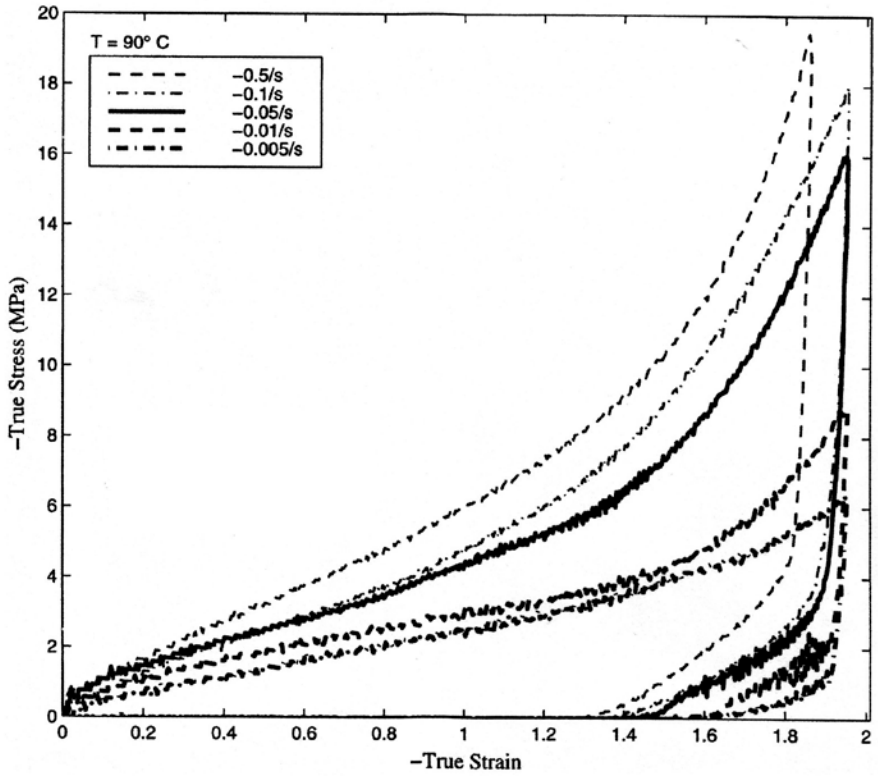

Figure 11. Stress-strain curves of polymers at different strain rates (reprinted from [116] with permission from Elsevier).

The next material phase in the TEC is the tissue cartilage itself. Many different approaches have been proposed to represent mathematically the behaviour of tissue cartilage. In one approach [117], the cartilage is modelled as a network of spring elements representing the fibrils pre-stressed by osmotic pressure. The Donnan osmotic pressure of the tissue is considered as a function of the tissue outer geometry, which can be altered to reflect its variation in a confined compression test. This model shows promise for reproducing the experimentally-observed behaviour of cartilage at a specific strain rate. Further development or modification of these existing models to include the strain rate-dependency of the fibril network is urged.

Because cartilage shares similarities with moistened soil, poroelastic models developed for the analysis of soils offer another possible avenue for the modelling of cartilage tissue. In one approach [118], the poroelastic soil analysis elements present in the commercial software ABAQUS were employed to model the mechanical behaviour of a cartilage tissue plug in confined compression. The results obtained were compared to a mechanical model based on a biphasic rule of mixtures (detailed below) and close agreement was found. In another study [119], ABAQUS was employed to model cartilage tissue behaviour under compression, with agreement found between the experimental results and model predictions.

Another model commonly employed to represent the load-deformation behaviour of cartilage is the biphasic model based on the rule of mixtures, which represents cartilage tissue as a linear elastic or non-linear visco-elastic matrix infused with an incompressible fluid phase. The governing equations for this model are the conservation of mass and momentum laws for a two phase liquid-solid mixture [120]. The conservation of mass for the solid fluid mixture is given by

$$div(\dot{\boldsymbol{u}}) + div(\dot{\boldsymbol{w}}) = 0 \tag{2.1}$$

where $\boldsymbol{u}$ is the displacement of the solid phase and $\boldsymbol{w}$ the displacement of the fluid phase with respect to the solid phase. The conservation of momentum for the two phase mixture is given by

$$div(\boldsymbol{\tau}) + \boldsymbol{f} = \rho_{sat}\ddot{\boldsymbol{u}} + \rho_w\ddot{\boldsymbol{w}} \tag{2.2}$$

where $\boldsymbol{\tau}$ is the effective stress tensor of the mixture, $\boldsymbol{f}$ the body force vector, ρ_{sat} the density of the saturated solid, and ρ_w the density of the fluid phase. Furthermore, the effective stress tensor $\boldsymbol{\tau}$ can be decomposed into contributions from the solid and liquid phases

$$\boldsymbol{\tau} = \boldsymbol{\tau}^{s} + \boldsymbol{\tau}^{w} \tag{2.3}$$

where $\boldsymbol{\tau}^{s}$is the stress tensor for the solid phase and $\boldsymbol{\tau}^{w}$ the stress tensor for the liquid phase of the tissue. In addition, the stress in the fluid phase can be represented as

$$\boldsymbol{\tau}^{w} = -\phi p \boldsymbol{I} \tag{2.4}$$

where p is the pore pressure, ϕ the porosity of the tissue, and $\boldsymbol{I}$ the identity matrix. Furthermore, the velocity of the fluid phase with respect to the solid phase may be related to the acceleration of the solid phase by

$$\dot{\boldsymbol{w}} = -\boldsymbol{k}\left(\frac{grad(\boldsymbol{p})}{\rho_w g}\right) - \frac{\boldsymbol{g}}{g} - \frac{1}{g}\boldsymbol{k}\ddot{\boldsymbol{u}} \tag{2.5}$$

where $\boldsymbol{k}$ is the hydraulic conductivity (permeability) matrix of the solid phase $\boldsymbol{p}$ the pore pressure distribution within the tissue, g the acceleration due to gravity, and $\boldsymbol{g}$ the gravity acceleration vector. The above governing equations may be solved using the finite element method. After being placed into the finite element matrix form, a Newmark based numerical integration scheme can be employed [120] to solve the governing equations (2.3), (2.4), and (2.5) and estimate the nodal displacements of the solid phase and the nodal pore pressure distribution within the saturated solid body. While the above formulation assumes a linear elastic solid phase and an incompressible fluid phase with small deformations, this approach [120] also results in a large deformation finite element formulation for the conservation of mass and momentum when the solid phase is assumed to be compressible and hyperelastic. A further development is the triphasic model of cartilage, which divides the liquid phase further into two separate fluids, i.e., intrafibrillar and extrafibrillar fluid phases. The intrafibrillar fluid phase contains intrafibrillar water, sodium ions, and chloride ions; the extrafibrillar fluid phase includes proteoglycans, extrafibrillar water, and sodium and chloride ions[121]. This model gave predictions in agreement with experimental results from confined compression tests [121].

Another approach [122] presents a generalized *n+2* phase theory for charged hydrated tissue. The charged and hydrated tissue is modelled as a continuum of three phases, i.e., solid phase, solvent phase, and *n* ion phases or species dissolved in the solvent. The solid phase and ions are assumed to carry charge, while the solvent phase is neutral. The continuity equation for such a system is given by

$$div(\dot{\boldsymbol{u}}^s) + div[\sum_\alpha \phi^\alpha(\dot{\boldsymbol{u}}^\alpha - \dot{\boldsymbol{u}}^s)] = 0 \tag{2.6}$$

where $\dot{\boldsymbol{u}}^s$ is the velocity of the solid, $\dot{\boldsymbol{u}}^\alpha$ the velocity of constituent α, and ϕ^α the volume fraction of constituent α. The momentum equation is given in terms of electrochemical potentials for the solvent and ions in the *n+2* phase mixture, i.e.,

$$-\rho^\alpha \nabla \tilde{\boldsymbol{\mu}}^\alpha + \sum_\beta \boldsymbol{f}_{\alpha\beta}(\dot{\boldsymbol{u}}^\beta - \dot{\boldsymbol{u}}^\alpha) = 0 \tag{2.7}$$

where ρ is the density of each phase, $\tilde{\boldsymbol{\mu}}^\alpha$(J/kg) the electrochemical potential of each constituent, and $\boldsymbol{f}_{\alpha\beta}$ the friction force between the various constituents in the mixture. These equations can be cast into their weak forms and integrated over the entire volume of the considered tissue sample, where the unknown parameters in the finite element implementation are the displacements of the *n*+2 constituents. Alternatively, the governing equations can be solved with a forward difference numerical method [122].

Another mathematical model developed to represent the constitutive behaviour of cartilage tissue in both tension and compression is based on the theory of quasilinear viscoelasticity (QLV) proposed by Fung [100]. This model represents tissue as a homogenous rheological fluid, where the stress in the body with time $\sigma(t)$ is given as function of the stretch ratio $\lambda(t)$ [123],

$$\sigma(\lambda(t); t) = \int_0^\infty G(t)T^e(\lambda)dt \tag{2.8}$$

where $T^e(\lambda)$ is elastic stress as a function of the stretch ratio and $G(t)$ the ratio of current stress to the elastic instantaneous stress present immediately after load application, which is given by

$$G(t) = \frac{\sigma(t)}{\sigma(t=0)} \tag{2.9}$$

The stress response of the system to an infinitesimal change in stretch when the object is initially in the state of stretch λ at the time τ is given by

$$\delta\sigma(t) = G(t-\tau)\frac{\partial T^e(\lambda(\tau))}{\partial\lambda}\delta\lambda(t) \tag{2.10}$$

where $\sigma(t)$is the first Piola-Kirchhoff stress as a function of time, which is evaluated from the forces in the deformed configuration of a body and the areas present in the original reference

configuration of the body. The stress history in the body with time is given by the time integral of Equation (2.10), i.e.,

$$\sigma(t) = \int_{-\infty}^{t} G(t-\tau) \frac{\partial T^e(\lambda(\tau))}{\partial \lambda} \frac{\partial \lambda(\tau)}{\partial \tau} d\tau = S^e(t) - \int_0^t \frac{\partial G(t-\tau)}{\partial t} S^e(\tau)\, d\tau \tag{2.11}$$

where S^e is the stress from the instantaneous nonlinear equilibrium response of the tissue, G the reduced relaxation function, $\frac{\partial T^e(\lambda(\tau))}{\partial \lambda}$ the instantaneous elastic response to an infinitesimal change in the stretch ratio, and $\frac{\partial \lambda(\tau)}{\partial \tau}$ the strain history. Once the mechanical property functions in the model $G(t)$ and $S^e(t)$ are known, the time-dependent stress $\sigma(t)$ can be determined for a known strain history. For the tensile response of cartilage, the following stress relaxation function is proposed [124],

$$G = 1 + \frac{\alpha}{1+\left(\frac{t}{\tau}\right)^{\beta}} \tag{2.12}$$

where α, t, and τ are the material property parameters that can be estimated from a stress relaxation test [124]. The instantaneous stress relaxation of the tissue in compression or tension is experimentally determined, typically taking the form of

$$S^e(\boldsymbol{\varepsilon}) = E(\boldsymbol{\varepsilon})\boldsymbol{\varepsilon} \tag{2.13}$$

where $\boldsymbol{\varepsilon}$ is strain (stretch ratio) and $E(\boldsymbol{\varepsilon})$ a non-linear function for compressive and tensile loading determined from the initial behaviour of a tissue sample under compression or tension. The above model was used to represent the tensile response of cartilage tissue, dominated by the viscoelastic behaviour of the cartilage solid matrix [124]. Under compression, the viscoelasticity of the tissue is fluid-flow dependent and is modelled by using a relaxation function to account for the effect of fluid flow on the cartilage. Because this modelling method represents the cartilage as a homogeneous solid, the resultant QLV model cannot represent the material properties of individual constituents within cartilage. If a TEC is considered, however, this method would be used to estimate the mechanical properties of the regenerating tissue within the scaffold from the measurements of the effective properties of the TEC. This is an inverse problem, where the known effective properties of the TEC are functions of the unknown properties of its constituents. The QLV model can be incorporated into biphasic theory to give a more accurate

representation of the behaviour of the cartilage matrix, which is assumed in classical biphasic theory to be only a simple linear elastic material [125].

With the availability of models for both the cartilage tissue and solid scaffold material phases, the next step in modelling the TEC's effective mechanical properties is to combine the material models based on the homogenization method. Considering a representative piece of the TEC, with strain-dependent stress strain curves for each material phase, finite element models of the TEC can be constructed and subjected to displacement boundary conditions that simulate the effect of a mechanical test. For cases with large displacements, non-linear material behaviour, and/or strain rate dependence, the non-linear problem can be linearized by applying the prescribed displacement boundary conditions as step loads and/or updating the modulus of material at the experienced strain level in each of the finite elements. During each step, the configuration of the nodes from the previous step is employed to assemble a linear stiffness matrix, and the strain in each element, determined in the previous load step, is employed to select an appropriate stiffness for each element in the body from the known stress-strain curves of the constituents. This approach may be executed using commercial software, such as ANSYS. Unfortunately, representation of the full TEC in a finite element model is a significant computational burden. An alternative is the use of a small representative piece of the TEC, which is known as a representative volume (RV). This is accomplished based on the homogenization method, in which a TEC is represented by a finite number of RVs that possess location-independent mechanical properties. A type of traction or deflection boundary condition is then applied to the RV such that the average stress within the body is an average of the stress distribution experienced by all of the assembled cells in the complete TEC. To effectively represent RV deformation in the presence of neighbouring cells, the deformation pattern of the RV's outer surface should be some type of average of the deformation shape experienced by all the unit cells in the TEC. One deflection boundary condition to achieve this objective is the periodic deflection boundary condition, where the displacements on opposite sides of the RV tile together. These displacement boundary conditions are represented mathematically as [126]

$$u_i = \bar{s}_{ij} x_j + v_i \tag{2.14}$$

where u_i is the displacement of a node on the boundary of the RV, $\bar{s}_{ij}$ the average strain experienced in the RV, x_j the location of the boundary node, v_i the periodic component of the boundary node displacement, and $i, j = 1,2,3$ indices indicating global coordinate directions. For a square RV, the above expression becomes

$$u_i{}^{K+} = \bar{s}_{ij} x_j{}^{K+} + v_i{}^{K+}, u_i{}^{K-} = \bar{s}_{ij} x_j{}^{K-} + v_i{}^{K-} \tag{2.15}$$

where $K+$ indicates the positive x_j direction and $K-$ the negative x_j direction. The difference between the deflections on opposite sides of the RV is therefore given by

$$u_i{}^{K+} - u_i{}^{K-} = \bar{s}_{ij}(x_j{}^{K+} + x_j{}^{K-}) \tag{2.16}$$

If the TEC considered is heterogeneous, the strategy of using averaged properties can be applied and expressed mathematically by

$$\bar{S}_{ij} = \frac{1}{V_{RV}} \int_{V_{RV}} S_{ij} dV, \bar{T}_{ij} = \frac{1}{V_{RV}} \int_{V_{RV}} T_{ij} dV \tag{2.17}$$

where S_{ij} T_{ij} are the strain and stress, respectively, and the over-bar indicates a volume average.

Representing or modelling the displacement-under-loading behaviour of hydrated tissues such as cartilage by solving the governing equations in the above shows promise. Constitutive relations for all of the material phases within the TEC can be incorporated into finite element models of the TEC to predict its mechanical behaviour. The primary source of error in such models is considered to mainly come from the assumption of homogenization in each structural level of the TEC. With the advance of computing technologies, future work should include more structural details in finite element models of the TEC to release or partially release the homogenization assumption of the TEC structure.

2.2.6 Methods to Enhance the Mechanical Properties of TECs

The mechanical properties of TECs for cartilage repair should match those of native articular cartilage. As discussed above, the mechanical properties of cartilage vary widely and depend on donor species and age, as well as joint location and sample orientation. As such, the mechanical properties of TECs should be defined and determined differently for specific

implantation sites. To make things more challenging, the TEC's mechanical properties are not constant during the healing process, but change dynamically with time as the tissue regenerates and the scaffold degrades. Thus, engineering functional cartilage with matching mechanical properties has proven to be extremely difficult and, so far, engineered cartilage has largely been mechanically inferior to native cartilage [105, 127-129]. A number of methods or techniques have been developed to enhance the mechanical properties of engineered cartilage, including control over the amount of ECM components that the chondrocytes produce, control over the fibre geometry within the scaffolds, and selection of scaffold materials with appropriate mechanical properties.

By modifying the amount of ECM components, i.e, proteoglycans and collagen, that the chondrocytes produce, the mechanical properties of the cartilage can be controlled. For example, the shear storage and tensile modulus can be enhanced by increasing collagen concentrations or the cross-linking of the collagen fibrils [99, 130]. On the other hand, decreasing the PG concentrations within the ECM can reduce the tensile and compressive moduli by 10-fold[82, 99]. One method for controlling collagen and proteoglycan levels within the ECM is the use of mechanical stimulation, such as hydrostatic pressure [131] and dynamic shear or compression[132]. The levels of PG and collagen vary, depending on the type of loading regimen [131], for example, if the loading frequency is low (0.3 Hz) or high (3 Hz), ECM production can be inhibited, with 1 Hz appearing optimal for ECM production [34, 107, 133]. The compression amplitude can also regulate both PG and collagen synthesis [107]. These findings have been recently applied to bioreactor design, so that they are able to mimic the dynamic forces seen in the native joints and thereby create cartilage with similar mechanical properties [134]. By altering the flow conditions within the bioreactor one can adjust the mechanical properties and possibly improve the mechanical properties of TECs [92, 129]. In the aforementioned processes, the interactions between cells and ECM play a critical role. These interactions, however, are complicated and many remain to be defined. In addition to experimental methods, the use of finite element methods would be a powerful tool to discover links between mechanical stimulation and cellular activity [135].

Another method of adjusting the levels of proteoglycans and collagens is the use of chemical stimulants, the most common of which is fetal bovine serum (FBS). FBS is a clear fluid

fraction prepared from clotted blood that contains various hormones, growth factors, and other bioactive stimulants. When added to cell culture, FBS increases cell proliferation and ECM production [136]. However, one large drawback is that this serum has a poorly defined composition, which can lead to problems with growing tissue in a repeatable manner [137]. Recent studies have used other individual stimulants, such as bone morphogenetic proteins and transforming growth factors [14, 15, 17-19], that have a more defined composition and give more repeatable results. In addition, natural cartilage ECM components such as HA and chondroitin sulphate (CS) can mechanically enhance TECs. The addition of HA to a cell medium or hydrogel enhances the production of GAG and collagen II as well as significantly increases cell proliferation [21, 22]; the addition of CS increases cell proliferation and PG synthesis [23, 24]. However, these individual stimulants are relatively costly and have problems including retention them within the TECs [43].

The mechanical properties of TECs can also be controlled via the design of scaffolds for the repair of cartilage. Increasing scaffold porosity would increase the loss angle and plastic deformation and decreases the storage modulus and aggregate modulus [51]. Changing the strand orientation within the scaffold, for example from a 0-90 to a 0-45 pattern (Figure 12), or using different types of honeycomb structures can significantly alter the mechanical properties [51, 138]. Another important consideration is the biological properties of the scaffold. Pore size cannot be made arbitrarily small for maximizing the aggregate modulus because a certain pore size and porosity is necessary to allow for cell delivery and tissue ingrowth. Mathematical models may allow one to optimize the trade-off between tissue growth and porosity before even entering the laboratory [139].

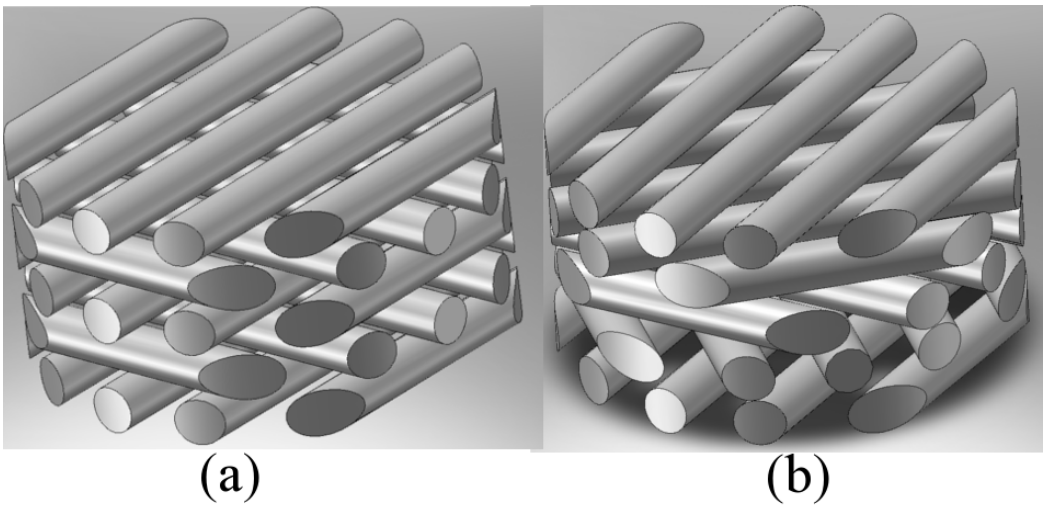

Figure 12. Schematic showing the strand orientation for the 0-90 (a) and 0-45 (b) solid scaffold geometries.

Different scaffold materials are recognized as having different mechanical and biological properties. These distinct yet diverse properties can be used to control and ensure the mechanical properties of the TEC. For example, a scaffold made out of poly(glycolic acid) (PGA) is stiffer than one with an identical geometry made of poly(lactic acid) [56]. Different materials also differentially stimulate chondrocytes. For example, a PGA scaffold stimulates PG synthesis while a collagen scaffold stimulates collagen II synthesis [140]. Further developments or investigations are urged to strategically combine different materials in scaffold designs to achieve synergistic properties of scaffolds.

2.2.7 Future Research Work

An initial goal of cartilage tissue engineering was to create a homogeneous tissue with the same bulk properties as the surrounding tissue [141]. However, current research has focused on creating mechanical property gradients within the TECs to more closely mimic the four zones found in native cartilage. The potential for stratification has been demonstrated through the creation of pore size, porosity, and stiffness gradients[50] within fabricated scaffolds. Recently, layered TECs were shown to reduce strain discontinuities between the TEC and the surrounding natural cartilage [27], demonstrating their promise for achieving mechanical property gradients within TECs. Hydrogels are well known for their biocompatibility and recently have been demonstrated as suitable for creating such layered scaffolds. Moreover, chondrocytes can be isolated from the different zones of native cartilage and cultured separately. These different cells

can then be encapsulated in separate hydrogel disks. Eventually, these disks can be layered on top of one another to produce a stratified culture [25], with the construct producing a smooth transition between the layers with time [142]. These constructs also have the potential to create layers with differing chemical stimulants and/or mechanical properties. One promising research avenue for the creation of stratified TECs is the development of a hybrid scaffold that incorporates the "cell friendly" environment of a hydrogel with the mechanical stability of a solid polymer scaffold. Control of the mechanical properties of these scaffolds would be easier than with hydrogels alone, and includes the opportunity to create different hydrogel layers (as discussed above) within the solid scaffold. Preliminary studies of these hybrid scaffolds have shown promising results[39]. More experiments will be needed with different types of cell stimulation and scaffold design before TECs are created with the desired bulk and local mechanical properties of natural articular cartilage.

To design TECs with the desired mechanical properties gradients, an alternative method to the experimental methods is the use of mathematical models. Mathematical models, including one based on modeling updating [143], have been developed to predict the time-dependent mechanical properties. Some mathematical models of the behaviour of cartilage tissue give good predictions of experimental tissue behaviour. The last component necessary for the complete mathematical analysis of cartilage TEC mechanical properties and their time dependent evolution is a model that can describe the time-dependent regeneration and behaviour of tissue within the TEC [144]. If such models can be improved to more accurately represent the strain-dependent mechanical properties of tissue/scaffold under compression and tension, and the gradual change in tissue/scaffold composition during scaffold degradation and tissue regeneration, they will provide an effective means to mathematically evaluate TEC designs and optimize their performance. This will require determining or modelling various interrelationships within the scaffold, such as the effects of living tissue and scaffold degradation products on the degradation rate of the solid scaffold.

As cartilage tissue engineering moves towards implanting TECs to repair damaged cartilage in human patients, non-invasive methods of testing the properties of the implanted TECs *in situ* must be developed. The only one of the aforementioned methods currently capable of testing implanted TECs *in situ* is indentation, and even this method would require surgery. In

order to track the properties of TECs after implantation, imaging methods such as magnetic resonance imaging [79] show the most promise. Typically, image-based methods are based on the idea of measuring the strain in the cartilage before and after loading in a joint and using these measurements to determine the aforementioned mechanical properties. These imaging methods will help researchers determine the success of TEC implants without subjecting the patient to another surgery.

2.2.8 Conclusions

Cartilage tissue engineering has made great strides towards growing cartilage substitutes with the mechanical properties necessary to withstand the loads found within joints. Mathematical modeling, in conjunction with tensile, compressive, and shear testing, provides researchers with the mechanical properties that govern both the equilibrium and the transient responses, and allows the accurate comparison of TECs to natural cartilage accurately.

Although current TECs have, for the most part, not achieved mechanical properties that match those of natural cartilage, considerable progress has been made in the development of methods to modify the mechanical properties of TECs. These methods include modifying the amount of ECM components produced by chondrocytes through mechanical or chemical stimulation, adjusting the internal scaffold structure, and choosing appropriate scaffold materials or their combinations. Further work or development to create stratified cartilage and mathematically model the time-dependent properties of TECs is encouraged to achieve mechanical property gradients within the TECs to mimic the four zones found in native cartilage.

2.2.9 Acknowledgements

The authors would like to acknowledge financial support from the Natural Sciences and Engineering Research Council of Canada (NSERC) and the Saskatchewan Health Research Foundation (SHRF).

2.2.10 Authors' Disclosure Statement

No competing financial interests exist for any of the authors.

Chapter 3: Materials and Methods

3.1 Introduction

This chapter outlines the methodology used in pursuit of the objectives outlined in Section 1.3. After fabrication, the solid scaffolds were photographed and then examined using microtomography to determine porosity, pore size, and to confirm that the pores were interconnected throughout the scaffolds. In addition, the Hoechst assay was used to determine cell population on disks of the scaffold material after a week of culture.

To determine the effects of hyaluronic acid (HA) and chondroitin sulphate (CS) on chondrocytes in hydrogel culture a number of tests were used to examine cell proliferation and matrix production. The 1,9-Dimethylmethylene Blue (DMMB) assay and immunostaining were used to examine ECM production, while the Hoechst DNA assay was used to quantify cell proliferation. Finally, Real-Time Quantitative Polymerase Chain Reaction (qPCR) was used to show concentration of the mRNA that encodes for aggrecan and collagen types I and II relative to GAPDH.

To examine the differences in cell population between the composite scaffold and solid scaffold controls the Hoechst DNA assay was used, while the differences in matrix production were elucidated using the DMMB assay. The preceding information is summarized in Figure 13.

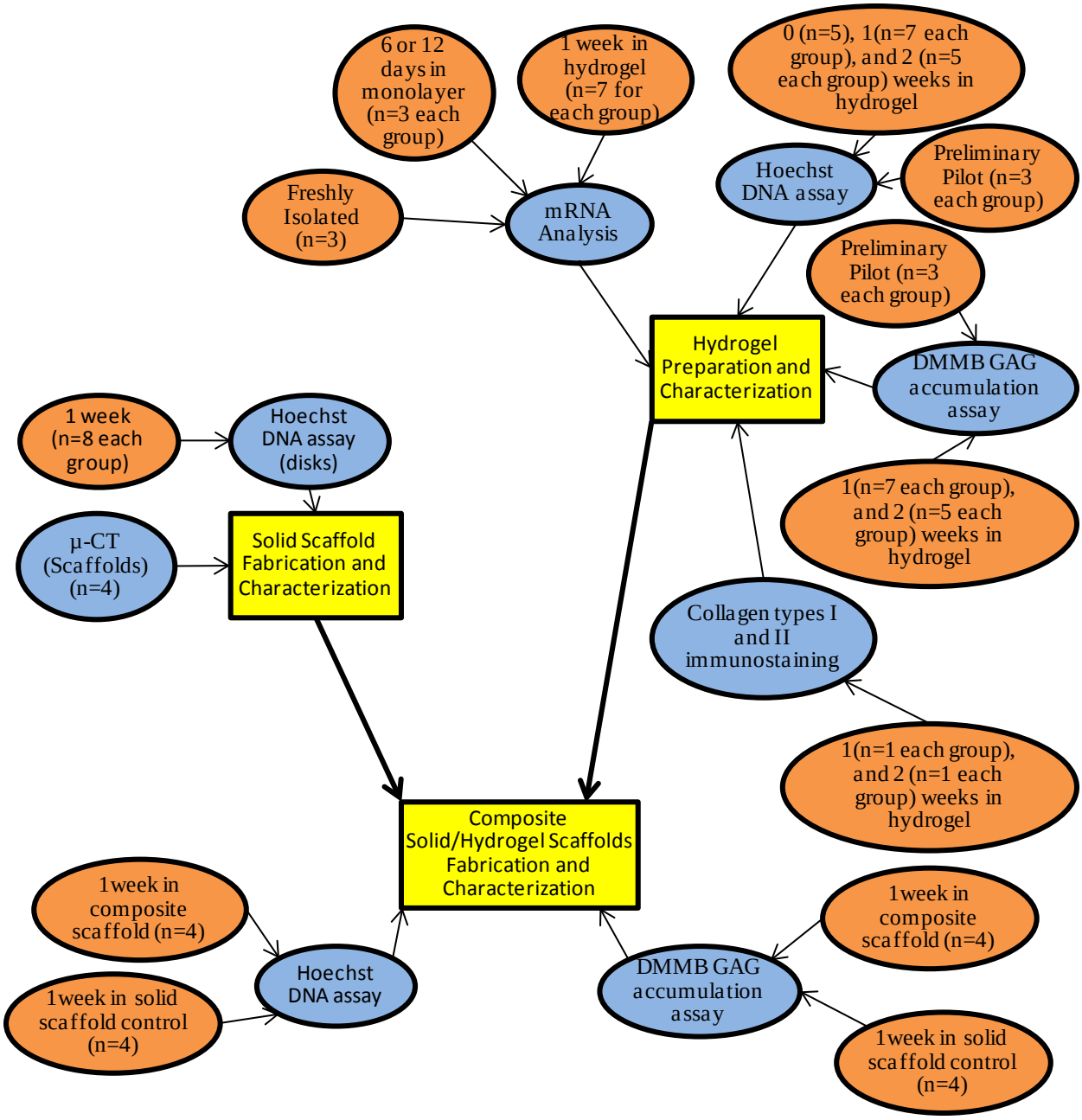

Figure 13. Flow chart summarizing the majority of the experimental work done in the present study. The brown entries represent the sample information, the blue entries represent the experimental test performed on said samples, and the yellow entries represent the final goal of the experimental tests. The ultimate goal of the study, as denoted by the thick arrows, was the fabrication and characterization of the solid/hydrogel scaffolds.

3.2 Solid Scaffold Fabrication and Characterization

3.2.1 Fabrication of Solid Scaffolds and Substrates

3D scaffolds were fabricated for the purpose of characterizing pore size and porosity and to ensure that overhanging structures existed throughout. 2.0 g of PLGA (50:50 copolymer of polylactic and polyglycolic acid; Lactel, CA) were dissolved in 5.0 ml of chloroform to make a 40 % (w/v) solution, and 3.0 ml of the PLGA-chloroform solution were then mixed with 1.2 g of iron(III) oxide (IO) powder (<50nm particle size, Sigma) and stirred thoroughly. This material slurry was then loaded into a 10 ml syringe and hooked up to a rapid-prototyping (RP) machine (C0720M, Asymtek, Figure 14). The programmed initial dimensions of each scaffold were 5.25 mm x 5.25 mm x 2.5 mm with a horizontal pore size and strand diameter of 250 μm, as shown in Figure 15. After deposition, scaffolds were placed in a fume hood overnight to allow the chloroform to evaporate and the scaffolds to harden. Some shrinking of the scaffolds occurred during this period.

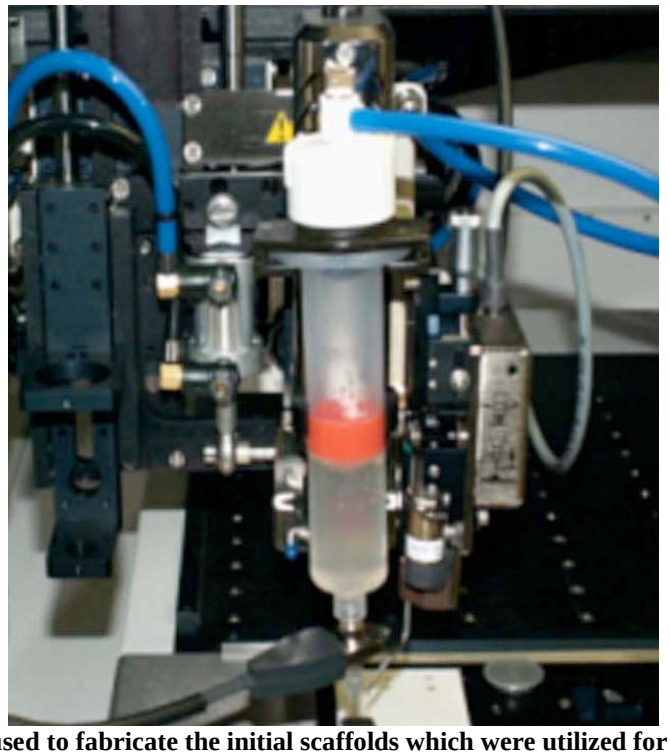

Figure 14. RP machine used to fabricate the initial scaffolds which were utilized for the purposes of scaffold characterization using microtomography. The material slurry is dispensed through a needle as the moving head that the syringe is attached to moves along a pre-programmed path. Layers were sequentially deposited on top of one another to create the 3D construct.

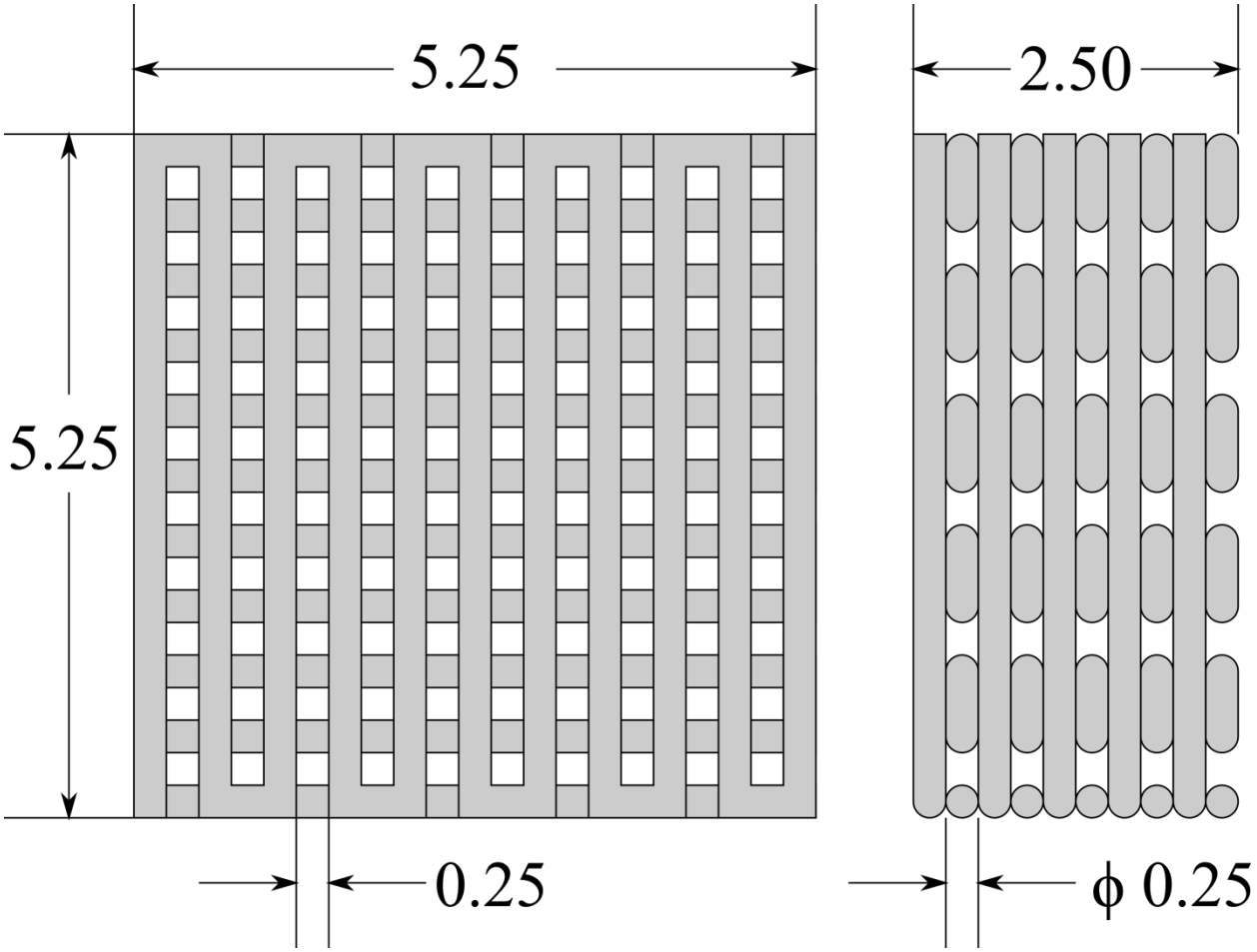

Figure 15. Schematic of the solid scaffolds showing top (left) and side (right) views with all dimensions in millimetres and the ϕ representing a diameter. The horizontal pore size and strand diameter were both 0.25 mm.

In some experiments, flattened discs of the above scaffold material were fabricated for the purpose of determining the material's ability to support chondrocyte culture. These discs were much easier to fabricate than the solid scaffolds, as they used a mould rather than a RP machine, which allowed for a larger number of samples in these experiments. The material slurry for these discs was comprised of 700 mg of either hydroxyapatite (HAP) or IO that was mixed with 3.0 ml of a 23.3% solution of PLGA in chloroform. The additional chloroform lowered the viscosity of the slurry, allowing it to be poured into a plastic mould, forming a 1 mm thick film without pores. After the chloroform evaporated, the final ratio of PLGA to iron oxide was the same as in the slurry used to fabricate the 3D scaffolds, and 5.0 mm discs were cut using a dermal biopsy punch.

3.2.2 Scaffold Characterization

After the scaffolds were fabricated it was necessary to confirm their final porosity, average pore size, and that the pores were indeed connected to one another throughout the construct. Photographs of the solid scaffolds were taken using a dissection microscope (Wild, Heerbrugg) to visually confirm that overhanging structures (i.e. interconnected pores) were present on the exterior of the scaffold. In addition, microtomography imaging was performed (Skyscan 1172 micro-CT instrument, Kontich, Belgium) on four of the scaffolds to determine average pore size, porosity, and strand diameter, as well as the internal structure of the scaffolds. Images were taken at an energy of 55 keV, with a 460 ms exposure and 0.5 mm Al filter used. The voxel size was 10 μm and an angular step of 0.21° was used. The resultant tomography data was analysed using CT-Analyser software (Skyscan).

3.2.3 Cell Culture

To demonstrate the biocompatibility of this scaffold material, primary chondrocytes were cultured on it *in vitro* for one week. Articular cartilage was harvested from the femoral and humeral heads, lateral and medial condyles, and patellae of newborn pigs. These piglets were obtained from the Prairie Swine Centre, and had died spontaneously no more than 24 hours prior to dissection. The cartilage was minced into 1-2 mm fragments using scalpels and subjected to a sequential digestion in which the tissue was incubated for 1 hour (37ºC, 5% CO_2, 100% RH) with 10 mg/ml pronase (Boehringer) in Dulbecco's Modified Eagle Medium (DMEM; Sigma) supplemented with GAK (0.292 mg/ml glutamine; 100 U/ml penicillin; 100 μg/ml streptomycin, 0.25 μg/ml amphotericin B, 100 μg/ml kanamycin), and then treated with 2 mg/ml collagenase (Type IA; Sigma) in DMEM supplemented with 10% Fetal Bovine Serum (FBS) and GAK and for 4 hr with intermittent agitation. The resulting digest was then passed through a 100 μm Nitex filter and the isolated chondrocytes were isolated by centrifugation (10 min, 300g) and resuspended in DMEM/10%FBS/GAK.

Both the PLGA-HAP (n=16) and PLGA-IO (n=16) substrate discs were sterilized in 95% ethanol for 15 minutes, rinsed twice with Hanks's saline[145], and placed in a sterile 96-well tissue culture plate. For each type of substrate, 8 discs and 8 empty culture wells were seeded at a density of 1.75×10^6 cells/cm^2 in DMEM/10%FBS/GAK. The remaining 8 discs and 8 additional

empty wells were not seeded with cells and had an equal amount of DMEM/10%FBS/GAK medium added to serve as a no-seed control. Seeded wells and no-seed controls were incubated for seven days with a medium change on day 4.

3.2.4 Hoechst DNA Assay

The Hoechst DNA assay uses a fluorescent dye that binds to DNA for the purposes of determining cell population (i.e. DNA concentration) within a sample.

After culture, all wells were rinsed with Hanks's saline and the substrates were removed and individually placed in a sterile 96-well plate. To account for the difference in culture surface area, 150 µl of 1.25 mg/ml trypsin in calcium and magnesium free Puck's saline[146] was added to each well containing a 5.0 mm substrate disc, whereas 216 µl of trypsin solution was added to each 6.0 mm empty well containing no substrate. Cultures were incubated for 10 minutes (37ºC, 5% CO_2, 100% RH) in the trypsin solution and the cells were dislodged by pipetting up and down, after which the cell suspensions were put in microtubes and frozen at -20ºC. Samples were later subjected a fluorometric DNA assay similar following a modification of the method of Labarca *et al*[147]. Briefly, samples were thawed and sonicated, then a 70 µl aliquot of each sample was mixed with 30 µl of 4 µg/ml Hoechst 33258 dye (Sigma), and 100 µl of 2X buffer (0.1 M NaH_2PO_4, 4 M NaCl, pH 7.4). Samples were then loaded into a black-plastic 96-well microtiter plate and read on a plate-reader fluorometer (Fluorolite 1000, Dynex) at an excitation wavelength of 365 nm and an emission wavelength of 458 nm. Samples were run alongside a set of DNA standards (0 - 4 µg/100µl chicken DNA, Sigma) for absolute quantification of DNA in each unknown sample.

3.2.5 Statistics

An analysis of variance combined with a Tukey's Honest Significant Differences *post-hoc* test was performed using R© (version 2.10.1)[148] to test for significant differences between treatment groups in the Hoechst assay. A p value less than 0.05 was considered to be significant.

3.3 Hydrogel Preparation and Characterization

This experiment had both a preliminary pilot study and a later full experiment component. Both experiments had similar hydrogel preparation protocols and mainly differed in their sample sizes, RNA extraction techniques, and time points. The main purpose of the preliminary pilot study was to ensure that the proposed methodology would work in the full experiment. However, this pilot study ended up providing some useful data and as such, is included within this thesis.

3.3.1 Fabrication of Supplemented Hydrogels for Full Experiment

Chondrocytes were isolated according to the procedure outlined in Section 3.2.3. Fibrin-alginate hydrogels were created using a protocol similar to those described previously[42, 149]. Briefly, solutions of 62.5 mg/ml of fibrinogen (Sigma) and 30 mg/ml alginate (Sigma) were filter sterilized using syringe filters specifically designed for viscous solutions (glass prefilter to 0.2 µm; Filtropur, Sarstedt, catalogue # 83.1826.102). The solutions of 102 mM $CaCl_2$ and 100 U/ml of thrombin were filter sterilized using conventional 0.2 µm syringe filters.

The alginate was supplemented with enough HA and/or CS for a final concentration of 0.1 mg/ml of each/either macromolecule in the final hydrogel. The alginate, fibrinogen and cell suspension ($5x10^7$ cells/ml) were mixed together in a 1.5 ml tube, and then the thrombin was added to cleave the fibrinogen into fibrin. The final concentrations of the gel components were 25 mg/ml fibrinogen, 12 mg/ml alginate, $5x10^6$ cells/ml, and 10 U/ml thrombin with each gel being 196 µl in total volume. The gel mixture was incubated at 37°C for 15 minutes to allow the fibrin portion of the gel to set. Then, 588 µl of $CaCl_2$ were added to the microtube and the mixture was incubated for an additional 20 minutes to crosslink the alginate. After crosslinking, the gels were moved to 12 well tissue culture plates (2.1 cm diameter each) containing DMEM/10% FBS/GAK supplemented with 0.1 mg/ml HA alone, 0.1 mg/ml CS alone, both HA and CS (HACS), or neither additive.

This was a factorial experiment with one set of samples (n=8 for each treatment) harvested at week 1, another harvested (n=6 for each treatment) at week 2, and 5 untreated samples being harvested immediately. Some samples (n=7 for week 1; n=5 for week 2 for each

of the four treatment groups) were used for biochemical analysis of total sulphated GAG content. The hydrogel samples were rinsed in Hank's saline for 10 minutes, after which they were incubated at 37ºC with 471 µl of hydrogel dissolution solution (90 mM NaCl, 55 mM sodium citrate, 30 mM EDTA, 0.1 mM Tris HCl, pH 7.5, 0.2mM $CaCl_2$, 0.2 mg/ml proteinase K (Invitrogen Life Technologies)) until the gels were completely dissolved. A 30.4 µl aliquot of this digest was removed and mixed with 70.6 µl triple-distilled water, then stored at 4°C for later use in the DMMB assay for GAG quantification. The remaining hydrogel digest was centrifuged (5 minutes, 4°C, 300 g), the supernatant was removed and the pelleted cells were resuspended in 110 µl of Hank's saline. A 10 µl aliquot of this cell suspension was mixed with 160 µl of Hank's saline and frozen for the Hoechst DNA quantification assay. For the week 1 samples, the remaining 100 µl of cell suspension was mixed with 300 µl of TRIzol® LS reagent (Invitrogen Life Technologies). The cells were then immediately lysed by repeated aspiration through a 27-gauge syringe needle and frozen at -80°C for later RNA analysis.

3.3.1.1 Fabrication of Hydrogels for Preliminary Pilot Experiment

A preliminary experiment performed earlier was almost the same that outlined above with a few notable exceptions. The hydrogel dissolution solution contained 10 mg/ml trypsin instead of proteinase K. The isolated cells were also lysed and stored in GTC lysis buffer (Omega Bio-Tek) rather than the TRIzol® LS. Attempts to isolate RNA from the preliminary pilot experiment were unsuccessful, leading to the development of the above protocol which used TRIzol® LS and proteinase K and better protected the RNA from degradation. The cell pellet was resuspended in 1 ml of Hank's saline and a 40 µl aliquot of this suspension was diluted in 110 µl of Hank's for the Hoechst assay samples. In addition, the sample size was much smaller (n=3 plus one sample for cryogenic sectioning, for each treatment) and there was only a single time point which was harvested at 10 days.

3.3.2 DMMB assay

The DMMB assay used for sulphated GAG analysis was adapted from a combination of several protocols found in the literature [21, 31, 32, 150] and modified for use with alginate by adjusting the pH of the dye to 1.5, which effectively protonates the alginate which would

otherwise compete with the GAGs for binding sites on the DMMB dye molecules[150]. Briefly, 21 mg of DMMB (Sigma) was dissolved in 5 ml absolute ethanol. Then 2 g of sodium formate was added, and this solution was mixed with 800 ml of triple-distilled water. Formic acid (95%, Sigma) was added to the solution until the pH was 1.5 and then triple-distilled water was added until the final volume was 1 L. A buffer solution lacking DMMB dye was also prepared in an identical manner. In addition, a set of GAG standards was created by mixing seeded hydrogels (as in Section 3.3.1) supplemented with known amounts of CS (0 – 100 µg/ml final concentration).

For the full experiment samples harvested after one week (week 1) samples, the DMMB dye solution was diluted with an equal part of buffer to increase the sensitivity of the assay. A 48 µl aliquot of the diluted hydrogel digests (both samples and standards) was added to 300 µl of the diluted DMMB dye, and then incubated at room temperature for 1 hour. Thereafter, the samples and standards were centrifuged (15 minutes, 16°C, 11,500 g) and 280 µl of each supernatant was pipetted into a 96-well plate. The absorbance was read at 600 nm using a plate reader (SLT, Spectra).

Because the full experiment samples harvested after two weeks (week 2) samples had higher GAG levels, a less sensitive assay was used. A 48 µl aliquot of each sample or standard was mixed with 300 µl of undiluted DMMB dye and incubated at room temperature for one hour. Samples and standards were centrifuged and 200 µl of the supernatant was pipetted into a 96-well plate so the absorbance could be measured.

The DMMB assay for the pilot preliminary experiment followed the same protocol as the week one samples, except that 40 µl of sample or standard were mixed with 250 µl of diluted DMMB dye. After centrifugation 200 µl of the supernatant were pipetted into the 96-well plates.

3.3.3 Hoechst DNA Assay

The Hoechst assay protocol for these experiments was the same as the one described in section 3.2.4.

3.3.4 RNA analysis

While doing the DMMB assay and immunostaining are excellent ways of determining accumulation of ECM molecules within the hydrogels, mRNA analysis provides a "snapshot" of which genes are actively being transcribed into mRNA (and ostensibly being translated into their corresponding proteins). In addition, the immunostaining for collagen types I and II is qualitative, while the mRNA analysis allows for the quantification of the mRNA coding for these proteins.

Samples for RNA analysis were thawed, then centrifuged (10 minutes, 12,000g, 4°C) to pellet any insoluble debris. The supernatant (approx. 390 µl) was moved to a fresh microtube, then 80 µl of chloroform was added and the mixture was incubated at room temperature for 5 minutes. Samples were then centrifuged (15 minutes, 12,000g, 4°C) to separate the aqueous and organic phases. 150 µl of the upper aqueous (RNA-containing) phase was drawn off and mixed with an equal volume of 70% ethanol. This solution was then added to a HiBind RNA column from an E.Z.N.A™ Total RNA Kit (Omega, BioTek) and the manufacturer's protocol for RNA isolation was followed.

After RNA isolation, the A_{260}/A_{280} ratio was measured to check for phenol or protein contamination. An A_{260}/A_{280} ratio of 1.8 to 2.2 is characteristic of high quality RNA and the A_{260} reading was used to determine RNA concentration. Then, cDNA was synthesised from this RNA using the QuantiTect® Reverse Transcription Kit (Qiagen) following the manufacturer's protocol. Once synthesised, the cDNA was used as template for Real-Time Quantitative Polymerase Chain Reaction (qPCR) using Maxima® SYBR Green (Fermentas) reagents system in accordance with the manufacturer's protocol. The amplification then took place in a thermal cycler (MJ Mini, BioRad) equipped with a mini-opticon fluorescence detection module. Expression levels of four types of gene transcripts were analyzed; the mRNAs which coded for collagen type I (col1α1), collagen type II (col2α1), aggrecan, and glyceraldehyde 3-phosphate dehydrogenase (GAPDH) as a reference gene. The sequences of all qPCR primers used are described in Table 4. We designed each primer pair using the National Center for Biotechnology Information's "Primer Blast" software, and following the qPCR primer design guidelines given by BioRad[151].

Table 4. List of qPCR primers used in the present study. The optimal annealing temperature range was determined by an annealing temperature gradient. All primers were designed using the NCIB primer BLAST software, and validated using melt curves and electrophoresis.

Gene	GenBank Accession Number	Forward Sequence (5'-3')	Reverse Sequence (5'-3')	Amplicon Size	Optimal Annealing Temperature Range (°C)
GAPDH	DQ403065	5'-ACGGCAAGTTCCACGGCACAGT-3'	5'-GTTGGCGGGATCTCGCTCCTGG-3'	95	53.0 – 69.0
Collagen Type II	AF201724	5'-CAAAGATGGCGAGACAGGTGCT-3'	5'-GAAGTCCCTGGAAGCCAGATGGC-3'	104	53.0 – 65.8
Collagen Type I	AF201723	5'-GACGCACGGCCAAGAGGAGG-3'	5'-CTGGCAGGGCACGGGTTTCC-3'	130	59.5 – 65.8
Aggrecan	NM_001164652	5'-GCTTCCGAGGTGTCTCGGCG-3'	5'-TCGTCTCCTCGCCCACAGGG-3'	141	56.4 – 69.0

To determine the optimum Polymerase Chain Reaction (PCR) annealing temperature for each gene-specific primer pair, a temperature gradient was run using cDNA from an untreated hydrogel which was fabricated in the manner described in Section 3.3.1 and cultured for 2 weeks. Then, a standard curve prepared by a 5-fold serial dilution of the cDNA (5x, 1x, 1/5x, 1/25x, 1/125x) was amplified at the optimum temperature to determine the efficiency of the PCR for each target gene. To ensure that each primer pair only amplified its specific target gene sequence, the PCR reaction products were separated by electrophoresis on a 15% polyacrylamide gel. In addition, a melt-curve analysis was carried out on all PCR products immediately following the amplification reaction to make sure that all products amplified were of the same size. No template controls (NTCs; i.e. PCR reaction mixtures lacking cDNA template) were run alongside the samples to check for amplification of primer-dimers or contamination of the reagents. In addition, 6 samples were randomly chosen for a "no reverse transcriptase controls" (NRTs) to check for genomic DNA contamination in the isolated RNA. For both the NTCs and NRTs if amplification took place more than 5 cycles after the lowest expressed transcript in the experimental samples it was considered negligible, as proposed by Bustin *et al*[152]. Finally, 6 randomly chosen samples were analyzed on an automated electrophoresis machine (BioRad Experion System) to check for integrity of the input RNA that was used for the cDNA synthesis step that preceded qPCR amplifications. The Experion System measures an "RNA quality

indicator" which is a scale from 1-10, with 7-10 representing high quality RNA with negligible levels of degradation.

Relative expression of each gene of interest normalised to GAPDH expression was calculated using the Pfaffl method[153]:

$$\text{Ratio} = (E_{target})^{\Delta CPtarget(control-sample)}/(E_{reference})^{\Delta CPreference(control-sample)} \quad (3.1)$$

where Ratio is the relative expression ratio, E_{target} and $E_{reference}$ are the measured PCR amplification efficiencies of the target and reference genes, respectively, and ΔCP_{target}(control-sample) and $\Delta CP_{reference}$(control-sample) are the differences in crossing points between a control versus a sample for the target and reference genes, respectively.

For the purposes of determining whether the CS, HA, and HACS hydrogel supplements had an effect on the levels of mRNAs for the aggrecan, collagen type I, and collagen type II genes, the untreated hydrogel samples served as the "control," whereas the CS, HA, and HACS supplemented hydrogels were each individually treated as "samples." In addition, untreated hydrogel cultures were compared to RNA from freshly isolated chondrocytes and chondrocytes that had been cultured in conventional two-dimensional monolayer to assess how well the hydrogels helped the chondrocytes retain their differentiated phenotype. Chondrocytes that retain their phenotype would be expected to synthesize significantly more collagen type II than collagen type I[154], so difference in expression of the mRNA transcripts in these two genes was determined.

3.3.5 Cryogenic Sectioning

One sample from each treatment group at each time point was used for histological sectioning and staining. Hydrogels were rinsed in Hank's saline solution for 2 minutes. The saline was then removed and the hydrogel was immersed in formaldehyde solution (3.7% formaldehyde in Lonza's phosphate buffered saline (PBS) supplemented with Mg^{++} and Ca^{++}) for 30 minutes to fix the cells. The fixed hydrogel samples were then soaked overnight in a sucrose cryopreservation solution (30% sucrose in PBS supplemented with Mg^{++} and Ca^{++}). Then samples were embedded in Optimal Cutting Temperature Compound (Tissue-Tek) and frozen at -20°C initially, then transferred to -80°C for long-term storage. The samples were later

cryogenically sectioned using a cryostat (HM 550, Thermo Scientific) at a thickness of 30 µm. The sections were placed on glass microscope slides (Superfrost Plus, Fisher Scientific) and stored at -20°C.

The sections were subjected to immunostaining to detect the presence of collagen types I and II. First the sections were washed 2x with PBS containing 0.01% Tween 20 (PBST), for 5 minutes per wash. The sections were then incubated in a blocking solution of PBST containing 5% sheep serum (Sigma) for one hour. The blocking solution was replaced with the diluted primary antibody and allowed to incubate at room temperature for 1 hour. The primary antibody solution for collagen type II (hybridoma supernatant, monoclonal, anti-chicken collagen II; II-II6B3, DSHB) was diluted 1:25 with PBST containing 5% sheep serum, while the collagen type I antibody solution (monoclonal, cat# 2456, Sigma) was diluted 1:200. Following the primary antibody treatment, the sections were washed 4x with PBST (10 minutes per wash). Then the sections were incubated for 1 hour at room temperature in a 1:200 dilution of alkaline phosphatase-conjugated goat anti-mouse secondary antibody (400 µg/ml stock; Santa Cruz Biotechnology) in PBST containing 5% sheep serum. Then, the sections were washed 3x with PBST containing 0.5 mg/ml levamisole (10 minutes per wash), followed by two washes in NTMT (100 mM Tris HCl, pH 9.5, 50 mM $MgCl_2$, 100 mM NaCl, 1 mg/ml Triton X-100, 0.5 mg/ml levamisole) (for 15 minutes per wash). Finally, the sections were incubated overnight at room temperature in colour development solution (NTMT supplemented with 0.34 mg/ml nitroblue tetrazolium chloride and 0.175 mg/ml 5-bromo-4-chloro-3-indolylphosphate). The colour development reaction was stopped by three, 5 minute washes in PBST. As a negative control, a parallel section was treated as above, except that the primary antibody incubation step was omitted.

3.3.6 Statistics

For both the DMMB and the Hoechst assays a minimally-adequate mixed-effects linear model, with the untreated group as the intercept, was used to identify significant interactions using the model simplification techniques presented in [155]. The reason for using a mixed-effects model was that during the initial mixing of the hydrogels, the fibrinogen and alginate for each treatment group were pre-mixed in a large batch. As the individual gels were fabricated,

this batch separated out and the later gels received slightly more fibrinogen than the earlier ones. Fortunately, the order that the gels were fabricated was recorded, thus allowing for gels that were fabricated at the same time to be blocked together. By listing these blocks (each containing one sample of each treatment) as a random effect in the model it effectively "filtered out" the effects of the differing hydrogel compositions and allowed the treatments of interest (in this case the HA/CS treatments) to be fairly compared to one another. The results of this minimally-adequate model were used solely to determine if there was a significant interaction between HA and CS.

To examine if the hydrogel samples supplemented with HA, CS, or HACS were significantly different from the untreated group, a separate mixed-effects linear model was fit to the data that treated the HACS group as a separate treatment, rather than as an interaction of the HA and CS treatments. The results from this model were used to determine which, if any, of the three groups of hydrogels treated with macromolecules were significantly different from the untreated control. In addition, to test for cell proliferation, only the untreated groups from weeks 0, 1, and 2 were compared to one another. In this case, it was not possible to use a mixed-effects model as we were not comparing the effects of treatments within the same block. Therefore, a simple analysis of variance (ANOVA) was used to see if total cell numbers were significantly different between the time points, and a Tukey's Honest Significant Differences *post-hoc* test was used to determine which time points were significantly different from one another. A box and whisker plot of the data was used to visually confirm that it was normally distributed.

The data from the preliminary pilot experiment did not require a mixed-effects linear model either as each gel was pre-mixed separately before seeding, eliminating the problem of the gel separating out. Therefore, a traditional general linear model was used for this data. Finally, the DMMB readings were normalised to the amount of DNA in each sample, to account for any differences in total cell numbers.

For qPCR data, conventional parametric statistical tests may not be used because the mRNA expression ratio data derived from equation 3.1 do not follow a normal distribution. In response to this, the Relative Expression Software Tool (REST)[156] was developed with the intention of enabling qPCR users to apply robust non-parametric statistical tests to their data. REST uses a randomized resampling algorithm to determine if a specific gene transcript is significantly up regulated or down regulated, and bootstrapping methods to derive a 95%

confidence interval for the calculated mRNA expression ratio. Both of these statistical tests have the advantage of not needing to assume any type of distribution, making them appropriate for the analysis of qPCR data.

Another qPCR analysis compared the expression levels of aggrecan, type I and type II collagens in hydrogel cultures to the corresponding levels of chondrocytes in traditional two-dimensional monolayer cultures. In this case, the "samples" in equation 3.1 were the week 1 untreated hydrogels (n=7), chondrocytes cultured in monolayer for 6 days (n=3), and 12 days (n=3), whereas freshly isolated chondrocytes (n=3) were used as the "control."

In addition to determining if collagen types I and II and aggrecan were significantly up or down regulated, the REST program was used to determine if more collagen type II was present than collagen type I. To do this, it was assumed that the genes had a common amplification efficiency of 102% (amplification efficiencies were empirically measured as 101.9 for collagen type II and 102.2 for collagen type I). With this assumption equation 3.1 becomes:

$$\text{Ratio} = (E_{\text{collagen}})^{\Delta CPtarget(\text{collagen type I-collagen type II})} \tag{3.2}$$

where collagen type I and collagen type II represent the amplification cycle at which the respective collagens cross the qPCR detection threshold. If the expression ratio is significantly different from one (Ratio=1 if the mRNAs for these collagens are present in equal quantities), then collagen type I and collagen type II mRNA concentrations are significantly different from one another. This analysis was done for chondrocytes that were freshly isolated (n=3), cultured for 6 days in monolayer (n=3), 12 days in monolayer (n=3), and the week 1 untreated hydrogels (n=7).

3.4 Composite Solid/Hydrogel Scaffolds Fabrication and Characterization

3.4.1 Composite Scaffold Fabrication

The solid portion of the composite scaffolds was fabricated in a manner similar to the scaffolds made in Section 3.2.1. In brief, the PLGA/IO material slurry was mixed identically to the slurry for the earlier scaffolds. These scaffolds were fabricated using a different RP machine (3D-Bioplotter, Envisiontec) than the previous dispensing system. The 3D-Bioplotter, shown in

Figure 16, is specifically designed for scaffold fabrication and makes the adjustment of pore size, bulk dimensions, and dispensing pressure much simpler. It was acquired after the scaffolds described in Section 3.2.1 were fabricated. The programmed (before shrinking) bulk dimensions of the scaffolds were 7.0 mm x 7.0 mm x 3.0 mm with a horizontal pore size of 450 µm and a strand diameter of 250 µm. The slightly larger pore size (compared to the scaffolds described in Section 3.2.1) was to ensure that a hydrogel mixture would be able to freely flow into the fabricated solid scaffold. After deposition, scaffolds were placed in a fume hood overnight to allow the chloroform to evaporate and the scaffolds to harden. Once hard, the scaffolds were cut into cylinders using a dermal biopsy punch with a 5 mm diameter. Before any cell culture work, scaffolds were sterilized in 70% ethanol for 30 minutes and rinsed with Hank's saline.

Figure 16. The 3D-Bioplotter was used to fabricate the solid scaffold portion of the composite scaffolds. It worked in a similar manner to the RP machined presented in Figure 14 except that it had software more appropriate for scaffold fabrication. That is, it moved along a pre-programmed path and sequentially deposited layers one on top of another.

Cells were isolated following the protocol outlined in Section 3.2.3 and the cell suspension was mixed with the fibrinogen and alginate hydrogel components as described in Section 3.3.1. The final cell density of the hydrogels was $2x10^7$ cells/ml. This cell concentration was chosen as it was the most concentrated cell concentration that could be accurately pipetted. Then, the cylindrical solid scaffolds were press-fit into 5 mm diameter plastic moulds (Figure 17). With the solid scaffolds ready, the thrombin was added to the fibrinogen/alginate/cell suspension mixture such that the final concentration was 2.5 U/ml in the hydrogel. The reason that the thrombin concentration employed was only ¼ the concentration of our previous hydrogels was to decrease the rate of fibrinogen polymerization, thereby allowing the gel to flow through the solid scaffold more easily without affecting the final consistency of the hydrogel[149]. For each of the four composite (n=4) scaffolds, 120 µl of hydrogel was pipetted into each well of a 4-well tissue culture plate and negative pressure was applied to immediately suck the hydrogel into the solid scaffold. The composite scaffolds were allowed to sit for 30 minutes to allow the fibrinogen to gel. Then the moulds containing scaffolds were submerged in 102 mM $CaCl_2$ for 30 minutes to crosslink the alginate. The composite scaffolds were then ejected from the moulds and rinsed with Hanks's saline, after which any excess hydrogel not encapsulated within the scaffold was trimmed off. Scaffolds were then placed in individual wells of a 96-well plate and bathed in DMEM/10%FBS/GAK medium supplemented with 0.1 mg/ml CS.

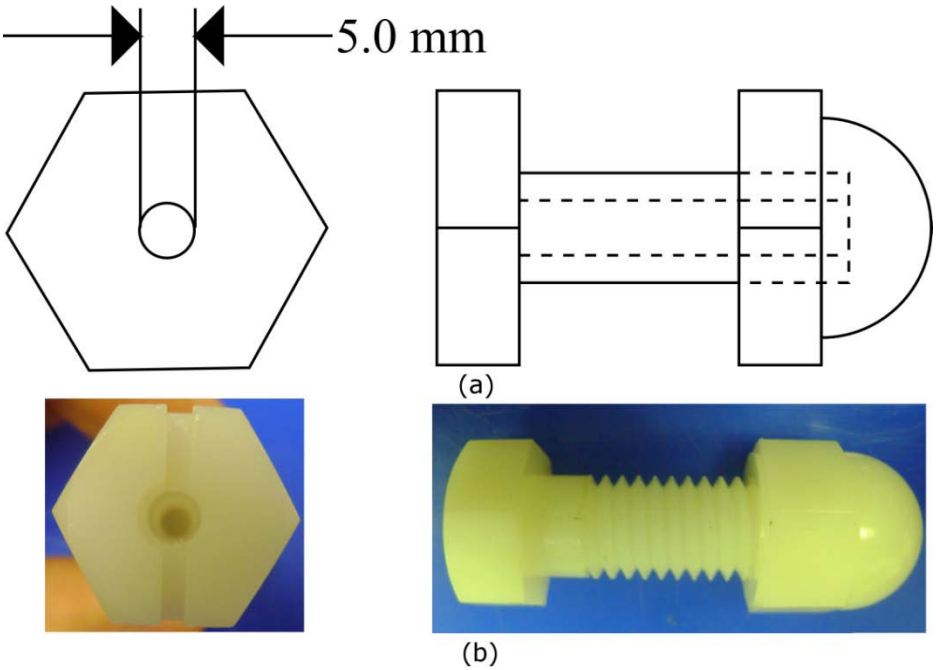

Figure 17. A (a) schematic and, (b) photographs of one of four identical moulds used in the composite scaffold fabrication process. Solid scaffold were pressed into the threaded end of the bolt and negative pressure was applied to the head end to suck the hydrogel into the solid scaffold. The cap nut was secured immediately afterwards to keep the hydrogel in place while gelation took place.

To determine the efficacy of these composite scaffolds, a set of four (n=4) solid scaffolds (without hydrogels) were also seeded with chondrocytes. The scaffolds, which were identical to those used for the composite scaffolds, were placed in a 96-well plate and a cell suspension of $2x10^7$ cells/ml was pipetted on top of them. Each well had 70 µl of cell suspension added to it, which represented just enough volume to completely cover the scaffold.

The cells were allowed 1 hour to settle to the bottom of the dish and start adhering to the solid scaffolds. After 1 hour, 250 µl of DMEM/10%FBS/GAK supplemented with 0.1 mg/ml CS was gently added to each well and the plates were incubated overnight (37ºC, 100% RH, 5% CO_2). The scaffolds were then transferred to individual wells of 4-well tissue culture plates and maintained in DMEM/10%FBS/GAK supplemented with 0.1 mg/ml CS for one week, with a single medium change on day 4.

3.4.2 Hoechst and DMMB Assays

After one week, the scaffolds were removed from the 4-well plates and placed in a 96-well plate. A 100 µl aliquot of hydrogel dissolution solution (described in Section 3.3.1) was

added to each well, and samples were digested for 4 hours. Then a 30 µl aliquot of the digest was diluted with 30 µl triple-distilled water to bring the concentration of alginate to 1 mg/ml, and this mixture was stored at 4ºC. The remaining digest was centrifuged (5 minutes, 4°C, 300 g), resuspended in 100 µl of Hank's saline, and frozen at -20ºC.

The DMMB assay was performed in a manner similar to the week 1 samples from Section 3.3.2 except that 40 µl of the diluted sample was mixed with 250 µl of diluted DMMB dye.

The Hoechst assay was performed using the same protocol outlined in Section 3.2.4.

3.4.3 Statistics

As this experimental design had only one treatment group and one control group a student's-t test was used to test for significance.

3.5 Preliminary Results

During the initial phases of this project, some preliminary work done to verify that viable chondrocytes could indeed be cultured in the hydrogels, and that the cells were producing proteoglycan-rich ECM. This work provided some excellent visual evidence of the cells' behaviour, but was not repeated in later experiments due to time constraints.

3.5.1 Hoechst Staining of Hydrogels

As an early test of cell viability, Hoechst 33342 dye was used to stain the nuclei of cells while in hydrogel culture. A 4 µg/ml solution of Hoechst 33342 was placed on top of the culture and incubated for 30 minutes at 37°C. Cultures were then rinsed twice with Hanks' saline, and allowed to sit in fresh Hanks' while being photographed under a fluorescence microscope (Olympus).

To determine if cells were surviving throughout the hydrogels, one sample was cryogenically sectioned as described in Section 3.3.5 and stained with Hoechst dye. The sections were rehydrated with PBS for five minutes, incubated in a 4 µg/ml Hoechst 33342 solution for

15 minutes, and rinsed 3x with PBS. The sections were then place in mounting solution (LabVision) and photographed using a fluorescence microscope.

3.5.2 Alcian Blue Staining of Hydrogels

Representative cultures of chondrocytes in hydrogels were stained overnight with Alcian blue dye (0.2% Alcian blue in 0.1 M HCl, pH=1) which binds to the GAG present in cartilage proteoglycans. The Alcian blue dye solution was removed and the cultures were briefly incubated with 0.1 M HCl to release any stain that was not bound to matrix GAGs. The cultures were then photographed using a dissection microscope (Wild, Heerbrugg).

Chapter 4: Results

4.1 Solid Scaffold Experiment

We employed microtomography to ensure that there were overhanging structures (i.e. interconnected pores) throughout the scaffold. These interconnected pores are crucial as they are the volume in which the chondrocytes proliferate, as well as allowing for medium exchange.

Scaffolds were successfully fabricated by the rapid-prototyping method using the PLGA-IO material slurry. As shown in Figure 18, the scaffolds had highly controlled and reproducible geometries. The micro-CT image analysis revealed that there were indeed overhanging structures throughout the scaffold (Figure 19). The mean pore size, strand diameter, and porosity for each of four replicate scaffolds produced are presented in Table 5.

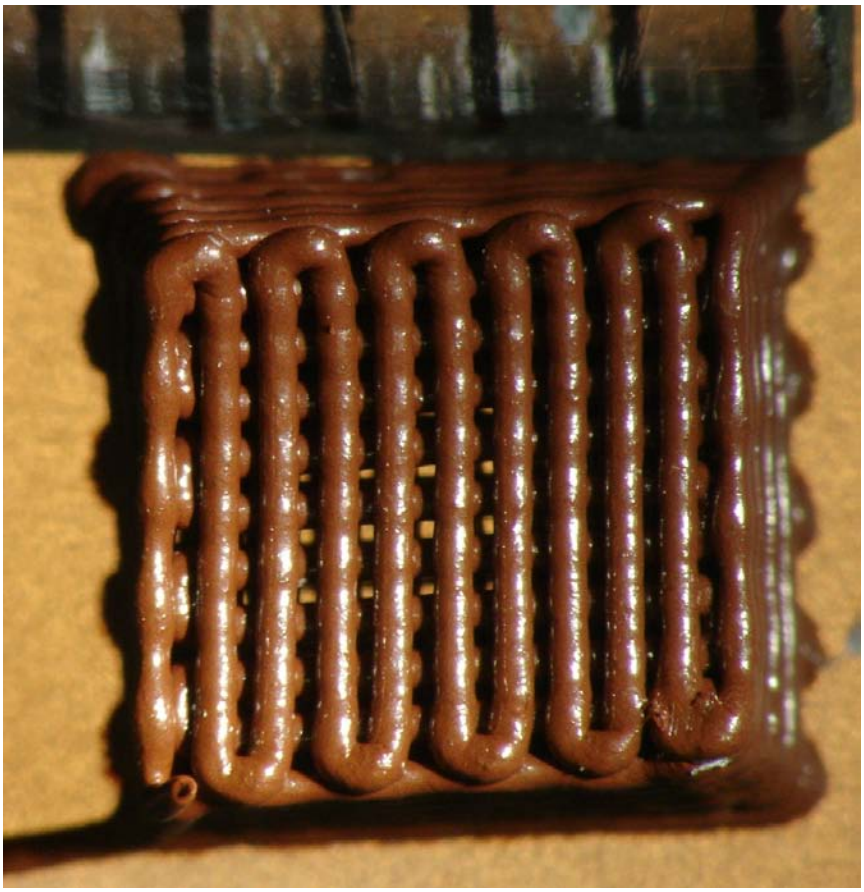

Figure 18. Photograph of solid scaffold taken with a dissecting microscope. The marks on the ruler at the top of the figure delineate 1mm increments.

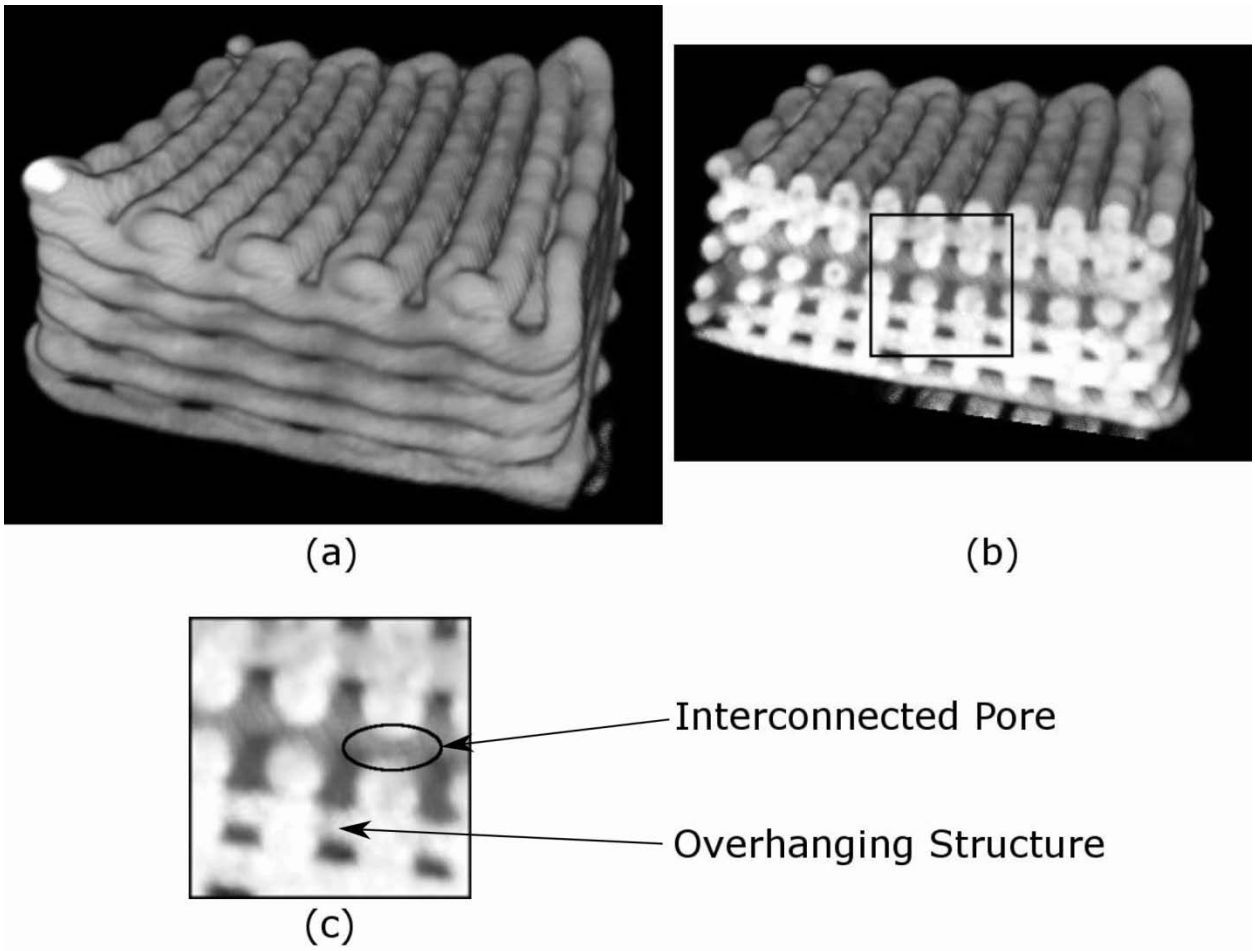

Figure 19. Three-dimensional model built from the microtomography data showing the (a) exterior and a (b) tomographic cross section. The cross section shows that there are overhanging structures (i.e. interconnected pores) throughout the scaffold as pointed out in the (c) magnified portion of this cross section.

Table 5. Summary of the scaffold parameters as measured by micro-CT image analysis. The 4 scaffolds measured were fabricated using the same RP program parameters. The pore size and strand diameters are presented as mean ± standard deviation. The cumulative average for each parameter is also presented.

Scaffold #	Pore Size (mm)	Strand Diameter (mm)	Porosity (%)
1	0.169±0.055	0.259±0.066	33.99
2	0.125±0.038	0.306±0.085	19.72
3	0.187±0.058	0.230±0.056	41.39
4	0.168±0.048	0.250±0.066	35.01
Cumulative Average	0.162	0.261	32.53

Once it was determined that a scaffold with interconnected pores could be fabricated using a PLGA-IO material slurry it was necessary to show that cells could be cultured on this

material. For this purpose, cells were cultured on disks of the PLGA-IO material slurry and on disks of PLGA-HAP and a tissue culture plate for comparison. A Hoechst DNA assay was used to determine cell number (as indicated by total DNA content) after one week of culture. This assay measured the amount of fluorometric dye bound to DNA within a homogenized sample. Therefore, the fluorometric intensity was assumed to be indicative of the amount of DNA in the sample. Moreover, the DNA content was assumed to reflect the total cell number because each chondrocyte contains an equivalent amount of nuclear DNA during most of the cell cycle.

Results of the Hoechst DNA assay (Figure 20) revealed that significant numbers of cells survived on both the PLGA-IO and PLGA-HAP scaffold materials. Unseeded scaffold materials had no detectable DNA. Seeded PLGA-IO had significantly more associated cellular DNA than either seeded PLGA-HAP substrates or the seeded wells of tissue culture dishes lacking these substrates. Hoechst staining provided visual evidence that the cells could attach to and survive on the PLGA-HAP and PLGA-IO scaffold materials (Figure 21). However, the cells on these substrates were not homogeneously distributed, making it impossible to count cells and thereby confirm the results of the Hoechst DNA assay (i.e. that the PLGA-IO substrate had significantly more cells than the PLGA-HAP substrate).

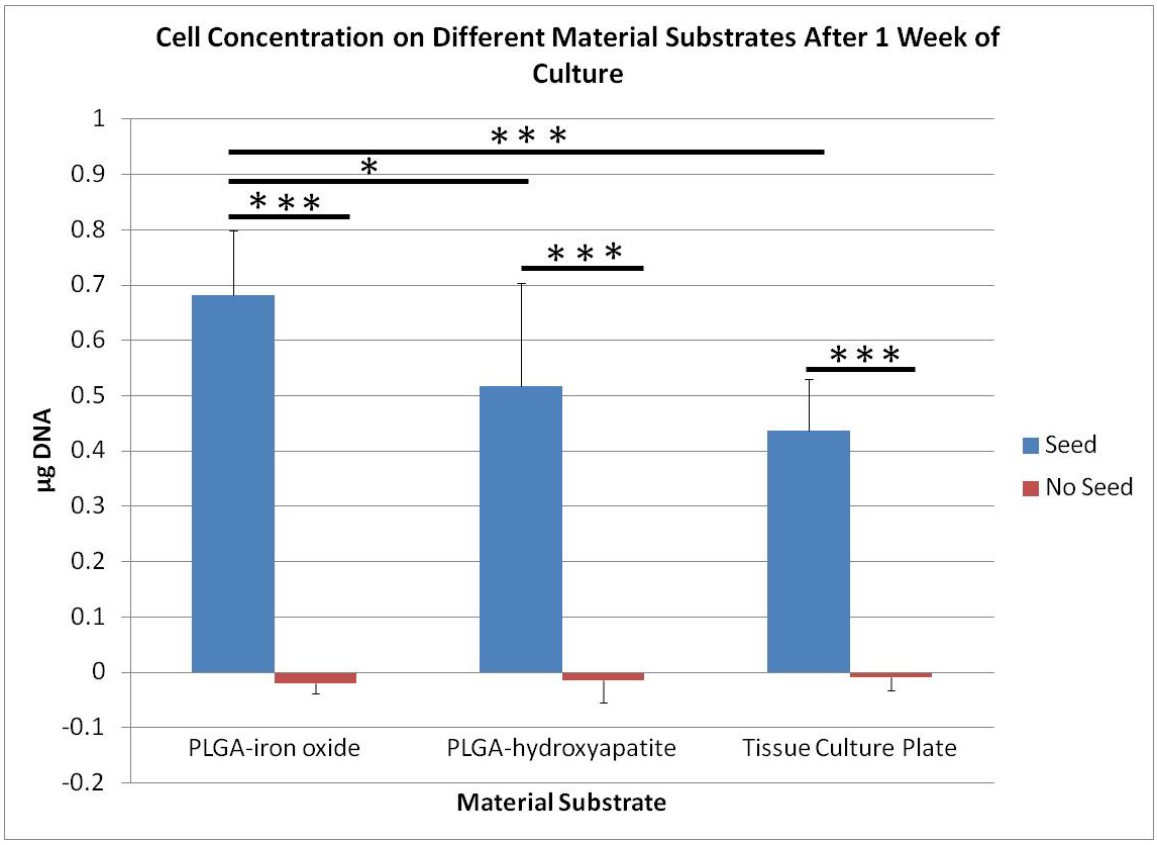

Figure 20. Hoechst DNA assay results from the scaffold substrate experiment (n=8 for each group). A * represents p<0.001, ** p<0.01, and * p<0.05, and the error bars represent one standard deviation for this and all following figures unless otherwise noted.**

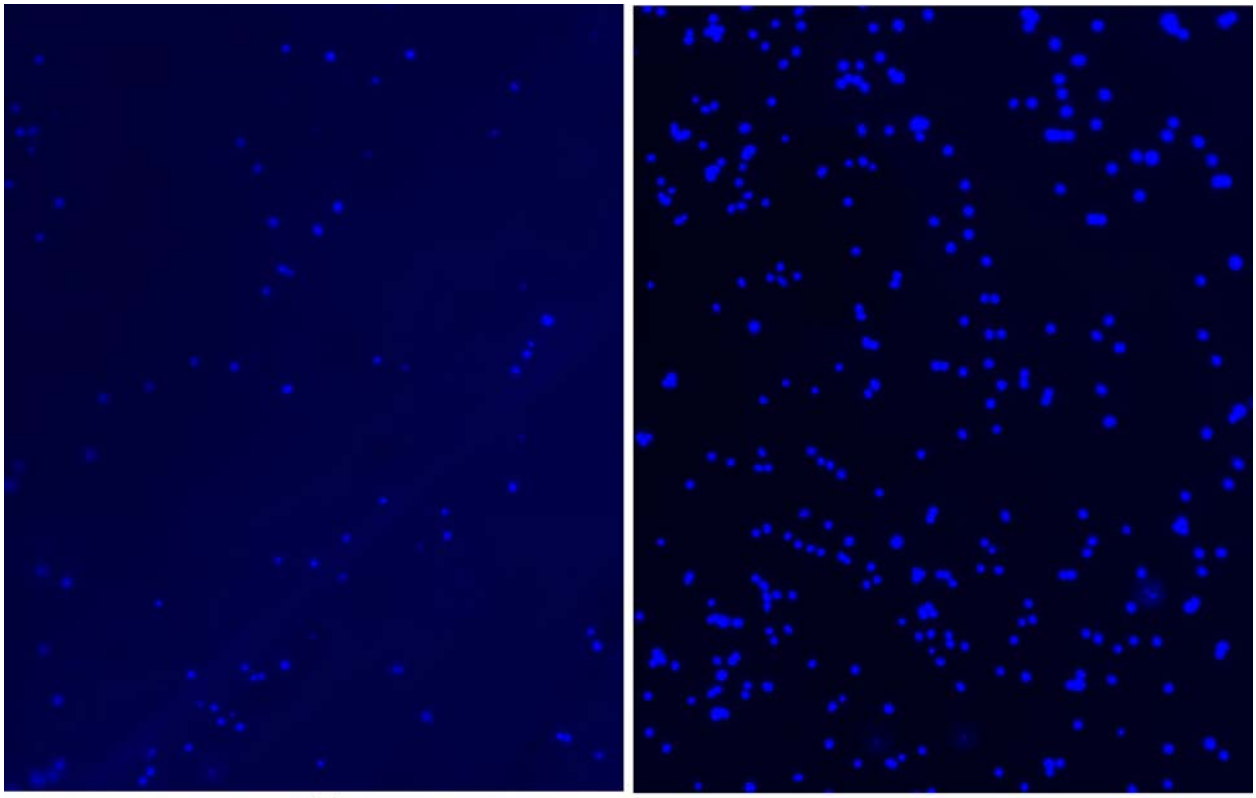

Figure 21. Hoechst DNA staining of porcine chondrocyte nuclei on the (a) PLGA-HAP and (b) PLGA-IO scaffold materials after two days of culture. Photographed using a 10x objective on a Olympus fluorescence microscope.

4.2 Hydrogel Preparation and Characterization

4.2.1 Results from Preliminary Pilot Experiment

The DMMB GAG quantification assay was used to quantify matrix production (indicated by sulphated GAG levels) in supplemented samples and non-supplemented hydrogels. Results from the DMMB GAG quantification assay showed that after ten days in culture there were significantly more total GAGs in the CS, HA, and HACS supplemented hydrogels compared to the untreated (without supplementation) hydrogel control. These treatments all had approximately twice as much total GAGs as the untreated group. In addition, the general linear model revealed that there was a significantly negative interaction between HA and CS ($p=0.027$). An inspection of Figure 22 shows that the effects of the CS and HA were not additive in the HACS group, supporting the results of the aforementioned general linear model.

It should be noted that the 10 minute rinse with Hanks's saline before digestion of the hydrogel (Section 3.3.1) sufficiently rinsed the solubilised CS and HA from the supplemented hydrogels so that they did not interfere with the DMMB GAG quantification assay (data not shown). In addition, the purpose of the lower pH in this assay is to reduce the binding of the DMMB dye to carboxyl group, thereby increasing the specificity of the assay for the sulphate groups present in suphated GAGs and reducing the effects of other carboxylated molecules like HA and alginate[150].

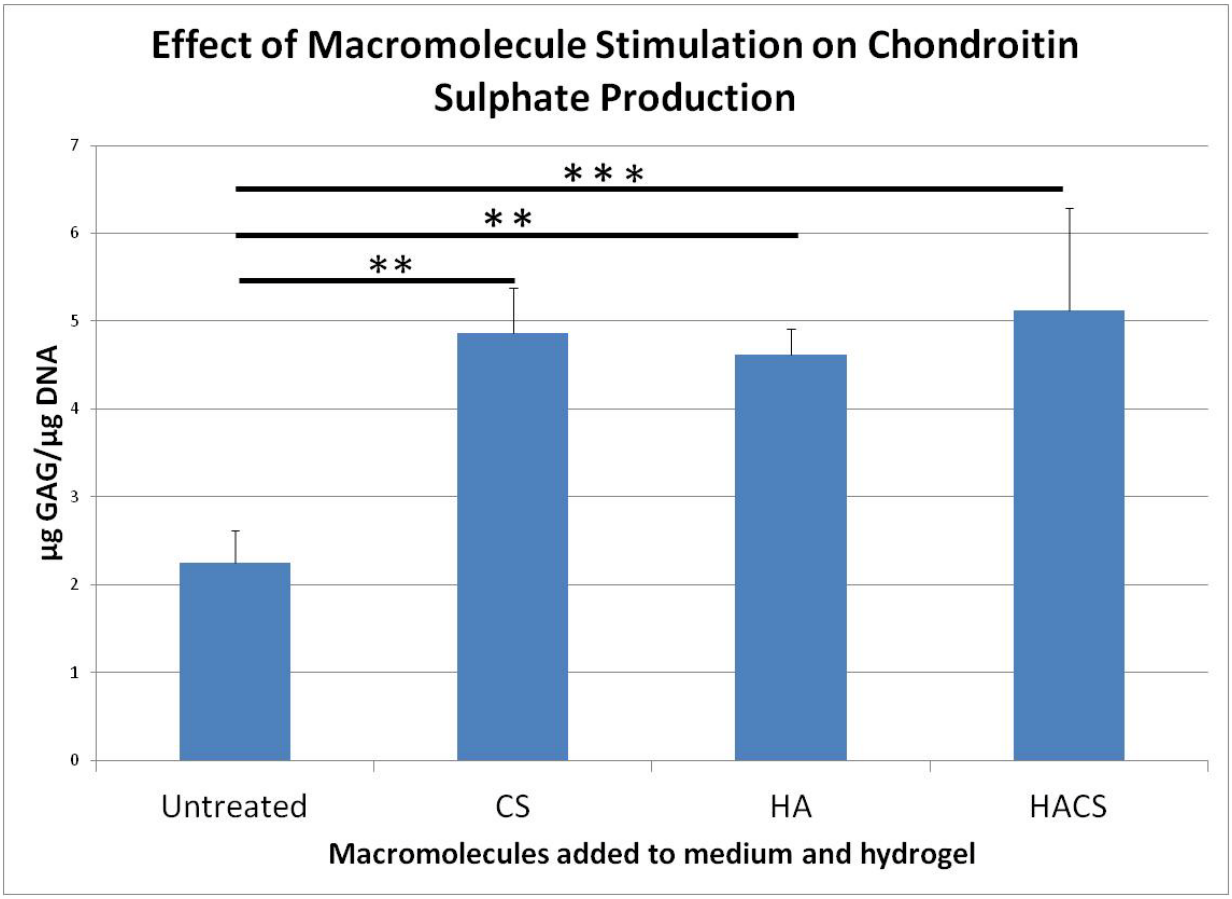

Figure 22. Amount of total GAG produced per each µg of DNA for each of the four treatments (n=3 for each group). The untreated controls were not supplemented with either HA or CS. A * represents p<0.001, ** p<0.01, and * p<0.05, and the error bars represent one standard deviation.**

The Hoechst DNA assay was used to quantify cell population within the hydrogels. The assay revealed that there was significantly less DNA (i.e. fewer cells) in the HA supplemented cultures compared to the untreated cultures after ten days of incubation, as shown in Figure 23. The DNA content of the CS and HACS supplemented hydrogels was not significantly different than the untreated control group.

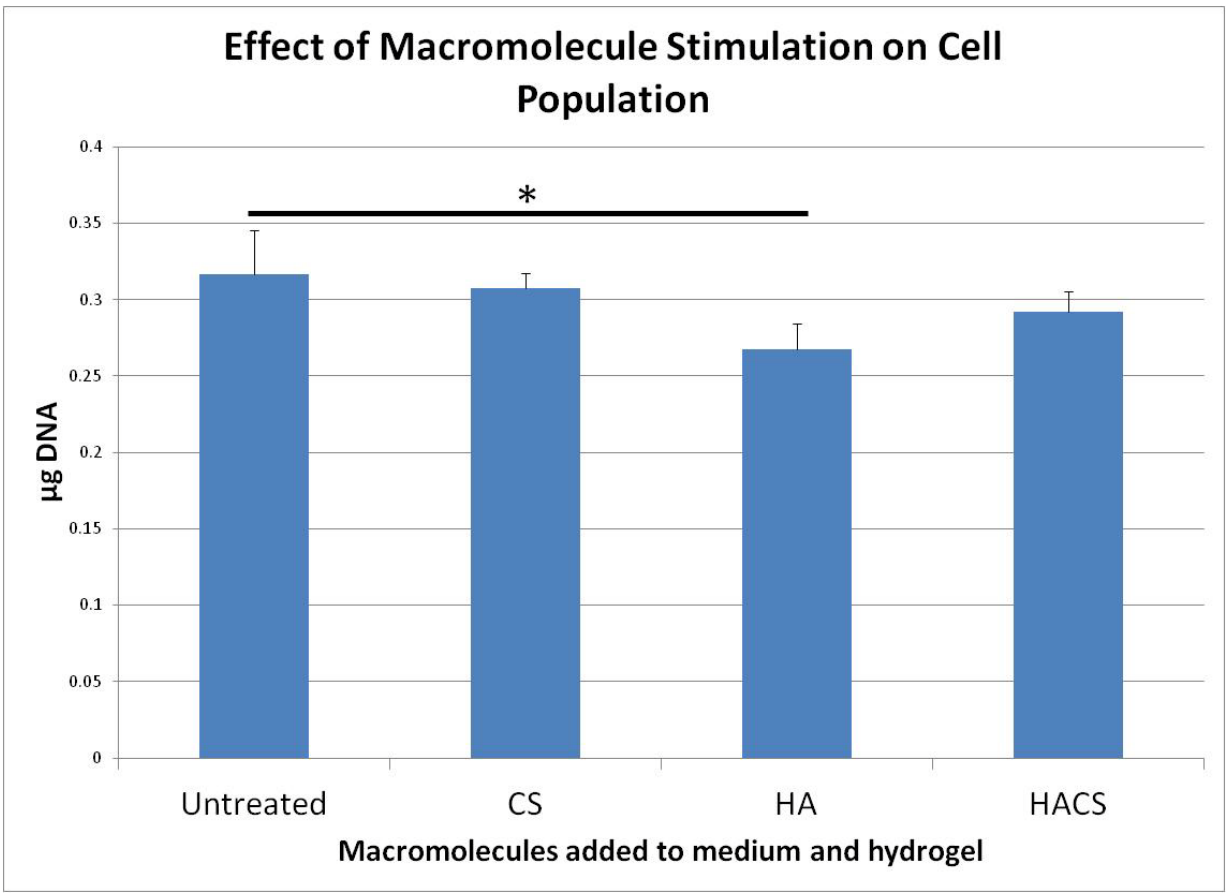

Figure 23. Amount of DNA for each of the four (n=3 for each) macromolecule treatments after ten days of culture. The untreated controls represent hydrogels that were not supplemented with HA or CS. A * represents p<0.001, ** p<0.01, and * p<0.05, and the error bars represent one standard deviation.**

4.2.2 Results from Full Hydrogel Supplementation Experiment

Again, this full hydrogel experiment was similar to the preliminary pilot study completed earlier. The main differences between these two studies were the increased number of replicates, performing two time points for the DMMB and Hoechst assays, and an initial time point for the Hoechst assay to measure cell proliferation, immunostaining of the week 1 and 2 samples, and RNA analysis of the week 1 samples.

The results of the DMMB GAG quantification assay indicate that after one week of culture, there was approximately twice as many GAG in the hydrogels supplemented with CS, HA, and HACS compared to untreated wells. This paralleled the results obtained in the preliminary pilot experiment. The mixed-effects linear model fit to the week 1 data suggests that there was a significant negative interaction between the HA and CS (p=0.0049). A negative

interaction in the context of this experiment suggests that the effects the HA and CS have individually on chondrocytes in hydrogel culture do not sum with one another when hydrogel cultures are supplemented with both macromolecules. Figure 24 shows that the effects of the CS and HA were indeed not additive, supporting the findings of the mixed-effects linear model.

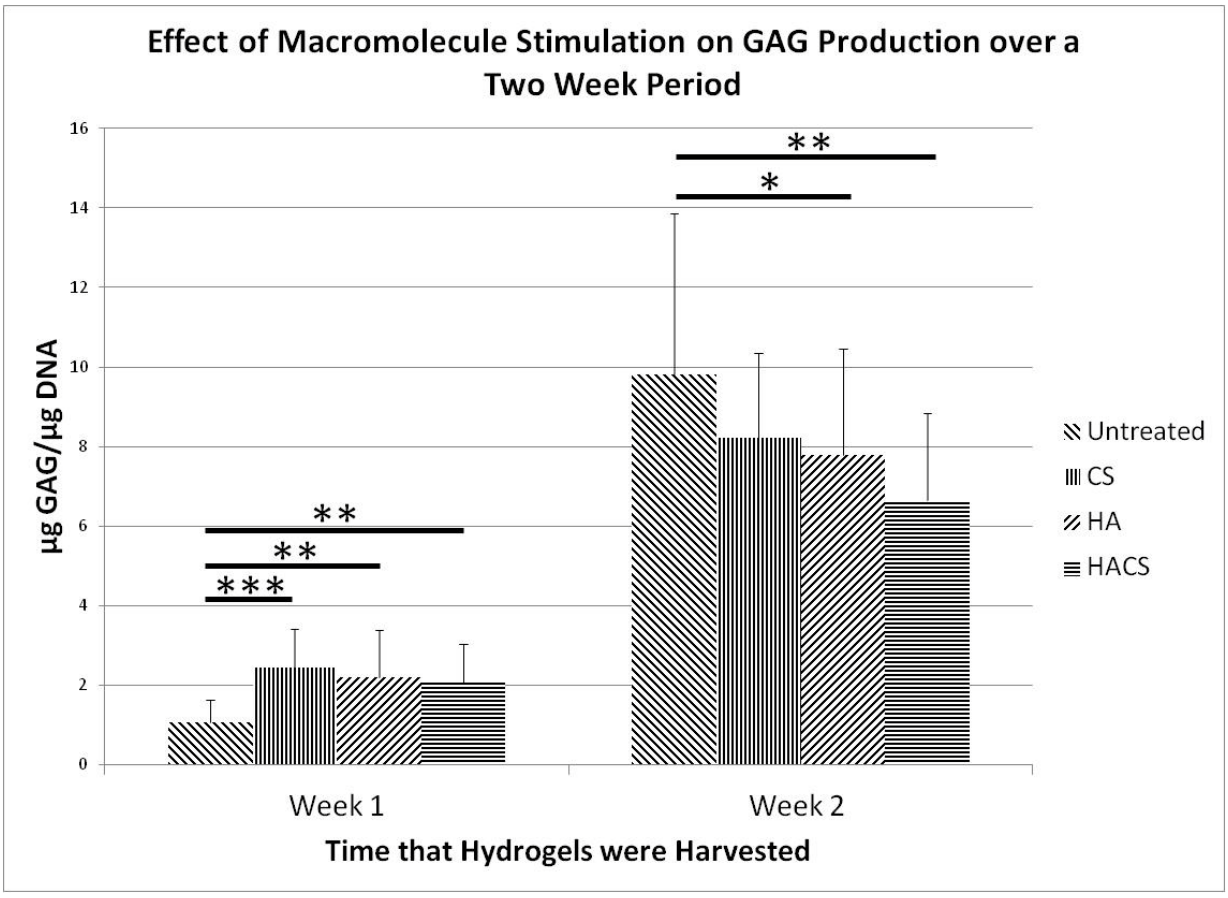

Figure 24. The effects of macromolecule stimulation on total GAG per µg DNA production at week 1 (n=7 for each treatment), and week 2 (n=5 for each treatment). A * represents p<0.001, ** p<0.01, and * p<0.05, and the error bars represent one standard deviation.**

The week 2 data showed a reversal of the trend found in week 1, with the untreated control hydrogels containing significantly more µg GAGs/µg DNA than either the HA or HACS treated groups. The CS supplemented hydrogels did not have significantly different levels of µg GAG/µg DNA than the non-supplemented hydrogels. In this case, there was not a significant statistical interaction (mixed-effects linear model) between the HA and the CS treatment effects (p=0.687), suggesting that their effects on GAG production per cell were neither antagonistic nor synergistic.

The Hoechst DNA assay showed that there was roughly a two-fold increase in cellular DNA (i.e. cell numbers) in the untreated hydrogel controls during the first week, but that the cell population did not significantly increase during the second week, as shown in Figure 25. As with the DMMB assay, the results for week 1 were similar to those observed in my earlier preliminary experiment. That is, that the HA, CS, and HACS treated hydrogels had slightly lower mean cellular DNA than the untreated hydrogel control, although the decrease was not significant at this time point. In addition, there was no significant interaction between the HA and CS treatment effects (p=0.112).

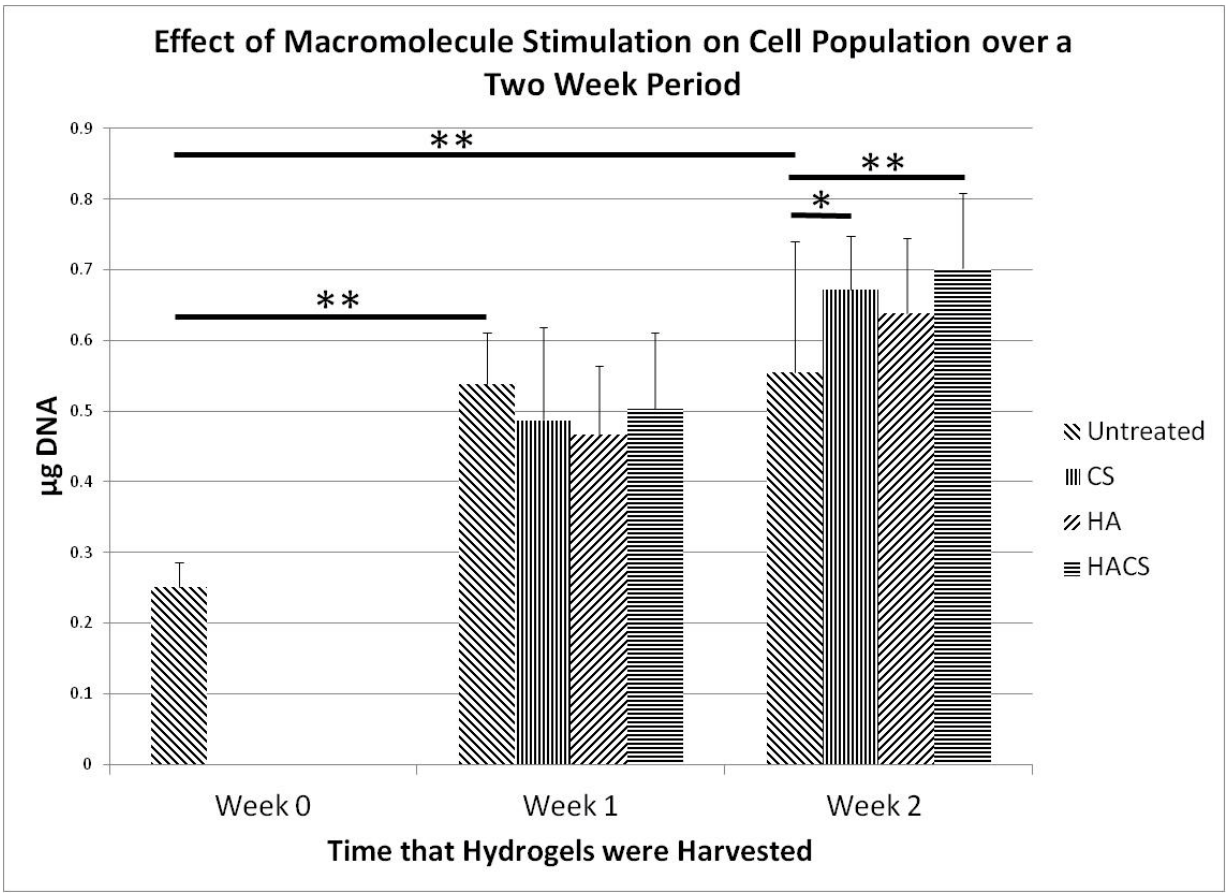

Figure 25. The effects of macromolecule stimulation on cell population at week 0 (n=5), week 1 (n=7 for each treatment), and week 2 (n=5 for each treatment). Untreated hydrogels were not supplemented with either HA or CS. A * represents p<0.001, ** p<0.01, and * p<0.05, and the error bars represent one standard deviation.**

In contrast, by week 2 of culture the CS and HACS treated hydrogels had accumulated significantly more cells than the untreated hydrogel control. There was no significant interaction between the HA and the CS treated hydrogels (p=0.394). Since the higher cell populations in the

week 2 CS and HACS treated hydrogels might account for the lower µg GAG/µg DNA in the week 2 samples (Figure 24). It was important to see what effects the macromolecule treatments had on the non-normalised GAG accumulation. As shown in Figure 26, there was still a roughly two-fold increase in GAG production in HA, CS, and HACS supplemented hydrogels after one week in culture, but that for the week 2 samples there was no significant difference in the total amount of GAG produced. Note that the mixed-effects linear model shows that there was a negative interaction between the HA and CS treatment effects for both week 1 ($p=0.0115$) and week 2 ($p=0.0378$).

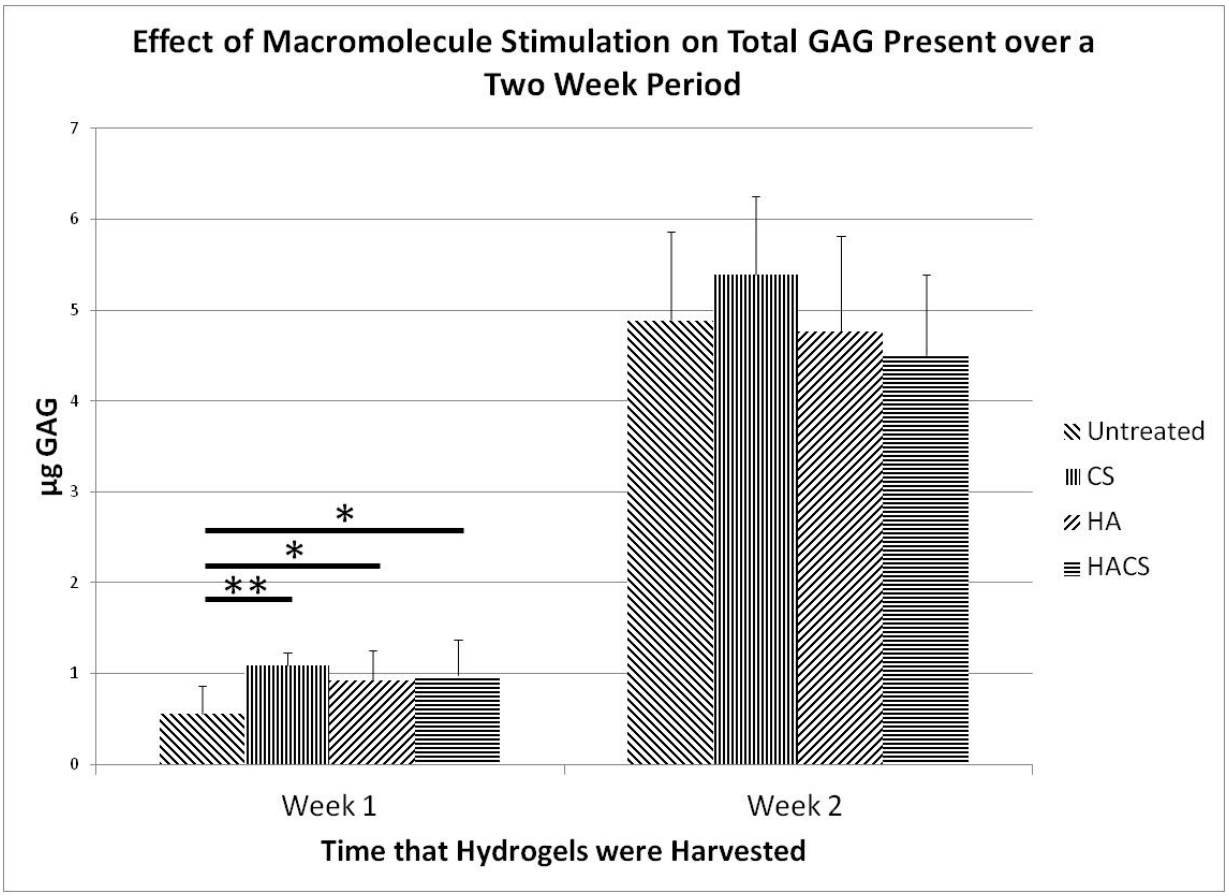

Figure 26. Amount of total GAG present in hydrogel cultures over a two week period when not normalised to DNA amount (n=7 for each treatment group in week 1; n=5 for each treatment group in week 2). Untreated hydrogels were supplemented with neither HA or CS. A * represents p<0.001, ** p<0.01, and * p<0.05, and the error bars represent one standard deviation.**

To determine the levels of mRNAs which coded for collagen type I (col1α1), collagen type II (col2α1), aggrecan, and glyceraldehyde 3-phosphate dehydrogenase (GAPDH), qPCR was used. To show matrix accumulation in the hydrogels during culture the DMMB GAG

quantification assay determined the amount of total sulphated GAG (present in proteoglycans), while the immunostaining provided qualitative information about the collagen types I and II levels. Determining mRNA levels for aggrecan (present in aggregating proteoglycans) and collagen types I and II ostensibly allowed for quantification of the production of these proteins at the time of RNA collection. As mentioned in Section 1.1, high levels of proteoglycans and collagen type II and low levels of collagen type I suggest that chondrocytes are retaining their phenotype. The GAPDH levels were used to normalise the expression levels of aggrecan and the collagen types I and II.

The temperature gradient optimization revealed that an annealing a PCR temperature of 65.8ºC gave a high efficiency value for all 4 genes of interest. In addition, the melt curve analysis and polyacrylamide gels showed that there was only a single amplification product for each of the genes at this temperature (Figure 27). Standard curves were run for each of the genes, as shown in Figure 28, with the 65.8ºC annealing temperature and these gave PCR amplification efficiencies of between 103.6 and 92.8%, which is within the acceptable range given by the thermal cycler's manufacturer[151] and MIQE guidelines[152].

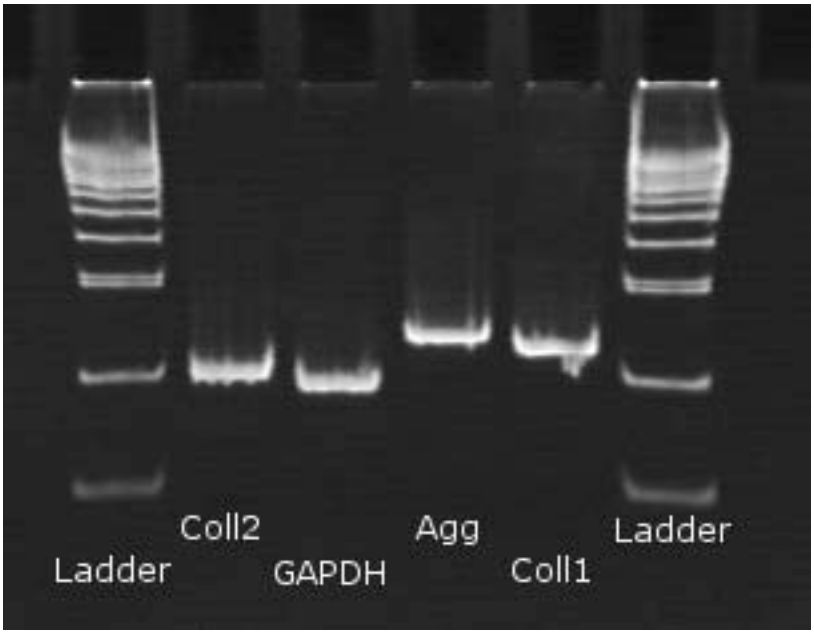

Figure 27. The PCR products, amplified at the optimized annealing temperature of 65.8°C, for the four genes of interest were run on a polyacrylamide gel and all showed only a single band at the designed amplicon length shown in Table 4. The bottom ladder band is 50 base pairs and the second from the bottom is 100 base pairs.

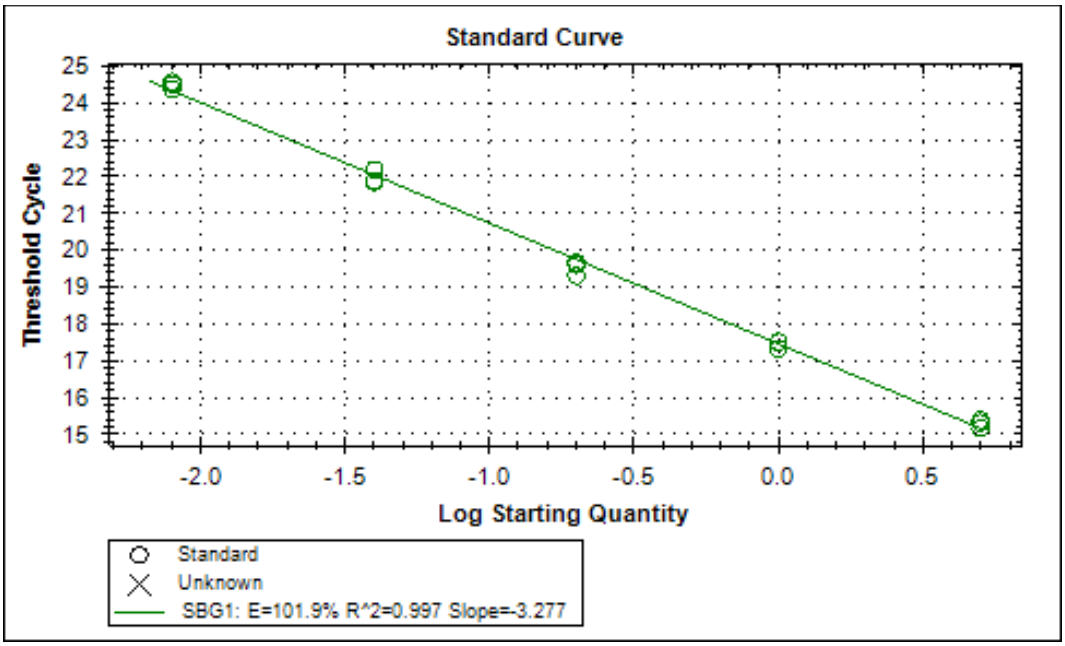

(a) Collagen type II

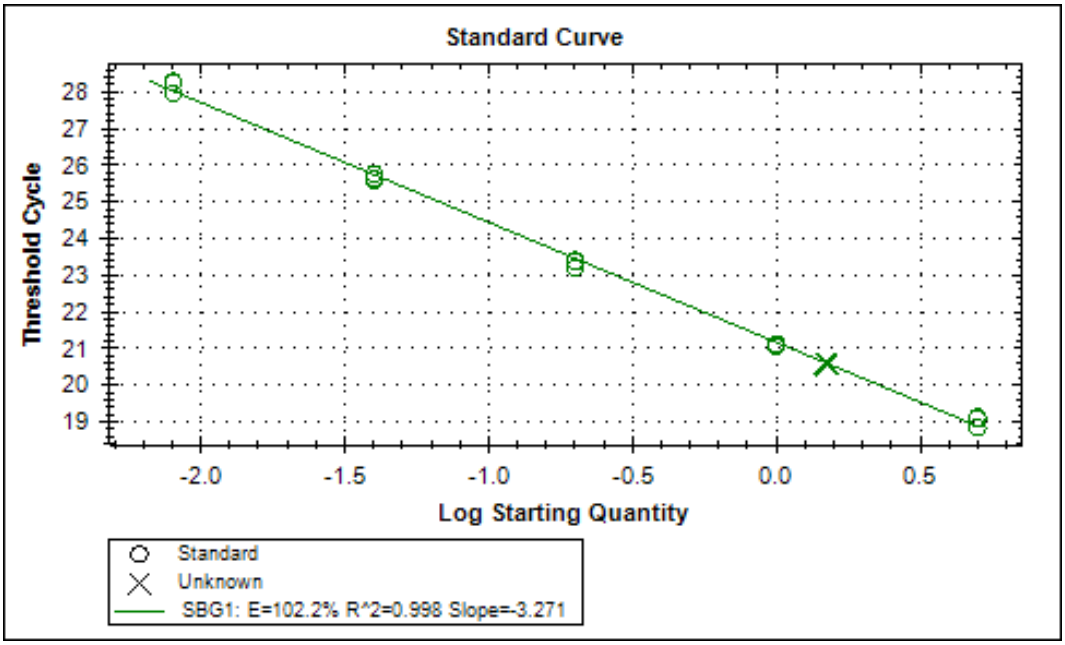

(b) Collagen type I

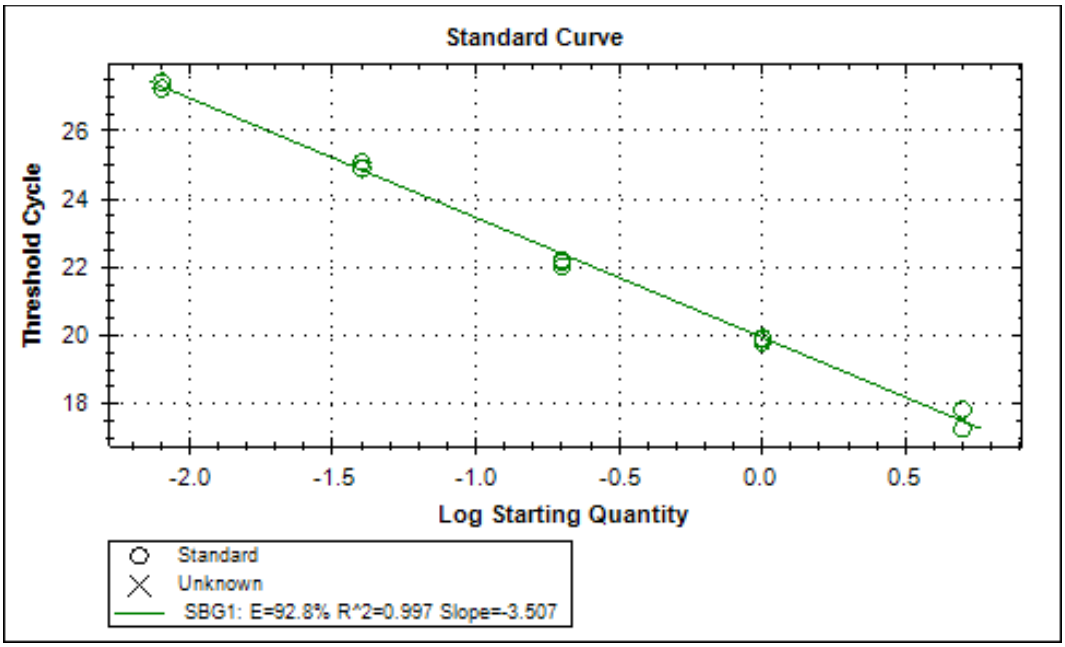

(c) Aggrecan

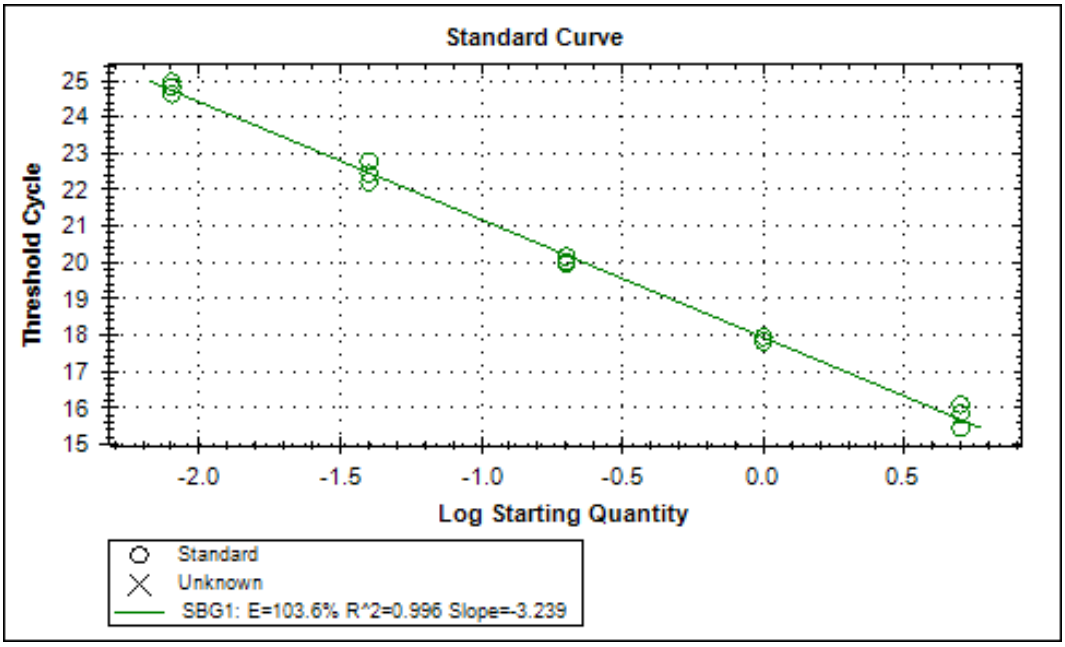

(d) GAPDH

Figure 28. Standard curves for the (a) collagen type II, (b) collagen type I, (c) aggrecan and, (d) GAPDH primers showing that all PCR efficiencies were close to 100%. Each standard curve is based on a 5-fold serial dilution of the cDNA (5x, 1x, 1/5x, 1/25x, 1/125x) with each concentration done in triplicate. All efficiencies and correlation coefficients were within the acceptable range given by the manufacturer of the thermal cycler[151] and MIQE guidelines[152].

With the PCR reactions optimized and the amplification efficiencies determined it was now possible to run the experimental samples and calculate their relative expression ratios using equation 3.1. Normalised gene expression is the amount of target gene (col1α1, col2α1, aggrecan) mRNA normalised to the amount of GAPDH mRNA. The relative expression ratio is the ratio of normalised gene expression in the HA, CS, and HACS supplemented hydrogels (samples), and the normalised gene expression in the non-supplemented hydrogels (controls). The REST software showed that there was no significant up or down regulation of any of the target genes when comparing the three different treatments to the untreated control group. In other words the relative expression ratios, R, for the CS, HA, and HACS treatments were not significantly different from 1 (R for the untreated control group), as shown in Figure 29.

It should be noted that for the HA treated group, one of the samples failed to amplify a PCR product. This could be due to some contaminant in the sample which inhibited either the reverse transcriptase step of the cDNA synthesis or the PCR reaction itself. Therefore, for the HA group there are only 6 samples as opposed to the 7 for all the other conditions. However, this would not compromise the statistical analysis as the randomization test used in REST can be used with groups of unequal size.

The comparisons of gene expression levels in chondrocytes cultured in the untreated hydrogel versus chondrocytes cultured on conventional tissue culture plates for 6 or 12 days versus freshly isolated (uncultured) chondrocytes shown in Figure 30. In this case, the relative expression ratio (equation 3.1) used the untreated hydrogels and conventional cultures as the samples, while the uncultured chondrocytes were used as the controls. The collagen type II mRNA levels were significantly higher in the non-supplemented hydrogel and the day 6 monolayer cultures, but were significantly lower in day 12 culture relative to the freshly isolated chondrocytes. The results for aggrecan gene expression were similar to the collagen type II results except that the aggrecan mRNA level in the day 12 sample was not significantly lower than the freshly isolated chondrocytes. The collagen type I gene expression was much higher in chondrocytes cultured for 6-12 days on standard tissue culture plastic than in chondrocytes within untreated hydrogels, again with all three measured relative to normalised mRNA expression levels in freshly isolated chondrocytes.

The collagen type II to collagen type I ratios presented in Figure 31, show that the 248x collagen type II is much higher than the 12x ratio for the untreated hydrogel, the 1.7x ratio for the day 6 chondrocytes, and the 0.1x ratio for the day 12 chondrocytes. In this case the collagen type II gene expression level was treated as the sample and the collagen type I level treated as the control as reflected in equation 3.2. These relative expression ratios were calculated using REST software, which used bootstrapping to determine the spread of data.

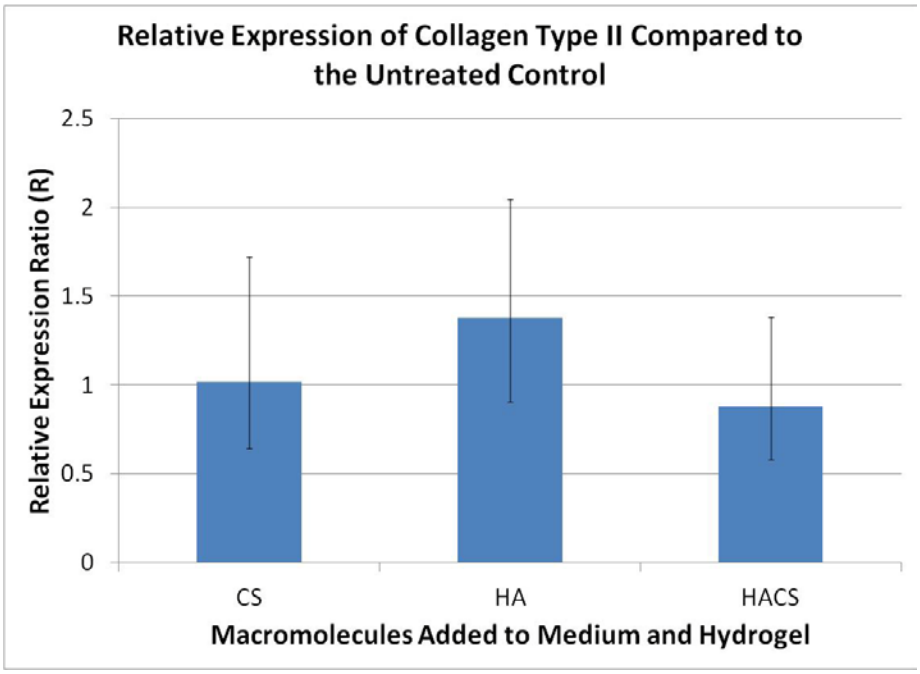
Relative Expression of Collagen Type II Compared to the Untreated Control
Relative Expression Ratio (R)
2.5
2
1.5
1
0.5
0
CS
HA
HACS
Macromolecules Added to Medium and Hydrogel

(a)

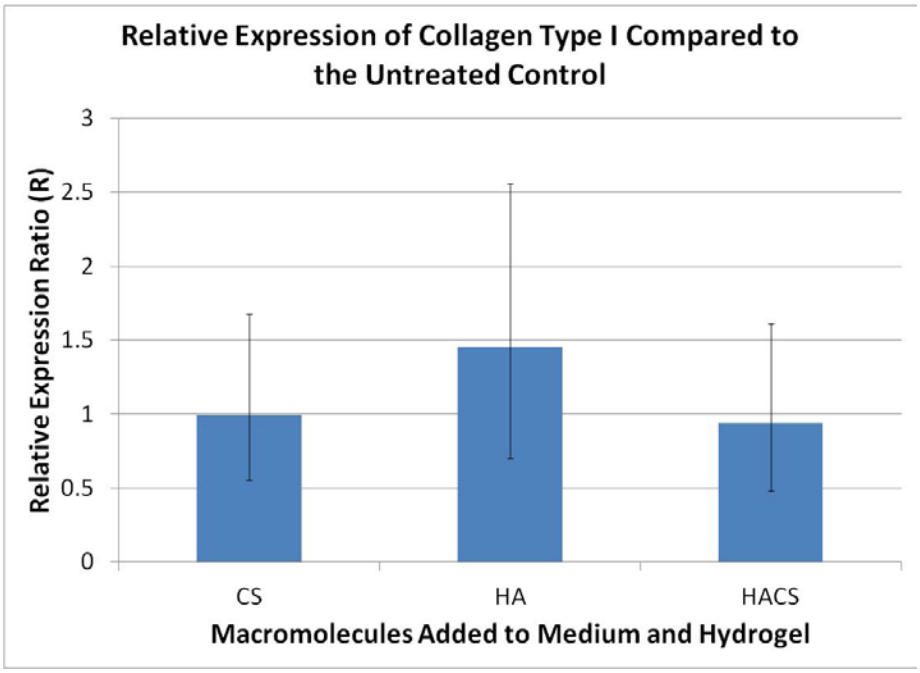
Relative Expression of Collagen Type I Compared to the Untreated Control
Relative Expression Ratio (R)
3
2.5
2
1.5
1
0.5
0
CS
HA
HACS
Macromolecules Added to Medium and Hydrogel

(b)

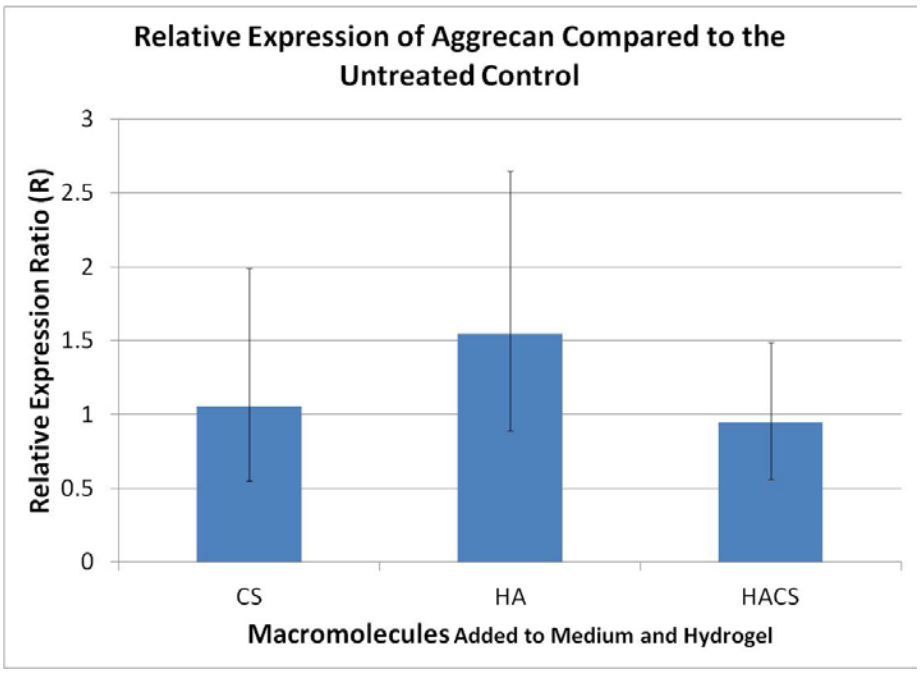

(c)

Figure 29. Plot of the relative expression of the mRNA that encodes for (a) collagen type II, (b) collagen type I and, (c) aggrecan in the CS (n=7), HA (n=6), and HACS (n=7) groups relative to the non-supplemented hydrogel control group. The bar height represents the median and the error bars represent standard error as calculated by REST. The relative expression ration (R) is 1 for the untreated hydrogel.

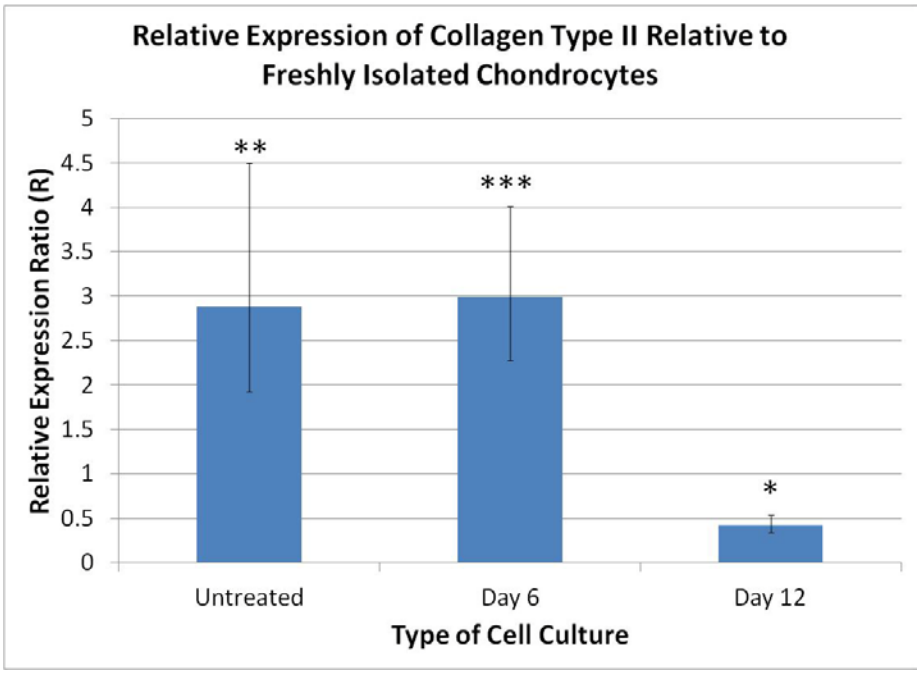
Relative Expression of Collagen Type II Relative to Freshly Isolated Chondrocytes
Relative Expression Ratio (R)
5
4.5
4
3.5
3
2.5
2
1.5
1
0.5
0
**
***
*
Untreated
Day 6
Day 12
Type of Cell Culture

(a)

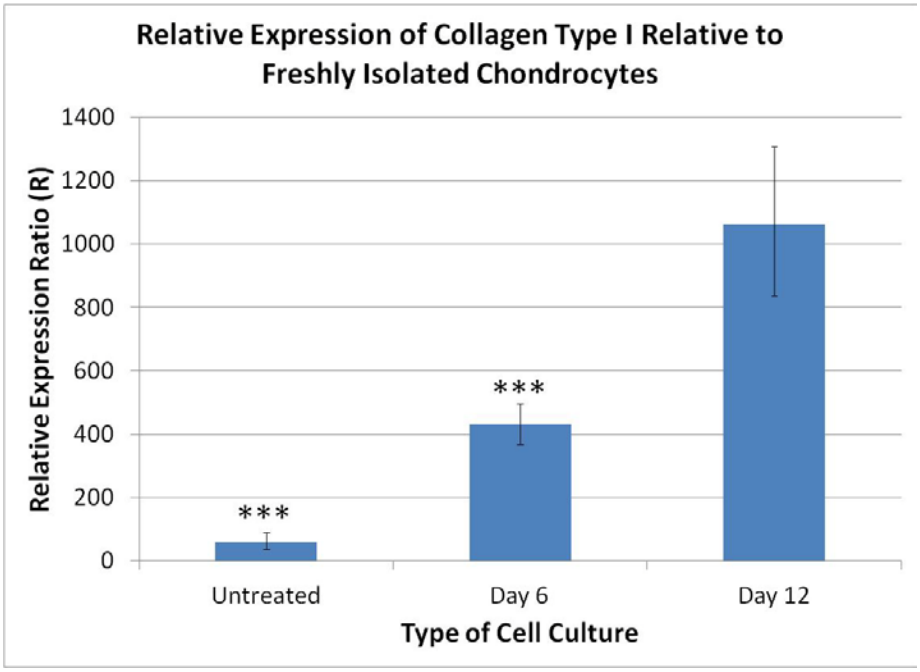
Relative Expression of Collagen Type I Relative to Freshly Isolated Chondrocytes
Relative Expression Ratio (R)
1400
1200
1000
800
600
400
200
0
***
***
Untreated
Day 6
Day 12
Type of Cell Culture

(b)

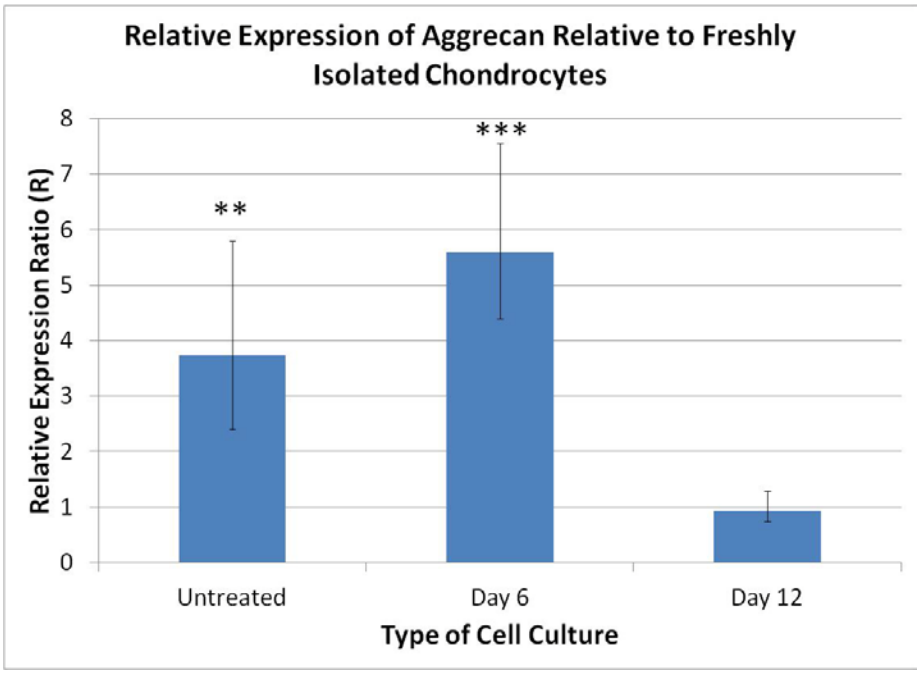

(c)

Figure 30. Results of the qPCR reaction showing how the mRNA expression of the target genes in the untreated hydrogel samples (n=7), and chondrocytes cultured on a conventional tissue culture plate for 6 (n=3) or 12 (n=3) relative to freshly isolated chondrocytes (n=3). The mRNA that encodes for (a) collagen type II, (b) collagen type I and, (c) aggrecan were investigated. Bar height represents the median value and error bars represent the standard error as calculated by REST. R=1 for the freshly isolated chondrocytes.

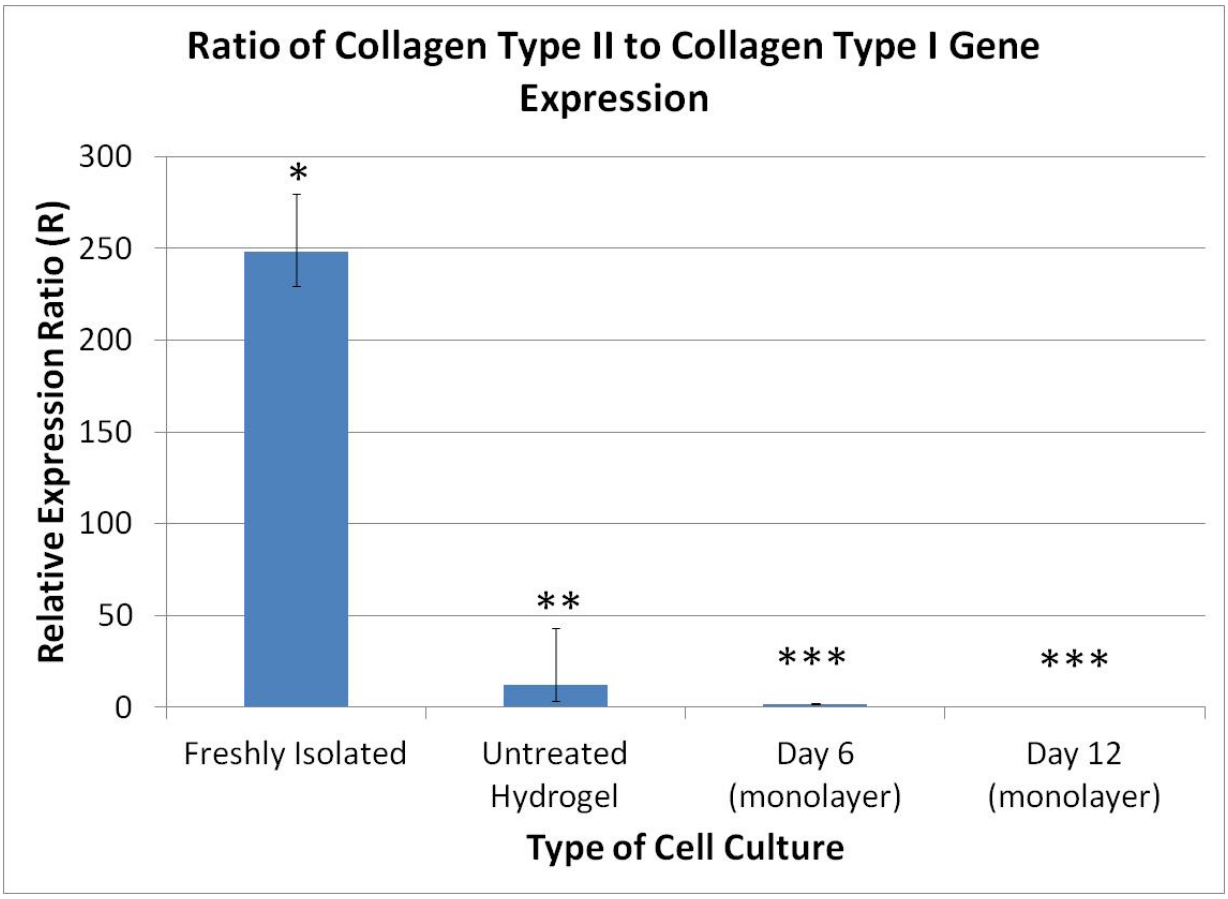

Figure 31. Relative amounts of collagen type II mRNA to collagen type I mRNA for chondrocytes that were freshly isolated (n=3), cultured in an untreated hydrogel for one week (n=7), or cultured in monolayer on a tissue culture plate for 6 (n=3) or 12(n=3) days. The relative expression ratio used the collagen type II mRNA expression level as the sample and the collagen type I level as the control, as indicated in equation 3.2. Bar height represents the median value and error bars represent the standard error as calculated by REST. R=1 when col2α1 and col1α1 have the same level of gene expression.

Immunostaining with antibodies specific for collagen type I and collagen type II proteins demonstrated the accumulation of both types of collagen in hydrogels at week 1 and 2 of culture (Figure 32). This staining suggests that the collagen type II and type I mRNAs detected by qPCR were indeed being translated into proteins.

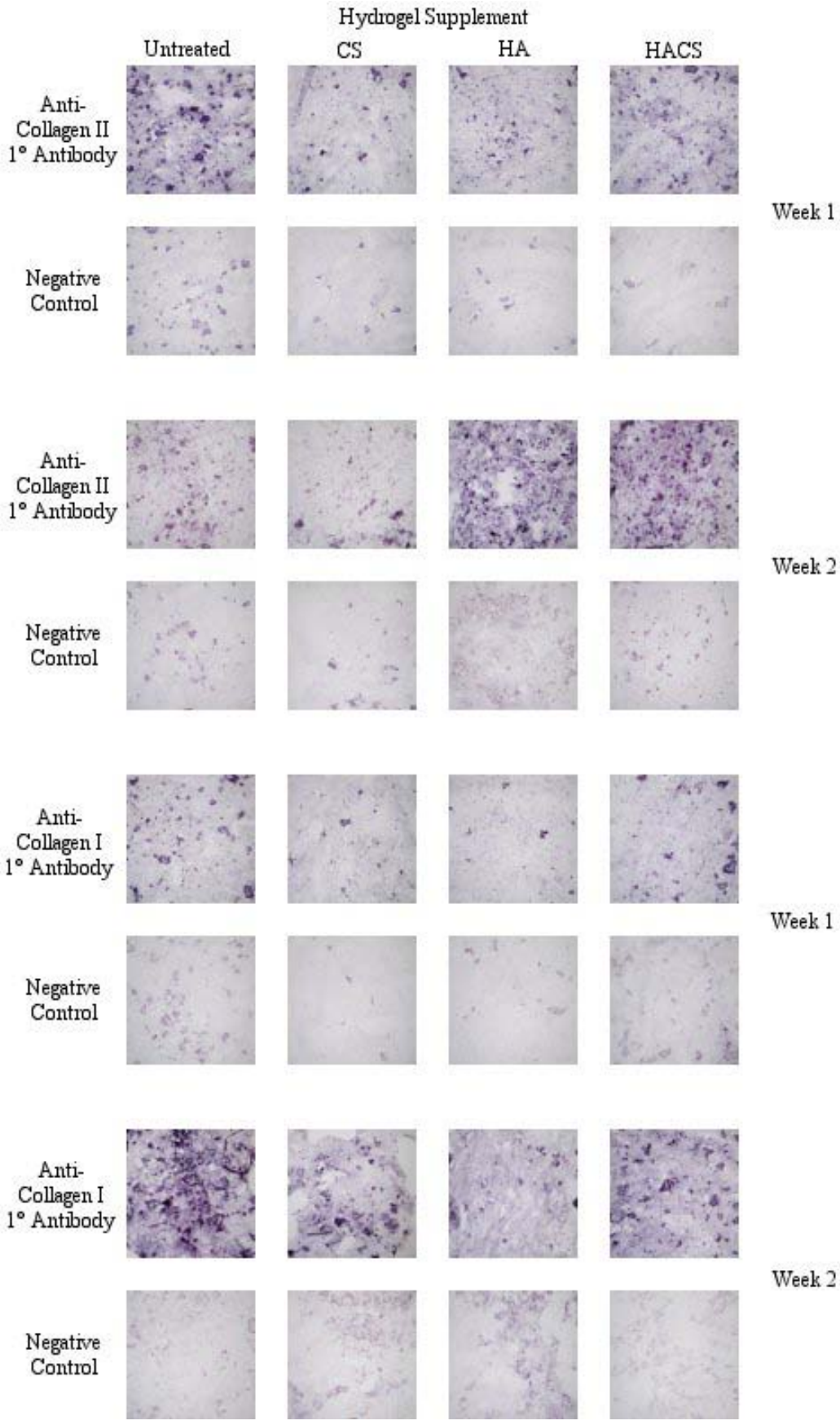
Hydrogel Supplement
Untreated
CS
HA
HACS
Anti-Collagen II 1° Antibody
Negative Control
Week 1
Anti-Collagen II 1° Antibody
Negative Control
Week 2
Anti-Collagen I 1° Antibody
Negative Control
Week 1
Anti-Collagen I 1° Antibody
Negative Control
Week 2

Figure 32. Immunostaining of cryogenic sections of the full hydrogel supplementation experiment. Staining revealed that there was an accumulation of collagen types I and II proteins over time. The negative controls were incubated with 5% Sheep Serum in PBST instead of the 1° antibodies. We used a Leica microscope using the 10x objective.

4.3 Composite Scaffold Fabrication and Characterization

The PLGA-IO scaffold proved suitable for both scaffold fabrication and chondrocyte culture. In addition, cells were successfully cultured within the fibrin-alginate hydrogel and it was demonstrated that supplementation had a positive short-term effect on sulfated GAG accumulation. This experiment infused a hydrogel supplemented with CS into a mechanically stable PLGA-IO solid scaffold in an attempt to demonstrate that cell proliferation and matrix accumulation was higher in a composite scaffold compared to a solid scaffold not impregnated with the hydrogel.

The solid scaffolds were successfully impregnated with the seeded hydrogel, as shown in Figure 33, whereas the solid scaffold controls (without hydrogel) sat in a dense cell suspension for seeding. The DMMB assay showed that there was significantly less sulphated GAG accumulation in the solid scaffold controls than in the composite scaffolds. The amount of GAG detected for the composite scaffold was essentially 0 µg while the amount in the solid scaffold controls was -1.5 µg. It is noted that there is not actually a negative mass of sulphated GAG, but rather that less of the DMMB dye was bound in the solid scaffold control samples than in the 0 µg/ml standard. This is likely due to some of the alginate present in the 0 µg/ml standard binding with the DMMB dye while the solid scaffolds without hydrogel lacked alginate. The Hoechst DNA assay showed that there were significantly more cells in the composite scaffolds than the controls, as shown in Figure 35.

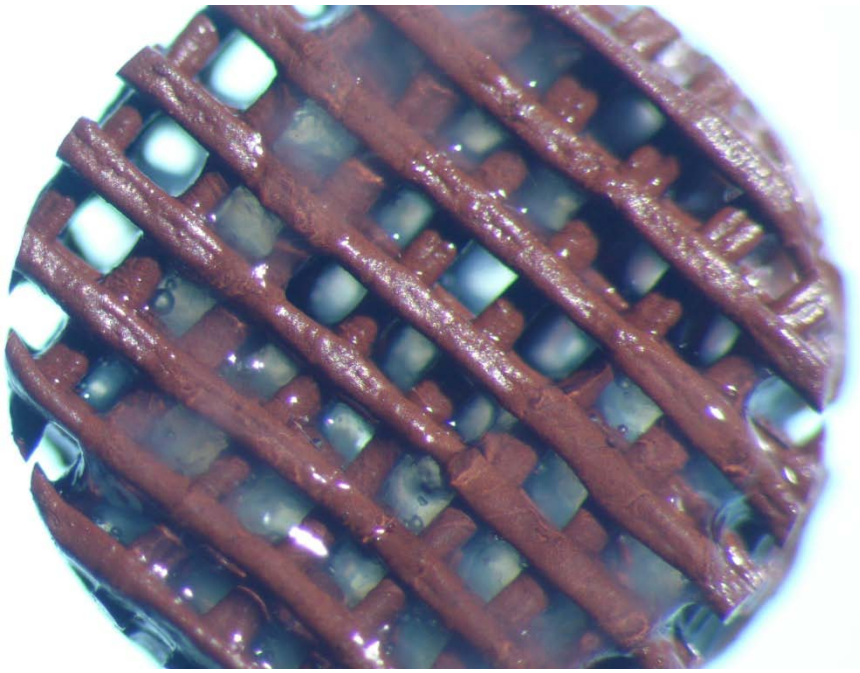

Figure 33. Photograph of the composite scaffold showing that the fibrin-alginate hydrogel could indeed be infused within the solid scaffold framework. The diameter of the solid scaffold is 5 mm.

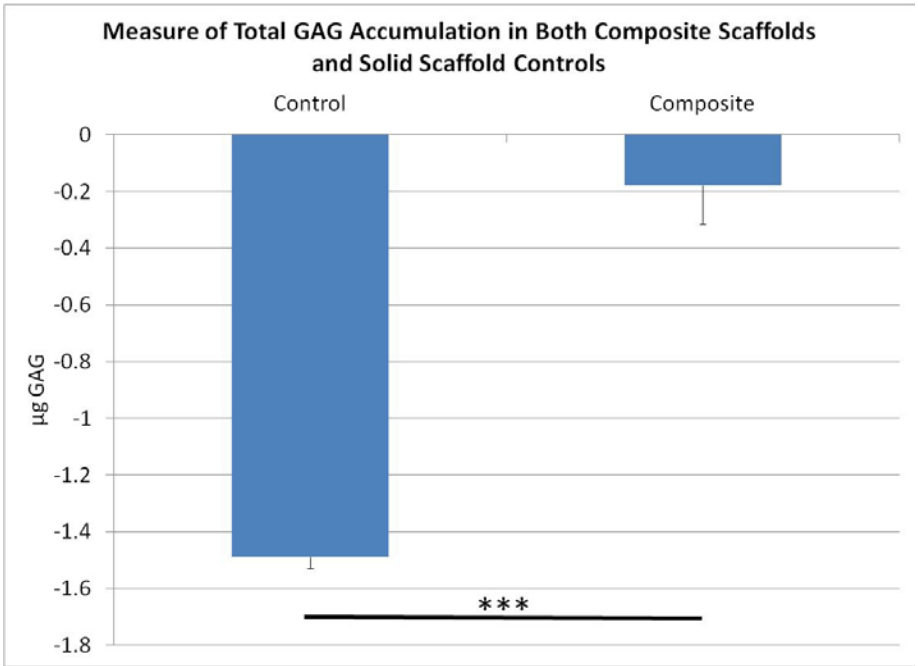

Figure 34. Results of the DMMB assay showing that the composite scaffolds (n=4) was almost identical to the 0 µg standard and the solid scaffold without hydrogel (n=4) had a DMMB reading significantly lower than the 0 µg standard. A * represents p<0.001, ** p<0.01, and * p<0.05, and the error bars represent one standard deviation.**

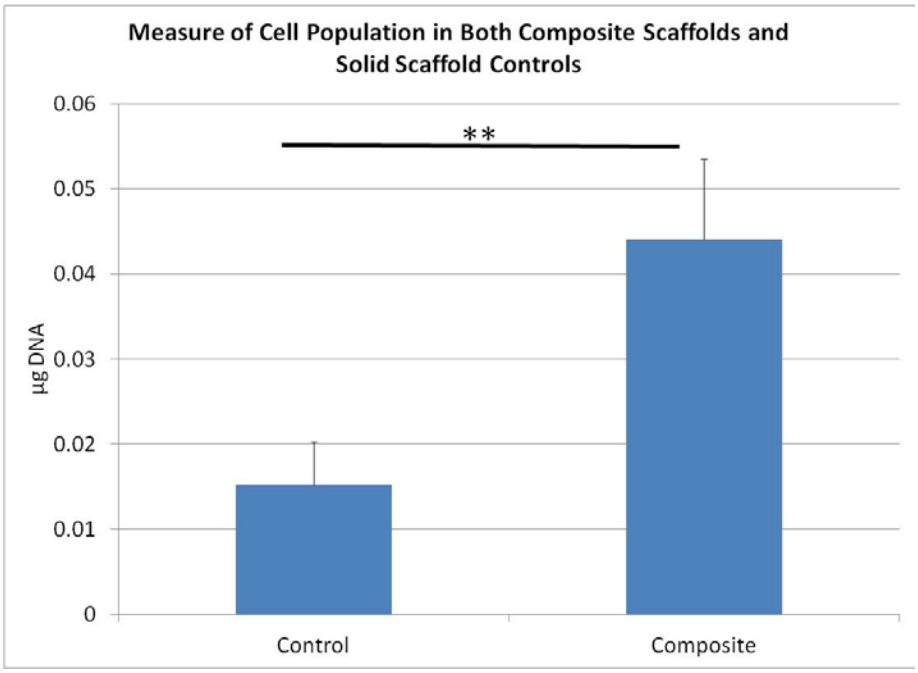

Figure 35. Results of the Hoechst DNA assay for the composite scaffold experiment showing that there were significantly more cells in the composite scaffolds (n=4) than in the solid scaffold controls (n=4). A * represents p<0.001, ** p<0.01, and * p<0.05, and the error bars represent one standard deviation.**

4.4 Preliminary Results

4.4.1 Hoechst Staining of Hydrogels

The Hoechst staining of the hydrogels, shown in Figure 36, showed that the cells were indeed surviving throughout the hydrogel and were evenly distributed.

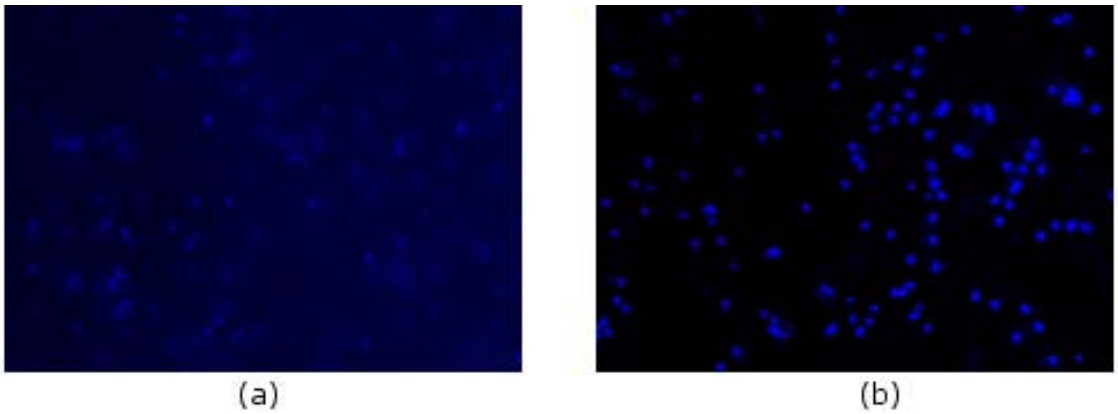

Figure 36. Hoechst staining of (a) chicken sternal chondrocytes after 5 days of culture while still in the hydrogel, and (b) porcine chondrocytes in a cryogenically sectioned cross-section from the preliminary pilot hydrogel experiment (Olympus microscope; 10x objective).

4.4.2 Alcian Blue Staining of Hydrogels

Alcian Blue histochemical staining, shown in Figure 37, of some of the early hydrogel cultures provided visual evidence that the embedded chondrocytes were indeed producing sulphated GAG. This indicates that the chondrocytes were retained their phenotype in the hydrogels.

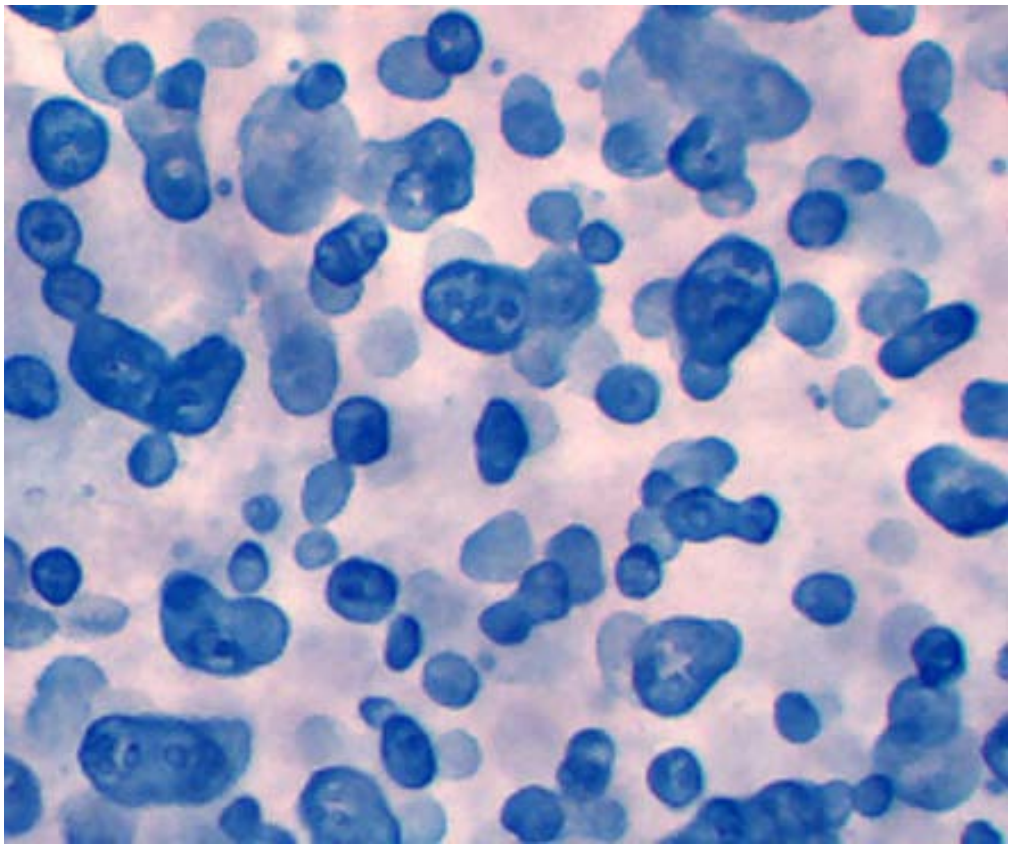

Figure 37. Alcian Blue staining of chicken sternal chondrocytes in the fibrin-alginate hydrogel after 8 days of culture showing a sphere of secreted proteoglycans around each of cluster of cells (dark spots in the centre of the blue spheres). Photograph taken using a dissecting microscope (Wild dissecting microscope, 40x objective).

Chapter 5: General Discussion

5.1 Solid Scaffold Fabrication and Experimentation

The purpose of this portion of the project was to determine if solid scaffolds could be fabricated with a PLGA-IO material slurry, and if so, to find if this material could support chondrocyte culture. This study represents the first time that IO has been used as the nanoparticle in a material slurry used for scaffold fabrication.

Both the photographic evidence and the microtomography showed that it is indeed feasible to fabricate scaffolds with overhanging structures (i.e. interconnected pores) with the PLGA-IO material slurry. The microtomography data allows the virtual sectioning of these scaffolds and confirms that the internal geometry contains repeating overhanging structures and that there is interconnectivity between the pores. This is important because interconnected pores are necessary for chondrocyte proliferation and medium exchange[47]. By examining the cross sections of scaffolds fabricated in the present study (Figure 19), obtained by microtomography, it is apparent that there is some fusion between the scaffold layers. This suggests that the IO concentration in the slurry was appropriate for solid scaffold fabrication. These overhanging structures would not be possible if the IO concentration was too low as the scaffold would fall in on itself, whereas an excessive IO content would prevent flow through the needle and sequentially fabricated layers from fusing with one another at their points of intersection, as demonstrated in an earlier study by Li *et al*[157].

By using the porosity equation[47] with the assumption that there is no fusion between the layers and no shrinking in the scaffolds as the chloroform evaporates, the porosity of these scaffolds was evaluated as 61% from the design parameters listed in Section 3.2.1. It is noted that the porosity measured using the microtomography data, shown in Table 5, was much smaller than the above evaluated value. This discrepancy is mainly caused by the partial fusion of the layers in the scaffold and the scaffolds undergoing some shrinking as they dried. It is important to take this shrinking into account when designing the initial dimensions of the scaffold as the final pore size will affect both chondrocyte proliferation and matrix production[50].

Culturing chondrocytes on this scaffold material as compared to a previously reported PLGA-hydroxyapatite (HAP) material slurry[48, 55] and a flat tissue culture surface showed that significantly more cells survived on the PLGA-IO material. Both the Hoechst DNA staining and

the Hoechst DNA assay showed that a significant number of cells survived on this material after one week of culture. This suggests not only that chondrocytes can be successfully cultured on a material comprised of both PLGA and IO, but that in terms of cell survivability this composite material is actually preferential to a PLGA-HAP scaffold material slurry.

These findings compared favourably to previous reports describing scaffolds that were fabricated with a PLGA-based material slurry which successfully created interconnected pores with pore sizes similar to the ones used in the present study[48, 55]. In addition, previous studies have also successfully used PLGA-based material for chondrocyte culture[52, 55, 57-60], while others have shown that IO has no detrimental effects on both chondrocyte phenotype[66] and survivability[65].

One of the real strengths of this study is the direct comparison to the biodegradable polymer and HAP scaffold material slurry that has previously been used for solid scaffold fabrication for the purposes of bone tissue engineering[48, 55, 62, 63]. In addition, the non-destructive microtomography imaging used in this study better preserves the internal structure of the solid scaffolds compared to traditional sectioning techniques. The shear-induced damage that can occur with sectioning may affect the pore structure of the interior of the solid scaffold.

Due to time restrictions, we were unable to ascertain the long-term effects of the PLGA-IO scaffold material on chondrocyte cultures. The long-term success of PLGA as a scaffold material for 3D chondrocyte culture was demonstrated in the 6 month *in vivo* study by Jiang *et al*[158]. Although information on the long-term effects of IO on chondrocytes is lacking, based on the positive results from the short-term studies done by Farell *et al*[66] and Heymer *et al*[65] chondrocyte proliferation and phenotype should not be affected by this material. We hypothesize, based on the aforementioned PLGA and IO studies, that chondrocytes will respond favourably to long-term culture on scaffolds fabricated from this PLGA-IO composite material.

Another limitation to the present study is the absence of any investigation into the phenotype of chondrocytes cultured on the PLGA-IO material. Due to the small culture surface area used in this experiment, we felt that all of the cells harvested after one week in culture would be required for the Hoechst DNA assay. However, after performing the DNA assay and measuring the high levels of cellular DNA, it became apparent that a portion of the harvested cell

suspension could have been used either for DMMB sulphated GAG analysis or qPCR. It is suggested that future investigations into this scaffold material include some form of investigation into chondrogenic phenotype retention.

For the purposes of our immediate research, we determined that the PLGA-IO scaffold material was well-suited for making the solid scaffold portion of our solid/hydrogel composite scaffolds. Using the material slurry is advantageous compared to using the high temperature polymer melts reported elsewhere[47] because the low-temperature deposition better protects the bioactivity of the polymer[48] and eliminates the need to have a rapid prototyper capable of high temperatures[159]. This material had greater cell survivability than the previously reported PLGA-HAP slurry, and since PLGA-HAP scaffolds have been shown to promote osteogenic phenotypes[62], it is presumed that the PLGA-IO will also be better suited for chondrogenic cell culture.

5.2 Hydrogel Preparation and Characterization

This portion of the project determined whether HA and CS supplements improved chondrocyte activity compared to an untreated hydrogel control. This represented the first such supplementation study that used a fibrin/alginate hydrogel to suspend the chondrocytes and also the first to explore the effects of supplementing cultures with both solubilised HA and CS. The concentration of HA and CS (0.1 mg/ml) was chosen as it has been shown to enhance matrix production and cell proliferation in HA[21, 22], and matrix production in CS supplemented hydrogels[23]. Finally, this represented the first time that the gene expression of chondrocytes cultured in fibrin/alginate hydrogels and chondrocytes cultured in monolayer was compared to gene expression in freshly isolated chondrocytes.

After 1 week of culture hydrogels supplemented with CS, HA, or HACS all had roughly twice as much µg GAG/µg DNA as untreated hydrogel controls did. Interestingly, the effects of the HA and the CS were not additive when they were combined together in the HACS supplemented hydrogels, inferring that there was no benefit (with respect to sulphated GAG production per cell) to adding both of these macromolecules to the cultures as opposed to just treating with one or the other. Unlike the situation in week 1 samples, after 2 weeks of culture the amount of GAG/µg DNA within the HA and HACS treated samples was significantly lower

than in untreated hydrogels. The CS treated hydrogels were also lower than the controls, though not significantly so. In this case effects of the HA and the CS were roughly additive. This suggests that individual cells in the supplemented hydrogels were producing more sulphated GAG than individual chondrocytes in the non-supplemented hydrogels during the first week, and less sulphated GAG during the second week. This eventual inhibition of sulphated GAG production is important as it infers that, on a per-cell basis, the supplementation of these hydrogels is actually slowing the rate of matrix production.

The effect of macromolecule stimulation on cell population was also examined in the present research. Comparison of the untreated controls for the week 1 and week 2 time points to hydrogels harvested initially showed that there was significant increase in cellular DNA during the first week but not during the second week. This increase in cellular DNA is interpreted as evidence of cell proliferation within the untreated hydrogels. Moreover, since all of the supplemented hydrogels had either DNA levels not significantly different from, or significantly greater than, the untreated hydrogels this inferred that there was chondrocyte proliferation in all treatment groups. This proliferation demonstrates both the biocompatibility of the fibrin/alginate hydrogel and the suitability of the cell seeding concentration used.

The Hoechst data for the week 1 samples showed that all treated hydrogel groups had roughly equivalent cell numbers as the untreated control. However, after 2 weeks of culture the CS and HACS treated samples both had significantly higher cell populations than the untreated controls, with the HA treated sample trending higher than the untreated control, though not significantly so. The higher levels of cellular DNA in the supplemented hydrogels after 2 weeks may be due to the earlier elevated sulphated GAG levels in the supplemented hydrogels harvested after 1 week of culture. This would suggest that while the solubilised CS and HA do not have an effect on cell proliferation, the accumulation of ECM molecules produced by the chondrocytes may.

The fact that cell population differed between treatments in the later time point, and that many of the previous studies on macromolecule stimulation [21, 22, 24] do not normalise their µg GAG readings to cell population, prompted the examination of the unnormalised DMMB readings as well. This unnormalised sulphated GAG accumulation data was similar to the normalised data in the week 1 samples, but the examination of the unnormalised week 2 data

showed that there were not significant differences between the treated samples and the untreated hydrogel controls.

It is probable that the matrix accumulation due to the embedded chondrocytes producing their own CS and HA had become so high during the second week that the stimulatory effects of the supplemented CS or HA became negligible. The similar levels of unnormalised sulphated GAG accumulation in all hydrogels after two weeks of culture regardless of cell population could be due to the cells reducing their proteoglycan production in response to the high levels of accumulated ECM surrounding them. This trend of decreasing matrix production with matrix accumulation was previously reported by van Susante *et al.*[24] and it would effectively allow the untreated hydrogel to "catch-up" to the three different supplementation treatments during the second week. This would also account for the lower sulphated GAG production per individual chondrocyte in the supplemented hydrogels which is discussed above. This is an important distinction, as it suggests that it is not the supplemented CS and HA directly decreasing matrix production (per cell) in week 2, but rather the early elevated levels of accumulated ECM which are due to the CS and HA supplements.

The mRNA analysis examined the gene expression of collagen types I and II and aggrecan mRNAs relative to GAPDH mRNA expression as an indicator of the production of those proteins at the time of cell harvest. The qPCR data showed no significant difference between mRNA expression of each of the three genes of interest (collagen types I and II and aggrecan) in the treatment groups when compared to the mRNA expression of these genes in the untreated control. From this, we infer that at the end of one week of culture none of the supplemented hydrogels were producing significantly more collagen type I, II or aggrecan than the untreated control.

The immunostaining data for collagen types I and II (Figure 32) showed a general trend of both of these proteins accumulating in the hydrogels over time. This suggests that the mRNAs for these collagens that are being detected in the qPCR reaction are in fact being translated into proteins. In addition, the fact that the accumulated sulfated GAG levels so drastically increased between the week 1 and week 2 samples suggests that the aggrecan mRNA that is being detected in the qPCR reaction is being translated into the aggrecan proteoglycan. Visual evidence of this

is displayed in the early Alcian Blue staining of chicken sternal chondrocytes as shown in Figure 37.

When comparing the mRNA expression of the three genes of interest in chondrocytes cultured within non-supplemented hydrogels, and in monolayer on a tissue culture plate for 6 days or 12 days with the mRNA expression of freshly isolated chondrocytes it became apparent that the hydrogel culture helped chondrocytes maintain their phenotype better than culturing in monolayer. Collagen type II and aggrecan gene expression is characteristic of hyaline chondrocytes while high levels of collagen type I indicate that the chondrocytes are de-differentiating. Both the untreated hydrogels (week 1) and the day 6 monolayer cultures showed a significant up-regulation of the aggrecan and collagen type II genes, while the chondrocytes cultured in monolayer for 12 days had collagen type II mRNA levels significantly lower than the freshly isolated chondrocytes. A visual indication of how much better the hydrogel helps chondrocytes maintain their phenotype is provided in Figure 30b, which shows that the collagen type I gene is much more strongly expressed in chondrocytes expanded out on a tissue culture plate than those cultured in the hydrogel.

If one was to view the amount of collagen type II mRNA relative to the amount of collagen type I mRNA as a sort of “differentiation index” as has been previously suggested[154, 160], then the data presented in Figure 31 provides an excellent perspective on how the chondrocytes are maintaining their phenotype. The freshly isolated chondrocytes expressed collagen type II mRNA at over 200 times the level of collagen type I mRNA. Though chondrocytes in the untreated hydrogels had a higher collagen II/collagen I expression ratio (approximately 12:1) than the chondrocytes in monolayer cultures, the ratio was much lower than for freshly isolated chondrocytes. This portion of the gene analysis suggests that while hydrogel cultures help chondrocytes retain their phenotype better than traditional culture techniques, there is most likely some de-differentiation of a portion of the chondrocyte population.

The early (week 1) results for normalised sulphated GAG accumulation and cellular DNA for the aforementioned full hydrogel experiment showed similar results to the preliminary pilot experiment. The primary difference between these experiments was sample size, with the full experiment having 7 samples and the preliminary study having 3 samples per treatment

group. In addition, the preliminary experiment was harvested at 10 days rather than 1 and 2 weeks. The one discrepancy in the results was that the preliminary pilot experiment showed that there were significantly fewer chondrocytes in the HA supplemented hydrogels compared to non-supplemented hydrogel controls. However, it was still only 15% less than the untreated control, which makes one question whether or not an effect size this small is actually biologically relevant. In addition, the week 1 HA supplemented samples of the more comprehensive full hydrogel supplementation experiment were not significantly different from the non-supplemented hydrogels, giving us further confidence that the early effect on HA on chondrocyte population, if any, is minimal.

The early elevated sulfated GAG levels in samples treated with CS relative to non-supplemented hydrogels in the week 1 (Figure 26) samples was not found in a previous study by van Susante *et al.*[24]. In contrast, the week 2 GAG/µg DNA data reported by this same study showed a similar result to those seen within the present work while the study put forward by Bassleer *et al.*[23] on clustered cultures of human chondrocytes showed significantly more GAG/µg DNA after 16 days of culture in samples treated with CS than in non-supplemented controls.

Both the studies presented by Kawasaki *et al.*[22] and Akmal *et al.*[21] found that there was no significant difference in GAG production after 1 week of culture and significantly more GAG production in HA treated samples cultured for 2 weeks, relative to untreated hydrogels. This differs from the results reported in Figure 26, which show a significantly higher amount of GAGs in the HA treated samples at week 1 and no significant difference between the HA treated samples and controls after 2 weeks of culture. This discrepancy may be due to the chondrocytes producing sulphated GAG at a faster rate in the fibrin/alginate hydrogel as opposed to the alginate or collagen I hydrogels used in these other studies. This would lead to a higher early accumulation of sulphated GAG in our study, with matrix production decreasing with increasing matrix accumulation as described above.

The DNA levels in CS treated hydrogels closely matched those reported in the van Susante *et al.* study[24]. Namely, samples treated with CS have previously been shown to have similar cell populations to non-supplemented hydrogel controls after 1 week of culture, but a significantly higher cell population after 2 weeks.

The literature is ambiguous when showing the short-term effect of HA supplementation on chondrocyte numbers in hydrogel culture with Akmal *et al.*[21] stating no significant difference in cell population after 1 week, while Kawasaki *et al.*[22] show a significantly higher cell population compared to non-supplemented hydrogel cultures. Our results closely correspond to the week 1 cellular DNA results presented by Akmal *et al*[21].

The literature is slightly more consistent regarding the effects of HA supplementation after 2 weeks of hydrogel culture relative to non-supplemented controls, with both of the aforementioned HA supplementation studies showing a significantly higher cell population after 2 weeks of culture, and a third study by Nishimoto *et al.* not showing a significant difference[161]. Though the week 2 DNA levels in the HA treated hydrogels were not significantly higher than untreated hydrogels, there was certainly a trend in the same direction, as shown in Figure 25, suggesting that our results correspond with those found in the literature.

Both the Nishimoto and van Susante findings for the effect of CS supplementation on gene expression were similar to what we report in this study (Figure 29). In the study performed by Nishimoto *et al.*[161], they found that after two weeks of culture in a collagen hydrogel supplemented with CS there was not a significant difference in either collagen type II or aggrecan mRNA expression. Van Susante *et al.*[24] also measured how much S^{35} uptake there was over a three hour period in both non-supplemented samples and samples treated with CS. This, like the mRNA analysis for aggrecan is an indicator of how many PGs are being produced at a certain point of time. The van Susante study showed that there was no significant difference in S^{35} uptake between the two treatments at both 1 and 2 weeks of culture[24]. When supplementing collagen hydrogels with HA, Nishimoto *et al*. did find a significant decrease in both aggrecan and collagen type II expression compared to untreated controls, which conflicts with the data found in the present work[161]. In addition, the dramatic increase in collagen type I mRNA and the initial increase and then eventual decrease in collagen type II mRNA in chondrocytes cultured in monolayer, reported in Figure 29, was also seen by Marlovits *et al.*[154].

There are a number of possible reasons for why some of the data reported within the present work does not align perfectly with those reported in the literature. For one, almost all of these studies with the exception of Nishimoto *et al.*[161] did not use porcine chondrocytes. There

may be differences in how newborn porcine chondrocytes react to this type of supplementation when compared to human or bovine adult specimens. Another reason could be that none of the other studies mentioned in this discussion section used the same type of three dimensional culturing material that was presented in this thesis. It has been shown previously, that the type of hydrogel used[105], or the use of a solid scaffold instead of a hydrogel[40, 57, 59] can greatly impact chondrocyte behaviour. Finally, the cell seeding density used in this study was different from the ones used in most of the other aforementioned macromolecule supplementation experiments[22-24, 161]. It has been shown that initial cell seeding density also has a significant effect on chondrocyte matrix accumulation and proliferation[32, 33].

A major strength of our study was that both gene expression and matrix accumulation of collagen type I, collagen type II and aggrecan was tested. This allowed us to ascertain in depth how well the chondrocytes were retaining their phenotypes in different culture conditions. Another strength was in the choice of the fibrin/alginate hydrogel, which provided a better long-term environment for chondrocyte culture than fibrin or alginate hydrogels alone would have[42].

One technical limitation we encountered was that the immunostaining signal intensity depended greatly on the quality of the section being stained. If the section was torn, or parts of it washed off during the staining process it would reduce the intensity of the final stain. It is likely that this variability was responsible for not being able to see significant differences between the non-supplemented hydrogel cultures and those treated with macromolecules. On the other hand, the expression of these proteins may truly not be affected by supplementation with CS and HA.

Another limitation was the small number of samples for the chondrocytes cultured in monolayer and freshly isolated chondrocytes. For example, the collagen type I expression for the day 12 culture was not as significantly different from collagen type I gene expression in freshly isolated chondrocytes even though its median value was over 1300 times higher. The reason for this is that for low samples sizes (such as n=3) the randomization test can be quite conservative. However, with an effect of this magnitude, it seems likely that if more samples had been analysed, a significant difference would have been detected.

Finally, while the gene expression data provided valuable information about how well the chondrocytes were retaining their phenotype, it failed to show the stimulation that caused the early matrix accumulation in the supplemented hydrogels. The gene expression analysis may have captured this stimulation if a set of samples had been harvested halfway through week one.

This study showed that, although HA and CS supplementation had a short-term stimulatory effect on sulphated GAG production, these effects were not additive and were short-lived. This suggests that it is not worth the expense of adding both stimulants to the medium. While the HA and CS both elicited roughly the same early matrix accumulation, the CS treated hydrogels had higher levels of cell proliferation after 2 weeks. This increase in cell numbers is important for integration with the surrounding tissue[162] when constructs are implanted *in vivo*. For the immediate purposes of this study, we have shown that since the preliminary composite solid/hydrogel scaffold experiment only has a culture time of one week, it would be advantageous (with regards to sulphated GAG production) to supplement the fibrin/alginate hydrogel with either CS or HA.

Current engineered cartilage still has matrix accumulation well below the levels seen in native cartilage[50]. The mechanical properties[70], cell proliferation and integration with the surrounding tissue[162] are all correlated with this matrix accumulation making it crucial to continue developing techniques that promote cell growth and matrix production.

5.3 Composite Scaffold Experiments

The purpose of this portion of the study was to demonstrate the higher cell survivability and matrix accumulation in composite solid/hydrogel scaffolds relative to solid scaffolds seeded with the same number of chondrocytes. This represents the first time that PLGA-IO has been used as the solid scaffold material and fibrin/alginate has been used as the hydrogel in a composite scaffold.

The impregnation of the PLGA-IO solid scaffolds with the fibrin/alginate hydrogel proved to be successful, as shown in Figure 33. The DMMB assay gave a significantly stronger signal for the composite scaffolds than for solid scaffolds that were not impregnated with a hydrogel. Moreover, the Hoechst DNA assay showed that there was significantly more cellular

DNA in the composite scaffold than in the solid scaffold controls. However, it is not believed that these readings are actually due to the superiority of the composite scaffolds over solid scaffolds without hydrogels.

As mentioned in Section 3.3.2, the standard curve for the DMMB assay was constructed using a set of standards made from dissolved fibrin/alginate hydrogels supplemented with a known amount of CS. Alginate contains a carboxyl group which competes with the sulphate group on the sulphated GAGs to create complexes with the DMMB dye molecules. The effect of these carboxyl groups is minimized by lowering the pH of the assay to 1.5 as demonstrated by Enobakhare *et al*[150]. However, the fact that the solid scaffold controls (without fibrin/alginate hydrogel) yielded a DMMB reading less than the 0 µg CS standard suggests that although the effects of the alginate on the DMMB assay had been minimized, the alginate still caused a background reading. Accordingly, the solid scaffold controls which contained no alginate would produce a lower DMMB reading than would a CS standard (with alginate) with a similar concentration of CS.

The aforementioned background reading due to the alginate means that one cannot use the dissolved hydrogel standards to accurately determine the level of sulphated GAGs in a sample that does not contain an equivalent amount of alginate. Accordingly, the GAG levels in the solid scaffold controls cannot be determined using the standard curve constructed with dissolved fibrin/alginate hydrogels standards. However, since the composite scaffolds and hydrogel standards had an equivalent concentration of alginate, the standards were a fair representation of these samples. Therefore, the fact that the composite scaffold reading was essentially the same as the 0 µg standard suggests that there was indeed not a detectable amount of GAG accumulation during the week of culture in the composite scaffolds.

It should be noted that the DNA readings obtained from the Hoechst assay were much lower than expected based on the large numbers of cells seeded in both the composite scaffolds and the solid scaffolds not impregnated with hydrogel. The DNA levels in the 3D solid scaffold controls (Figure 35) were much lower than when a similar number of cells were cultured on flattened disks of the PLGA-IO scaffold material, as presented in Figure 20. Since the dissociated chondrocytes were frozen in almost the exact same amount of Hanks's saline one

would not expect to see only 6% of the DNA in the solid scaffold controls compared to the earlier substrate experiment.

This low Hoechst reading and the fact that no GAG accumulation was detected suggests that many of the cells initially seeded in both the composite scaffolds and solid scaffolds did not survive the week in culture. This cell death is almost certainly not due to either the PLGA-IO scaffold or the fibrin-alginate hydrogel materials themselves, as my earlier experiments had shown that chondrocytes could be successfully cultured on these materials for at least a week. The most likely explanation is that a large proportion of the chondrocytes died during the initial cell seeding process into both scaffold types. The cells had been subjected to a Trypan Blue dye exclusion assay prior to seeding which showed that the chondrocytes were initially viable. However, after the high cell density overnight incubation to allow the cells to attach to the solid scaffold controls, it was observed that the Phenol Red indicator in the culture medium had turned from red to yellow, indicating that the culture medium had acidified. After the composite scaffolds and the solid scaffold controls were transferred to fresh tissue culture dishes, the cells remaining in the original plates were subjected to a Trypan Blue viability assay which confirmed that over 95% of the cells were dead (results not shown).

The concentrated cell suspension used during the seeding process described in Section 3.4.1 may have depleted the DMEM of nutrients which led to chondrocyte death and cell lysates being released into the medium, causing acidification. On the other hand, the small volume of culture medium may have become inundated with acidic metabolites which caused the chondrocytes to lyse. In either case, since both the solid scaffold controls and the composite scaffolds experienced roughly the same levels of cell death, it is unlikely that the hydrogel impregnation process killed the cells but rather the high cell seeding density. This acidification may be ameliorated by using a less concentrated cell suspension, or by using a medium perfusion system that constantly exchanges the medium.

The low number of viable cells is almost certainly the cause of the undetectable matrix accumulation and the low Hoechst readings. Though the Hoechst assay indicates a greater cell population in the composite scaffolds, it is unclear whether this is due to the superiority of the composite scaffold or not. It could be that the hydrogel was able to better protect the cells from

medium acidification, or was able to better preserve the DNA within dead cells so that it could be detected by the Hoechst assay.

As mentioned earlier, this was a preliminary experiment and as such, had a number of limitations. First, the aforementioned cell death during seeding made it impossible to ascertain matrix accumulation and confidently say whether the DNA levels actually reflected improved chondrocyte retention and survivability. However, previous studies by Lee *et al*.[69] and Gong *et al.*[59] showed significantly higher sulphated GAG accumulation and cell population immediately after seeding and after 1 week of culture in composite scaffolds compared to chondrocytes cultured in solid scaffolds not impregnated with hydrogel. In addition, this preliminary experiment lacked a gene analysis portion which would be a powerful indicator of matrix production at the time of harvest. Malicev *et al*[68]. performed a gene analysis on human chondrocytes in composite scaffold culture for 3 weeks using the same target genes analysed in our hydrogel supplementation experiments and found that collagen type II and aggrecan were upregulated relative to solid scaffold controls, while collagen type I levels were not significantly different. Finally, while this short-term *in vitro* experiment would shed little light on how these composite scaffolds would perform for extended periods of time *in vivo*, there are previously published studies by Fan *et al.*[39] and Eyrich *et al*.[40] which showed that composite scaffolds had superior ECM production and integration with the surrounding tissue after 6 months of *in vivo* culture compared similarly implanted solid scaffold controls.

The composite scaffold reported here has the potential to be a significant improvement over other previously manufactured composite scaffolds [39, 40, 57, 59, 68, 69]. As mentioned in Section 5.1, the PLGA-IO solid scaffold can be fabricated at low temperatures and is more cytocompatible than PLGA-HAP. Moreover, there is evidence that this solid scaffold material will better help chondrocytes preserve their phenotype[62, 65, 66]. In addition, the fibrin/alginate hydrogel utilized here has been shown have better long-term stability than the fibrin hydrogel commonly used in composite scaffolds[42]. Composite scaffolds have previously shown enhanced cytocompatibility and mechanical properties over solid scaffold and hydrogel controls, respectively[59, 70]. Therefore, these scaffolds show great promise in moving cartilage tissue-engineers toward their goal of a long-term, mechanically stable, and cytocompatible engineered cartilage.

Chapter 6: Conclusions and Future Directions

6.1 Conclusions

Based on the aforementioned findings it can be concluded that the PLGA-IO material slurry is suitable for creating scaffolds with porous structure and that a dried film of this slurry has the ability to support chondrocyte culture. The fact that this material had significantly more cells on it than a PLGA-HAP film seeded with an identical number of chondrocytes suggests that this may be a significant advancement in the study of possible scaffold materials for use in tissue engineering scaffolds.

The results of the macromolecule supplementation experiment indicated that there was an initial stimulatory effect on sulphated GAG production when chondrocytes were cultured in fibrin/alginate hydrogels containing HA and/or CS. However, this stimulation of GAG production was not seen in the hydrogel samples cultured for 2 weeks, suggesting that the effects of treating the HA and CS supplements are short-lived.

The higher initial GAG accumulation in the HA, CS, and HACS supplemented hydrogels relative to non-supplemented controls may have stimulated higher chondrocyte proliferation in these supplemented hydrogels during the second week of culture. This proliferation may be due to enhanced cell-cell interactions via the freshly synthesized ECM.

Since the effects of HA and CS were not additive it appeared that, for the most part, there was no advantage to treating with both HA and CS together. Therefore, it is not worth the extra expense of adding both components. The HA and CS supplements elicited roughly the same initial stimulation of matrix accumulation. However, in the week 2 samples, the CS treated hydrogels had a higher cell population and final matrix accumulation than HA supplemented hydrogels (unnormalised). This suggests that of the treatments examined here, supplementing with 0.1 mg/ml CS has the most beneficial effects on chondrocyte proliferation and phenotype retention.

A method for impregnating the solid scaffolds with the fibrin/alginate hydrogel was successfully implemented, as shown in Figure 33. However, the preliminary experiment did not definitively show that the composite scaffolds had higher sulphated GAG accumulation and cell population than solid scaffold controls as a large number of the cells died off during the seeding process. Previous studies [39, 40, 57, 59, 68, 69] which examined composite scaffolds with

different solid scaffold materials and hydrogels have demonstrated the superiority this culture method over solid scaffolds not impregnated with hydrogels. Therefore, if the seeding process can be modified to enhance cell survival the superior matrix production and cell population in these composite scaffolds should also be demonstrated here.

6.2 Future Directions

The next step of the solid scaffold material research should be to repeat the substrate experiment and do a gene analysis of the chondrocytes cultured on these materials. This gene analysis should examine the same target genes as the qPCR analysis used in the hydrogel supplementation experiment (collagen type II, aggrecan, and collagen type I normalised to GAPDH). This will help confirm which of the materials are helping the chondrocytes maintain their phenotype the best.

Since the porosity of these solid scaffolds differed from the designed porosity, it would be of interest to see how closely they coincide with the more detailed pore size model put forward by Li *et al*.[163] which takes into account the fusion of the layers. If it is found that the calculated pore sizes still differ significantly from the ones measured by microtomography, then it may be of interest to create a mathematical model that also takes the shrinking of the scaffolds as they dry into account. With this model, the fabricators of TECs would be able to more accurately design for the final pore sizes of the solid scaffolds.

To further elucidate the effects of the CS and HA macromolecules on hydrogel cultured chondrocytes it would be of interest to examine the mRNA expression halfway through the first week to see if the cells in the treated hydrogels were more strongly expressing the collagen type II and aggrecan mRNA than the untreated control. In addition, examining the mRNA expression halfway between the week 1 and week 2 time points would allow one to see if the untreated controls were in fact more strongly expressing the aggrecan mRNA as it “catches up” to the other treatments. It would also be interesting to see whether or not the hydrogels had reached their steady-state values for cell population and matrix accumulation by taking some later time points for biochemical analysis.

The doses of CS and HA chosen here were previously reported to be optimal for the enhancement of matrix production and cell proliferation in HA[21, 22], and matrix production in CS supplemented hydrogels[23]. However, it would be of interest to know if adjusting these doses would have an impact on the interaction of the effects of HA and CS supplementation. In addition, a study by Hwang *et al*.[164] explored the effects of copolymerizing HA and CS with hydrogels. This copolymerization reduces the solubility of these supplements and, like the present study, showed an increase in sulphated GAG accumulation compared to hydrogels that were not copolymerized. This copolymerization method may be better suited to *in vivo* studies of these supplemented hydrogels, as they would allow the macromolecules to be better retained by the hydrogel after implantation.

It would also be of interest to directly compare the efficacy of stimulating chondrocytes with HA and CS relative to different growth factors currently in use by cartilage tissue engineers. Some of these include: transforming growth factor betas [14-17], bone morphogenetic proteins [15, 18, 19], fibroblast growth factor 2, and insulin-like growth factor 1[15, 17].

The large amount of cell death during the seeding process in the composite scaffold experiment may be ameliorated by lowering the chondrocyte concentration to reduce the acidification of the culture medium. If the cell concentration is lowered, it may be necessary to increase the size of the constructs so that there is a detectable amount of sulphated GAG and cellular DNA. In addition, a medium change during the seeding process or a medium perfusion system would reduce the depletion of media nutrients and the accumulation of toxic metabolites.

To ensure that the DMMB assay is accurately measuring the GAG production in the solid scaffold controls it is recommended to create a second set of standards that are a known amount of CS in Hank's saline. This second set of samples would be used to measure the GAG production in the solid scaffold controls while the existing set of standards would still be used to measure GAG production in the composite scaffolds.

Once cells can be successfully cultured in the composite scaffolds and sulphated GAG accumulation can be measured, it would be of interest to measure the mechanical properties of these scaffolds using the methods outlined in Chapter 2. The small amount of mechanical testing that has been done on composite scaffolds[59] fails to report properties such as hydraulic

permeability and aggregate modulus, which are important for comparison to the mechanical behaviour of natural cartilage. Once known, these properties could be modified to more closely match those of native cartilage using the various methods outlined in Section 2.2.6.

While testing the short-term behaviour of porcine chondrocytes in composite scaffolds *in vitro* provides a relatively simple measure of their efficacy, before these scaffolds can be used to treat patients with osteoarthritis a number of research milestones must be achieved. First, the long-term (1 to 6 month) *in vivo* culture of these constructs would show if chondrocytes were stably maintaining their phenotype and viability. These composite scaffolds and solid scaffold controls could be implanted in articular defects in a model animal to compare their rate of degradation and rate of integration with the surrounding native cartilage.

The porcine chondrocytes used here served as a suitable model for these early investigations. However, the use of primary human chondrocytes would provide further insight into the potential of these composite scaffolds to create a cartilaginous tissue suitable for implantation into humans. Another potential cell source is bone-marrow derived stem cells which could be induced into differentiating into chondrocytes by supplementing either CS, HA, or other ECM components, or growth factors (such as TGF-βs, BMPs, FGF-2, etc).

Once these composite scaffolds have the appropriate mechanical properties, been proven capable of supporting human chondrocyte culture, and have an appropriate regimen of supplements they could prove to be an effective treatment for patients suffering from osteoarthritis.

References

1. Mansour, J.M. Biomechanics of cartilage. In: Oatis, C., ed. Kinesiology: The Mechanics and Pathomechanics of Human Movement. Philadelphia, PA: Lippincott Williams and Wilkins, 2003, pp. 66-79.

2. Brittberg, M., and Lindahl, A. Tissue engineering of cartilage. In: Blitterswijk, C., ed. Tissue Engineering. New York, NY: Academic Press, 2008, pp. 533-557.

3. Eyre, D. Collagen of articular cartilage. Arthritis Res **4**, 30, 2002.

4. Hunziker, E.B., Quinn, T.M., and Hauselmann, H.J. Quantitative structural organization of normal adult human articular cartilage. Osteoarthritis Cartilage **10**, 564, 2002.

5. Athanasiou, K., Darling, E., and Hu, J. Articular cartilage tissue engineering. San Rafael, CA: Morgan and Claypool Publishers, 2010.

6. Inerot, S., Heinegard, D., Audell, L., and Olsson, S.-E. Articular-Cartilage Proteoglycans in Aging and Osteoarthritis. Biochemical Journal **169**, 143, 1978.

7. Lawrence, R.C., Felson, D.T., Helmick, C.G., Arnold, L.M., Choi, H., Deyo, R.A., Gabriel, S., Hirsch, R., Hochberg, M.C., Hunder, G.G., Jordan, J.M., Katz, J.N., and Kremers, H.M. Estimates of the prevalence of arthritis and other rheumatic conditions in the United States part II. Arthritis Rheum **58**, 26, 2008.

8. Hart, D.J., Doyle, D.V., and Spector, T.D. Incidence and risk factors for radiographic knee osteoarthritis in middle-aged women: the Chingford study. Arthritis & Rheumatism **42**, 17, 1999.

9. Jackson, D.W., Simon, T.M., and Aberman, H.M. The articular cartilage repair dilemma: symptomatic articular cartilage; the impact in the new millennium. Clin Orthop Relat Res **391S**, S14, 2001.

10. Lee, J., Kisiday, J., and Grozonsky, A. Tissue-engineered versus native cartilage: linkage between mechano-transduction and biomechanical properties. In: Bock, G., and Goode, J., eds. Tissue-engineering of cartilage and bone. Hoboken, NJ: J. Wiley, 2003, p. 52.

11. Steadman, J.R., Rodkey, W.G., and Rodrigo, J.J. Microfracture: surgical technique and rehabilitation to treat chondral defects. Clin Orthop Relat Res **391S**, S362, 2001.

12. Marlovits, S., Zeller, P., Singer, P., Resinger, C., and Vecsei, V. Cartilage repair: generations of autologous chondrocyte transplantation. European journal of radiology **57**, 24, 2006.

13. Buckwalter, J.A. Articular Cartilage Injuries. Clin Orthop Relat Res **402**, 21, 2002.

14. Barry, F.P. Biology and clinical applications of mesenchymal stem cells. Birth Defects Res C Embryo Today **69**, 250, 2003.

15. Khalafi, A., Schmid, T.M., Neu, C., and Reddi, A.H. Increased accumulation of superficial zone protein (SZP) in articular cartilage in response to bone morphogenetic protein-7 and growth factors. J Orthop Res **25**, 293, 2007.

16. Schantz, J.-T., Hutmacher, D.W., Lam, C.X.F., Brinkmann, M., Wong, K.M., Lim, T.C., Chou, N., Guldberg, R.E., and Teoh, S.H. Repair of calvarial defects with customised tissue-engineered bone grafts I. Evaluation of osteogenesis in a three-dimensional culture system. Tissue Eng **9**, S113, 2003.

17. Jakob, M., Demarteau, O., Schafer, D., Hintermann, B., Dick, W., Heberer, M., and Martin, I. Specific growth factors during the expansion and redifferentiation of adult human articular chondrocytes enhance chondrogenesis and cartilaginous tissue formation in vitro. J Cell Biochem **81**, 368, 2001.

18. Ando, W., Tateishi, K., Hart, D.A., Katakai, D., Tanaka, Y., Nakata, K., Hashimoto, J., Fujie, H., Shino, K., Yoshikawa, H., and Nakamura, N. Cartilage repair using an in vitro generated scaffold-free tissue-engineered construct derived from porcine synovial mesenchymal stem cells. Biomaterials **28**, 5462, 2007.

19. Niikura, T., and Reddi, A.H. Differential regulation of lubricin/superficial zone protein by transforming growth factor beta/bone morphogenetic protein superfamily members in articular chondrocytes and synoviocytes. Arthritis Rheum **56**, 2312, 2007.

20. Cooper, G.M. The Cell; A Molecular Approach. Washington, D.C.: ASM Press, 2000.

21. Akmal, M., Singh, A., Anand, A., Kesani, A., Aslam, N., Goodship, A., and Bentley, G. The effects of hyaluronic acid on articular chondrocytes. J Bone Joint Surg Br **87**, 1143, 2005.

22. Kawasaki, K., Ochi, M., Uchio, Y., Adachi, N., and Matsusaki, M. Hyaluronic acid enhances proliferation and chondroitin sulfate synthesis in cultured chondrocytes embedded in collagen gels. J Cell Physiol **179**, 142, 1999.

23. Bassleer, C.T., Combal, J.P., Bougaret, S., and Malaise, M. Effects of chondroitin sulfate and interleukin-1 beta on human articular chondrocytes cultivated in clusters. Osteoarthritis Cartilage **6**, 196, 1998.

24. van Susante, J.L.C., Pieper, J., Buma, P., van Kuppevelt, T.H., van Beuningen, H., van der Kraan, P.M., Veerkamp, J.H., van den Berg, W.B., and Veth, R.P.H. Linkage of chondroitin-sulfate to type I collagen scaffolds stimulates the bioactivity of seeded chondrocytes in vitro. Biomaterials **22**, 2359, 2001.

25. Klein, T., Schumacher, B.L., Schmidt, T.A., Li, K.W., Voegtline, M.S., Masuda, K., Thonar, E.J.M.A., and Sah, R.L. Tissue engineering of stratified articular cartilage from chondrocyte subpopulations. Osteoarthritis Cartilage **11**, 595, 2003.

26. Bryant, S.J., Davis-Arehart, K.A., Luo, N., Shoemaker, R.K., Arthur, J.A., and Anseth, K.S. Synthesis and characterization of photopolymerized multifunctional hydrogels: water-soluble poly(vinyl alcohol) and chondroitin sulfate macromers for chondrocyte encapsulation. Macromolecules **37**, 6726, 2004.

27. Klein, T.J., Malda, J., Sah, R.L., and Hutmacher, D.W. Tissue engineering of articular cartilage with biomimetic zones. Tissue Eng Part B Rev **15**, 143, 2009.

28. Drury, J., and Mooney, D.J. Hydrogels for tissue engineering: scaffold design variables and applications. Biomaterials **24**, 4337, 2003.

29. Ahmed, T.A.E., Dare, E.V., and Hincke, M. Fibrin : A Versatile Scaffold for Tissue Engineering Applications. Tissue Eng Part B Rev **14**, 199, 2008.

30. Klein, T.J., Chaudhry, M., Bae, W.C., and Sah, R.L. Depth-dependent biomechanical and biochemical properties of fetal, newborn, and tissue-engineered articular cartilage. J Biomech **40**, 182, 2007.

31. Lee, C.S.D., Gleghorn, J.P., Nak, Cabodi, M., Stroock, A.D., and Bonassar, L.J. Integration of layered chondrocyte-seeded alginate hydrogel scaffolds. Biomaterials **28**, 2987, 2007.

32. Williams, G.M., Klein, T.J., and Sah, R.L. Cell density alters matrix accumulation in two distinct fractions and the mechanical integrity of alginate-chondrocyte constructs. Acta biomaterialia **1**, 625, 2005.

33. Mauck, R., Wang, C.C., Oswald, E.S., Ateshian, G.A., and Hung, C.T. The role of cell seeding density and nutrient supply for articular cartilage tissue engineering with deformational loading. Osteoarthritis Cartilage **11**, 879, 2003.

34. Mauck, R.L., Soltz, M.A., Wang, C.C., Wong, D.D., Chao, P.H., Valhmu, W.B., Hung, C.T., and Ateshian, G.A. Functional tissue engineering of articular cartilage through dynamic loading of chondrocyte-seeded agarose gels. J Biomech Eng **122**, 252, 2000.

35. Mauck, R.L., Yuan, X., and Tuan, R.S. Chondrogenic differentiation and functional maturation of bovine mesenchymal stem cells in long-term agarose culture. Osteoarthritis Cartilage **14**, 179, 2006.

36. Chen, G., Sato, T., Tanaka, J., and Tateishi, T. Preparation of a biphasic scaffold for osteochondral tissue engineering. Materials Science and Engineering: C **26**, 118, 2006.

37. Liao, E., Yaszemski, M., Krebsbach, P., and Hollister, S. Tissue-engineered cartilage constructs using composite hyaluronic acid/collagen I hydrogels and designed poly(propylene fumarate) scaffolds. Tissue Eng **13**, 537, 2007.

38. Nawata, M., Wakitani, S., Nakaya, H., Tanigami, A., Seki, T., Nakamura, Y., Saito, N., Sano, K., Hidaka, E., and Takaoka, K. Use of bone morphogenetic protein 2 and diffusion chambers to engineer cartilage tissue for the repair of defects in articular cartilage. Arthritis Rheum **52**, 155, 2005.

39. Fan, H., Hu, Y., Zhang, C., Li, X., Lv, R., Qin, L., and Zhu, R. Cartilage regeneration using mesenchymal stem cells and a PLGA-gelatin/chondroitin/hyaluronate hybrid scaffold. Biomaterials **27**, 4573, 2006.

40. Eyrich, D., Wiese, H., Maier, G., Skodacek, D., Appel, B., Sarhan, H., Tessmar, J., Staudenmaier, R., Wenzel, M.M., Goepferich, A., and Blunk, T. In vitro and in vivo cartilage engineering using a combination of chondrocyte-seeded long-term stable fibrin gels and polycaprolactone-based polyurethane scaffolds. Tissue Eng **13**, 2207, 2007.

41. Hoemann, C.D., Sun, J., Légaré, A., McKee, M.D., and Buschmann, M.D. Tissue engineering of cartilage using an injectable and adhesive chitosan-based cell-delivery vehicle. Osteoarthritis Cartilage **13**, 318, 2005.

42. Perka, C., Spitzer, R.S., Lindenhayn, K., Sittinger, M., and Schultz, O. Matrix-mixed culture: new methodology for chondrocyte culture and preparation of cartilage transplants. J Biomed Mater Res A **49**, 305, 2000.

43. Lindenhayn, K., Perka, C., Spitzer, R., Heilmann, H., Pommerening, K., Mennicke, J., and Sittinger, M. Retention of hyaluronic acid in alginate beads: aspects for in vitro cartilage engineering. J Biomed Mater Res A **44**, 149, 1999.

44. Homminga, G.N., Buma, P., Koot, H.W., van der Kraan, P.M., and van den Berg, W.B. Chondrocyte behavior in fibrin glue in vitro. Acta orthopaedica Scandinavica **64**, 441, 1993.

45. Park, S.H., Park, S.R., Chung, S.I., Pai, K.S., and Min, B.H. Tissue-engineered cartilage using fibrin/hyaluronan composite gel and its *in vivo* implantation. Artif Organs **29**, 838, 2005.

46. Reneker, D.H., Yarin, A.L., Fong, H., and Koombhongse, S. Bending instability of electrically charged liquid jets of polymer solutions in electrospinning. Journal of Applied Physics **87**, 4531, 2000.

47. Woodfield, T.B.F., Malda, J., de Wijn, J., Peters, F., Riesle, J., and van Blitterswijk, C.A. Design of porous scaffolds for cartilage tissue engineering using a three-dimensional fiber-deposition technique. Biomaterials **25**, 4149, 2004.

48. Xiong, Z., Yan, Y., Wang, S., Zhang, R., and Zhang, C. Fabrication of porous scaffolds for bone tissue engineering via low-temperature deposition. Scripta Materialia **46**, 771, 2002.

49. Yan, H., and Yu, C. Repair of full-thickness cartilage defects with cells of different origin in a rabbit model. Journal of Arthroscopic & Related Surgery **23**, 178, 2007.

50. Woodfield, T.B.F., Van Blitterswijk, C.A., De Wijn, J., Sims, T.J., Hollander, A.P., and Riesle, J. Polymer scaffolds fabricated with pore-size gradients as a model for studying the zonal organization within tissue-engineered cartilage constructs. Tissue Eng **11**, 1297, 2005.

51. Moroni, L., de Wijn, J.R., and van Blitterswijk, C.A. 3D fiber-deposited scaffolds for tissue engineering: influence of pores geometry and architecture on dynamic mechanical properties. Biomaterials **27**, 974, 2006.

52. Zwingmann, J., Mehlhorn, A.T., Sudkamp, N., Stark, B., Dauner, M., and Schmal, H. Chondrogenic differentiation of human articular chondrocytes differs in biodegradable PGA/PLA scaffolds. Tissue Eng **13**, 2335, 2007.

53. Chen, X.B., Li, M.G., and Ke, H. Modeling of the Flow Rate in the Dispensing-Based Process for Fabricating Tissue Scaffolds. Journal of manufacturing science and engineering **130**, 021003, 2008.

54. Mariani, M., Rosatini, F., Vozzi, G., Previti, A., and Ahluwalia, A. Characterization of tissue-engineered scaffolds microfabricated with PAM. Tissue Eng **12**, 547, 2006.

55. Liu, L., Xiong, Z., Zhang, R., and Jin, L. A Novel Osteochondral Scaffold Fabricated via Multi-nozzle Low-temperature Deposition Manufacturing. Journal of Bioactive and Compatible Polymers **24**, 18, 2009.

56. van Dijkhuizen-Radersma, R., Moroni, L., van Apeldoorn, A., Zhang, Z., and Grijpma, D. Degradable polymers for tissue engineering. In: van Blitterswijk, C.A., ed. Tissue Engineering. New York, NY: Academic Press, 2008, pp. 193-221.

57. Ameer, G.A., Mahmood, T.A., and Langer, R. A biodegradable composite scaffold for cell transplantation. J Orthop Res **20**, 16, 2002.

58. Caterson, E.J., Nesti, L.J., Li, W.-j., Danielson, K.G., Albert, T.J., Vaccaro, A.R., and Tuan, R.S. Three-dimensional cartilage formation by bone marrow-derived cells seeded in polylactide / alginate amalgam. J Biomed Mater Res A **57**, 394, 2001.

59. Gong, Y., He, L., Li, J., Zhou, Q., Ma, Z., Gao, C., and Shen, J. Hydrogel-filled polylactide porous scaffolds for cartilage tissue engineering. J Biomed Mater Res B Appl Biomater **82B**, 192, 2006.

60. Revell, C.M., and Athanasiou, K.A. Success rates and immunologic responses of autogenic, allogenic, and xenogenic treatments to repair articular cartilage defects. Tissue Eng Part B Rev **15**, 1, 2009.

61. Jain, R.A. The manufacturing techniques of various drug loaded biodegradable poly(lactide-co-glycolide) (PLGA) devices. Biomaterials **21**, 2475, 2000.

62. Attawia, M.A., Herbert, K.M., and Laurencin, C.T. Osteoblast-Like Cell Adherance and Migration Through 3-Dimensional Porous Polymer Matrices. Biochemical and Biophysical Research Communications **213**, 639, 1995.

63. Marra, K.G., Szem, J.W., Kumta, P.N., Dimilla, P.A., and Weiss, L.E. In vitro analysis of biodegradable polymer blend / hydroxyapatite composites for bone tissue engineering. J Biomed Mater Res **47**, 324, 1999.

64. Lide, D.R. CRC Handbook of Chemistry and Physics. New York, NY: CRC Press, 2002.

65. Heymer, A., Haddad, D., Weber, M., Gbureck, U., Jakob, P.M., Eulert, J., and NÃ¶th, U. Iron oxide labelling of human mesenchymal stem cells in collagen hydrogels for articular cartilage repair. Biomaterials **29**, 1473, 2008.

66. Farrell, E., Wielopolski, P., Pavljasevic, P., Kops, N., Weinans, H., Bernsen, M.R., and van Osch, G.J.V.M. Cell labelling with superparamagnetic iron oxide has no effect on chondrocyte behaviour. Osteoarthritis Cartilage **17**, 961, 2009.

67. Frank, J.A., Zywicke, H., Jordan, E.K., Mitchell, J., Lewis, B.K., Miller, B., Bryant, L.H., and Bulte, J.W.M. Magnetic intracellular labeling of mammalian cells by combining (FDA-approved) superparamagnetic iron oxide MR contrast agents and commonly used transfection agents. Acad Radiol **9 Suppl 2**, S484, 2002.

68. Malicev, E., Radosavljevic, D., and Velikonja, N.K. Fibrin gel improved the spatial uniformity and phenotype of human chondrocytes seeded on collagen scaffolds. Biotechnol Bioeng **96**, 364, 2007.

69. Lee, C.R., Grad, S., Gorna, K., Gogolewski, S., Goessl, A., and Alini, M. Fibrin-polyurethane composites for articular cartilage tissue engineering: a preliminary analysis. Tissue Eng **11**, 1562, 2005.

70. Little, C.J., Bawolin, N.K., and Chen, X.B. Mechanical properties of natural cartilage and tissue engineered constructs. Tissue Eng Part B Rev **17**, 213, 2011.

71. Poole, A.R., Yasuda, T., and Kobayashi, M. Composition and structure of articular cartilage. Clin Orthop Relat Res **391S**, S26, 2001.

72. Roth, V., and Mow, V.C. The intrinsic tensile behaviour of the matrix of bovine articular cartilage and its variations with age. J Bone Joint Surg **62**, 1102, 1980.

73. Schinagl, R.M., Gurskis, D., Chen, A.C., and Sah, R.L. Depth-dependent confined compression modulus of full-thickness bovine articular cartilage. J Orthop Res **15**, 499, 1997.

74. Mow, V.C., and Guo, X. Mechano-electrochemical properties of articular cartilage: their inhomogeneities and anisotropies. Annu Rev Biomed Eng **4**, 175, 2002.

75. Kwan, M.K., Lai, W.M., and Mow, V.C. Fundamentals of fluid transport through cartilage in compression. Annals of Biomedical Engineering **12**, 537, 1984.

76. Ateshian, G.A., Wang, H., and Lai, W.M. The role of interstitial fluid pressurization in articular cartilage lubrication. J Tribol **120**, 241, 1998.

77. Setton, L.A., Zhu, W., and Mow, V.C. The biphasic poroviscoelastic behavior of articular cartilage: Role of the surface zone in governing the compressive behavior. J Biomech **26**, 581, 1993.

78. Ateshian, G.A., Lai, W.M., Zhu, W.B., and Mow, V.C. An asymptotic solution for the contact of two biphasic cartilage layers. J Biomech **27**, 1347, 1994.

79. Eckstein, F., Tieschky, M., Faber, S., Englmeier, K.H., and Reiser, M. Functional analysis of articular cartilage deformation, recovery, and fluid flow following dynamic exercise in vivo. Anatomy and Embryology **200**, 419, 1999.

80. Mow, V.C., Kuei, S.C., Lai, W.M., and Armstrong, C.G. Biphasic creep and stress relaxation of articular cartilage in compression: theory and experiments. J Biomech Eng **102**, 73, 1980.

81. Woo, S.L.-Y., Mow, V.C., and Lai, W.M. Biomechanical properties of articular cartilage. In: Skalak, R., and Chien, S., eds. Handbook of Bioengineering. New York, NY: Mcgraw-Hill, 1987, p. 4.1.

82. Gu, W.Y., and Chen, F.H. Structure and function of articular cartilage and meniscus. In: Mow, V.C., and Huiskes, R., eds. Basic Orthopaedic Biomechanics and Mechano-Biology. Philadelphia, Pa: Lippencott Williams and Wilkins, 2005, pp. 181-258.

83. Korhonen, R.K., and Jurvelin, J.S. Compressive and tensile properties of articular cartilage in axial loading are modulated differently by osmotic environment. Med Eng Phys **32**, 55, 2010.

84. Williamson, A.K., Chen, A.C., Masuda, K., Thonar, E.J.-M.A., and Sah, R.L. Tensile mechanical properties of bovine articular cartilage: Variations with growth and relationships to collagen network components. J Orthop Res **21**, 872, 2003.

85. Kempson, G.E. Relationship between the tensile properties of articular cartilage from the human knee and age. Ann Rheum Dis **41**, 508, 1982.

86. Kempson, G.E. Age-related changes in the tensile properties of human articular cartilage: a comparative study between the femoral head of the hip joint and the talus of the ankle joint. Biochim Biophys Acta **1075**, 223, 1991.

87. Williamson, A.K., Masuda, K., Thonar, E.J.M.A., and Sah, R.L. Growth of immature articular cartilage in vitro: correlated variation in tensile biomechanical and collagen network properties. Tissue Eng **9**, 625, 2003.

88. Woo, S.L., Akeson, W.H., and Jemmott, G.F. Measurements of nonhomogeneous, directional mechanical properties of articular cartilage in tension. J Biomech **9**, 785, 1976.

89. Charlebois, M., McKee, M.D., and Buschmann, M.D. Nonlinear tensile properties of bovine articular cartilage and their variation with age and depth. J Biomech Eng **126**, 129, 2004.

90. Armstrong, C.G., and Mow, V.C. Variations in the intrinsic mechanical properties of human articular cartilage with age, degeneration, and water content. J Bone Joint Surg **64**, 88, 1982.

91. Buschmann, M.D., Soulhat, J., Shirazi-Adl, A., Jurvelin, J.S., and Hunziker, E.B. Confined compression of articular cartilage: linearity in ramp and sinusoidal tests and the importance of interdigitation and incomplete confinement. J Biomech **31**, 171, 1998.

92. Vunjak-Novakovic, G., Martin, I., Obradovic, B., Treppo, S., Grodzinsky, A.J., Langer, R., and Freed, L.E. Bioreactor cultivation conditions modulate the composition and mechanical properties of tissue-engineered cartilage. J Orthop Res **17**, 130, 1999.

93. Ma, P.X., Schloo, B., Mooney, D.J., and Langer, R. Development of biomechanical properties and morphogenesis of *in vitro* tissue engineered cartilage. J Biomed Mater Res **29**, 1587, 1995.

94. DiSilvestro, M.R., and Suh, J.K. A cross-validation of the biphasic poroviscoelastic model of articular cartilage in unconfined compression, indentation, and confined compression. J Biomech **34**, 519, 2001.

95. Korhonen, R.K., Laasanen, M.S., Toyras, J., Rieppo, J., Hirvonen, J., Helminen, H.J., and Jurvelin, J.S. Comparison of the equilibrium response of articular cartilage in unconfined compression , confined compression and indentation. J Biomech **35**, 903, 2002.

96. Hayes, W.C., Keer, L.M., Herrmann, G., and Mockros, L.F. A mathematical analysis for indentation tests of articular cartilage. J Biomech **5**, 541, 1972.

97. Mow, V.C., Gibbs, M.C., Lai, W.M., Zhu, W.B., and Athanasiou, K.A. Biphasic indentation of articular cartilage--II. A numerical algorithm and an experimental study. J Biomech **22**, 853, 1989.

98. Armstrong, C.G., Lai, W.M., and Mow, V.C. An analysis of the unconfined compression of articular cartilage. J Biomech Eng **106**, 165, 1984.

99. Hayes, W.C., and Bodine, A.J. Flow-independent viscoelastic properties of articular cartilage matrix. J Biomech **11**, 407, 1978.

100. Woo, S.L.Y., Simon, B.R., Kuei, S.C., and Akeson, W.H. Quasi-linear viscoelastic properties of normal articular cartilage. J Biomech Eng **102**, 85, 1980.

101. Spirt, A.A., Mak, A.F., and Wassell, R.P. Nonlinear viscoelastic properties of articular cartilage in shear. J Orthop Res **7**, 43, 1989.

102. LeRoux, M.A., Guilak, F., and Setton, L.A. Compressive and shear properties of alginate gel: effects of sodium ions and alginate concentration. J Biomed Mater Res **47**, 46, 1999.

103. Kwan, M.K., Coutts, R.D., Woo, S.L., and Field, F.P. Morphological and biomechanical evaluations of neocartilage from the repair of full-thickness articular cartilage defects using rib perichondrium autografts: a long-term study. J Biomech **22**, 921, 1989.

104. Setton, L.A., Mow, V.C., and Howell, D.S. Mechanical behavior of articular cartilage in shear is altered by transection of the anterior cruciate ligament. J Orthop Res **13**, 473, 1995.

105. Awad, H.A., Wickham, M.Q., Leddy, H.A., Gimble, J.M., and Guilak, F. Chondrogenic differentiation of adipose-derived adult stem cells in agarose, alginate, and gelatin scaffolds. Biomaterials **25**, 3211, 2004.

106. Mow, V.C., Mak, A.F., Lai, W.M., Rosenberg, L.C., and Tang, L.H. Viscoelastic properties of proteoglycan subunits and aggregates in varying solution concentrations. J Biomech **17**, 325, 1984.

107. Waldman, S.D., Spiteri, C.G., Grynpas, M.D., Pilliar, R.M., and Kandel, R.A. Long-term intermittent compressive stimulation improves the composition and mechanical properties of tissue-engineered cartilage. Tissue Eng **10**, 2004.

108. Jurvelin, J.S., Buschmann, M.D., and Hunziker, E.B. Optical and mechanical determination of poisson's ratio of adult bovine humeral articular cartilage. J Biomech **30**, 235, 1997.

109. Mak, A.F., Lai, W.M., and Mow, V.C. Biphasic indentation of articular cartilage--I. Theoretical analysis. J Biomech **20**, 703, 1987.

110. Moutos, F.T., Freed, L.E., and Guilak, F. A biomimetic three-dimensional woven composite scaffold for functional tissue engineering of cartilage. Nat Mater **6**, 162, 2007.

111. Jurvelin, J.S., Arokoski, J.P., Hunziker, E.B., and Helminen, H.J. Topographical variation of the elastic properties of articular cartilage in the canine knee. J Biomech **33**, 669, 2000.

112. Zhu, W., Mow, V.C., Koob, T.J., and Eyre, D.R. Viscoelastic shear properties of articular cartilage and the effects of glycosidase treatments. J Orthop Res **11**, 771, 1993.

113. Athanasiou, K., Agarwal, A., and Dzida, F.J. Comparative study of the intrinsic mechanical properties of the human acetabular and femoral head cartilage. J Orthop Res **12**, 340, 1994.

114. Athanasiou, K., Rosenwasse, M.P., Buckwalter, J.A., Malinin, T.I., and Mow, V.C. Interspecies comparisons of in situ intrinsic mechanical properties of distal femoral cartilage. J Orthop Res **9**, 330, 1991.

115. Setton, L.A., Mow, V.C., Müller, F.J., Pita, J.C., and Howell, D.S. Mechanical properties of canine articular cartilage are significantly altered following transection of the anterior cruciate ligament. J Orthop Res **12**, 451, 1994.

116. Boyce, M.C., Socrate, S., and Llana, P.G. Constitutive model for the finite deformation stress–strain behavior of poly(ethylene terephthalate) above the glass transition. Polymer **41**, 2183, 2000.

117. Bursac, P.M., McGrath, V., Eisenberg, S.R., and Stamenovic, D. A microstructural model of elastostatic properties of articular cartilage in confined compression. J Biomech Eng **122**, 347, 2000.

118. Prendergast, P.J., and Kuiper, J.H. A comparison of finite element codes for the solution of biphasic poroelastic problems. Proc Inst Mech Eng H **210**, 131, 1996.

119. Guptaa, S., Linb, J., Ashbyc, P., and Pruitte, L. A fiber reinforced poroelastic model of nanoindentation of porcine costal cartilage: A combined experimental and finite element approach. J Mech Behav Biomed Mater **2**, 326, 2009.

120. Finite element formulation of poro-elasticity suitable for large deformation dynamic analysis [Research Report]. Department of Civil and Environmental Engineering, Stanford University, 2005.

121. Loret, B., and Simoes, F.M.F. Articular cartilage with intra- and extrafibrillar waters: a chemo-mechanical model. Mech Mater **36**, 515, 2004.

122. Gu, W.Y., Lai, W.M., and Mow, V.C. A mixture theory for charged-hydrated soft tissues containing multi-electrolytes: passive transport and swelling behaviours. J Biomech Eng **120**, 169, 1998.

123. Fung, Y. Biomechanics: Mechanical Properties of Living Tissues. New York: Springer, 1993.

124. Park, S.H., and Ateshian, G.A. Dynamic response of immature bovine articular cartilage in tension and compression, and nonlinear viscoelastic modelling of the tensile response. J Biomech Eng **128**, 623, 2006.

125. Suh, J.K., and Bai, S. Finite element formulation of biphasic poroviscoelastic model for articular cartilage. J Biomech Eng **120**, 195, 1998.

126. Berger, H., Kari, S., Gabbert, U., Rodriguez-Ramos, R., Bravo-Castillero, J., and Guinovart-Diaz, R. A comprehensive numerical homogenisation technique for calculating effective coefficients of uniaxial piezoelectric fibre composites. Mater Sci Eng A Struct Mater **412**, 53, 2005.

127. Chang, S.C., Rowley, J.A., Tobias, G., Genes, N.G., Roy, A.K., Mooney, D.J., Vacanti, C.A., and Bonassar, L.J. Injection molding of chondrocyte/alginate constructs in the shape of facial implants. Journal of biomedical materials research. Part A **55**, 503, 2001.

128. Gratz, K.R., Wong, V.W., Chen, A.C., Fortier, L.A., Nixon, A.J., and Sah, R.L. Biomechanical assessment of tissue retrieved after in vivo cartilage defect repair: tensile modulus of repair tissue and integration with host cartilage. J Biomech **39**, 138, 2006.

129. Martin, I., Obradovic, B., Treppo, S., Grodzinsky, A.J., Langer, R., Freed, L.E., and Vunjak-Novakovic, G. Modulation of the mechanical properties of tissue engineered cartilage. Biorheology **37**, 141, 2000.

130. Kempson, G.E., Muir, H., Pollard, C., and Tuke, M. The tensile properties of the cartilage of human femoral condyles related to the content of collagen and glycosaminoglycans Biochim Biophys Acta **297**, 456, 1973.

131. Hansen, U., Schunke, M., Domm, C., Ioannidis, N., Hassenpflug, J., Gehrke, T., and Kurz, B. Combination of reduced oxygen tension and intermittent hydrostatic pressure: a useful tool in articular cartilage tissue engineering. J Biomech **34**, 941, 2001.

132. Waldman, S.D., Spiteri, C.G., Grynpas, M.D., Pilliar, R.M., Hong, J., and Kandel, R.A. Effect of biomechanical conditioning on cartilaginous tissue formation in vitro. J Bone Joint Surg Am **85-A Suppl 2**, 101, 2003.

133. Lee, D.A., Noguchi, T., Frean, S.P., Lees, P., and Bader, D.L. The influence of mechanical loading on isolated chondrocytes seeded in agarose constructs. Biorheology **37**, 149, 2000.

134. Wimmer, M.A., Grad, S., Kaup, T., Hanni, M., Schneider, E., Gogolewski, S., and Alini, M. Tribology approach to the engineering and study of articular cartilage. Tissue Eng **10**, 1436, 2004.

135. Guilak, F., and Mow, V.C. The mechanical environment of the chondrocyte: a biphasic finite element model of cell-matrix interactions in articular cartilage. J Biomech **33**, 1663, 2000.

136. Freyria, A.M., Cortial, D., Ronziere, M.C., Guerret, S., and Herbage, D. Influence of medium composition, static and stirred conditions on the proliferation of and matrix protein

expression of bovine articular chondrocytes cultured in a 3-D collagen scaffold. Biomaterials **25**, 687, 2004.

137. Heng, B.C., Cao, T., and Lee, E.H. Directing stem cell differentiation into the chondrogenic lineage in vitro. Stem Cells **22**, 1152, 2004.

138. Hutmacher, D.W., Schantz, T., Zein, I., Ng, K.W., Teoh, S.H., and Tan, K.C. Mechanical properties and cell cultural response of polycaprolactone scaffolds designed and fabricated via fused deposition modeling. J Biomed Mater Res **55**, 203, 2001.

139. Hollister, S.J., Maddox, R.D., and Taboas, J.M. Optimal design and fabrication of scaffolds to mimic tissue properties and satisfy biological constraints. Biomaterials **23**, 4095, 2002.

140. Grande, D.A., Halberstadt, C., Naughton, G., Schwartz, R., and Manji, R. Evaluation of matrix scaffolds for tissue engineering of articular cartilage grafts. J Biomed Mater Res **34**, 211, 1997.

141. Vunjak-novakovic, G., Obradovic, B., Martin, I., Bursac, P.M., Langer, R., and Freed, L.E. Dynamic cell seeding of polymer scaffolds for cartilage tissue engineering. Biotechnol Prog **14**, 193, 1998.

142. Ng, K.W., Wang, C.C., Mauck, R.L., Kelly, T.N., Chahine, N.O., Costa, K.D., Ateshian, G.A., and Hung, C.T.A. A layered agarose approach to fabricate depth-dependent inhomogeneity in chondrocyte-seeded constructs. J Orthop Res **23**, 134, 2005.

143. Bawolin, N.K., Li, M.G., Chen, X.B., and Zhang, W.J. Modeling material degradation induced time-dependent elastic property of tissue engineering scaffolds. J Biomech Eng (in press), 2010.

144. Bawolin, N.K., Zhang, W.J., and Chen, X.B. A brief review of the modelling of the time dependent mechanical properties of tissue engineering scaffolds. J Biomim Biomater Tissue Eng (in press), 2010.

145. Hanks, J.H. Hanks' balanced salt solution and pH control. Methods in Cell Science **1**, 3, 1975.

146. Puck, T.T., Cieciura, S.J., and Fisher, H.W. CLONAL GROWTH IN VITRO OF HUMAN CELLS WITH FIBROBLASTIC MORPHOLOGY. Journal of Experimental Medicine **106**, 145, 1957.

147. Labarca, C., and Paigen, K. A simple, rapid, and sensitive DNA assay procedure. Analytical Biochemistry **102**, 344, 1980.

148. R Development Core Team. R: A language and environment for statistical computing. Vienna, Austria: R Foundation for Statistical Computing, 2009.

149. Eyrich, D., Brandl, F., Appel, B., Wiese, H., Maier, G., Wenzel, M., Staudenmaier, R., Goepferich, A., and Blunk, T. Long-term stable fibrin gels for cartilage engineering. Biomaterials **28**, 55, 2007.

150. Enobakhare, B.O., Bader, D.L., and Lee, D.A. Quantification of sulfated glycosaminoglycans in chondrocyte/alginate cultures, by use of 1,9-dimethylmethylene blue. Analytical biochemistry **243**, 189, 1996.

151. Real-Time PCR Applications Guide Technical Document. N.D.

152. Bustin, S.A., Benes, V., Garson, J.A., Hellemans, J., Huggett, J., Kubista, M., Mueller, R., Nolan, T., Pfaffl, M.W., and Shipley, G.L. The MIQE Guidelines : Minimum Information for Publication of Quantitative Real-Time PCR Experiments. Clinical Chemistry **55**, 611, 2009.

153. Pfaffl, M.W. A new mathematical model for relative quantification in real-time RT-PCR. Nucleic acids research **29**, e45, 2001.

154. Marlovits, S., Hombauer, M., Truppe, M., Vecsei, V., and Schlegel, W. Changes in the ratio of type-I and type-II collagen expression during monolayer culture of human chondrocytes. J Bone Joint Surg **86-B**, 286, 2004.

155. Crawley, M.J. The R Book. West Sussex, England: John Wiley and Sons, 2007.

156. Pfaffl, M.W., Horgan, G.W., and Dempfle, L. Relative expression software tool (REST) for group-wise comparison and statistical analysis of relative expression results in real-time PCR. Nucleic acids research **30**, e36, 2002.

157. Li, J.P., de Wijn, J.R., Van Blitterswijk, C.A., and de Groot, K. Porous Ti6Al4V scaffold directly fabricating by rapid prototyping: preparation and *in vitro* experiment. Biomaterials **27**, 1223, 2006.

158. Jiang, C.-C., Chiang, H., Liao, C.-j., Lin, Y.-j., Kuo, T.-f., Shieh, C.-S., Huang, Y.-Y., and Tuan, R.S. Repair of porcine articular cartilage defect with a biphasic osteochondral composite. J Orthop Res **25**, 1277, 2007.

159. Leong, K.F., Cheah, C.M., and Chua, C.K. Solid freeform fabrication of three-dimensional scaffolds for engineering replacement tissues and organs. Biomaterials **24**, 2363, 2003.

160. Gebhard, P.M., Gehrsitz, A., Bau, B., Eger, W., Aigner, T., and Soder, S. Quantification of expression levels of cellular differentiation markers does not support a general shift in the cellular phenotype of osteoarthritic chondrocytes. J Orthop Res **21**, 96, 2003.

161. Nishimoto, S., Takagi, M., Wakitani, S., Nihira, T., and Yoshida, T. Effect of Chondroitin Sulfate and Hyaluronic Acid on Gene Expression in a Three-Dimensional Culture of Chondrocytes. Journal of Bioscience and Bioengineering **100**, 123, 2005.

162. Obradovic, B., Martin, I., Padera, R.F., Treppo, S., Freed, L.E., and Vunjak-Novakovic, G. Integration of engineered cartilage. J Orthop Res **19**, 1089, 2001.

163. Li, M.G., Tian, X.Y., and Chen, X.B. Modeling of Flow Rate, Pore Size, and Porosity for the Dispensing-Based Tissue Scaffolds Fabrication. Journal of manufacturing science and engineering **131**, 034501, 2009.

164. Hwang, N.S., Varghese, S., Lee, H.J., Theprungsirikul, P., Canver, A., Sharma, B., and Elisseeff, J. Response of zonal chondrocytes to extracellular matrix-hydrogels. FEBS Letters **581**, 4172, 2007.